

3)

Testing a Physically-Based Distributed Model (KINEROS):  
Predicting Runoff and Erosion from a Semi-Arid Hillslope  
in the Southwestern United States

by

Nicole L. Gotti

B.S., Environmental Engineering (1995)

Massachusetts Institute of Technology

Submitted to the Department of Civil and Environmental Engineering  
in Partial Fulfillment of the Requirements for the Degree of  
Master of Science in Civil and Environmental Engineering

at the

Massachusetts Institute of Technology

May 1996

© 1996 Massachusetts Institute of Technology  
All rights reserved

Signature of Author.....  
Department of Civil and Environmental Engineering  
May 24, 1996

Certified by.....  
Harold F. Hemond  
Professor of Civil and Environmental Engineering  
Thesis Supervisor

Accepted by.....  
Joseph M. Sussman  
Chairman, Departmental Committee on Graduate Studies

Eng.

MASSACHUSETTS INSTITUTE  
OF TECHNOLOGY

JUN 05 1996

LIBRARIES

**Testing a Physically-Based Distributed Model (KINEROS):  
Predicting Runoff and Erosion from a Semi-Arid Hillslope  
in the Southwestern United States**

by

**NICOLE L. GOTTI**

**Submitted to the Department of Civil and Environmental Engineering  
on May 24, 1996 in partial fulfillment of the requirements for the  
Degree of Master of Science in Civil and Environmental Engineering**

**ABSTRACT**

The practical implementation of a physically-based, distributed, watershed model is demonstrated by an application of KINEROS, a Kinematic Runoff and Erosion Model, in which an approximate calibration and validation of the model for a semi-arid pinon-juniper hillslope in the southwest United States is achieved on the basis of physical reasoning and through consideration of runoff response from storms with wide range of intensity and duration over a three year period. The erosion response was tested with data from one monsoon season only. Basic parameter values used in the application were derived from field measurements or published data. An approximated calibration was achieved for one hydrograph varying two parameters, relative saturated hydraulic conductivity and Manning's roughness coefficient, and was then validated against 12 different hydrographs, largely on the basis of peak watershed outflow. Some drawbacks of the model noted include the inability of KINEROS to predict small, low outflow producing storms and the extreme model dependence on the relative saturated hydraulic conductivity. Also noted was the paucity of guidance for the use of the erosion prediction capability of KINEROS and the possible inapplicability of the proposed transport equations for the type of watershed under study. However, the general good agreement between observed and simulated runoff and erosion responses for the class of large, intense storms and the use of watershed parameters based largely on field measurements indicate the potential usefulness of this model for land management purposes.

**Thesis Supervisor: Harold F. Hemond**

**Title: Professor of Civil and Environmental Engineering**

## ACKNOWLEDGMENTS

First and foremost, I would like to thank my family, especially my parents. It is only because of their support and encouragement that I have become the person that I am today and have been able to succeed. To Eddie, thanks for making the the last 3 years of my life better than I could have ever imagined.

In addition, this thesis would not have been possible without the work of Brad Wilcox at Los Alamos National Lab. His wisdom as well as his encouragement and support of my work the last three summers have been fundamental in the completion of my degree. Working with Brad and the rest of the folks at EES-15 was a great experience and I will miss not being able to return to Los Alamos.

Finally, thanks to Prof. Harry Hemond for helping me bring it all together in the end. Your encouraging words helped more than you know.

## Table of Contents

I. Introduction .....	5
II. Background .....	7
A. What is a physically-based model? .....	7
B. Erosion and Sedimentation - Current Technology and Limitations .....	7
C. Model Analysis .....	8
1. Validation .....	8
2. Sensitivity Analysis .....	9
3. Evaluation of Confidence Limits .....	9
III. Model Description .....	9
A. General Description .....	9
B. Upland Hydrology .....	10
C. Channel Phase .....	13
D. Erosion and Sediment Transport .....	14
E. Watershed Geometry .....	16
F. Parameter Estimation .....	16
G. Previous Validation of KINEROS .....	20
IV. Study Site .....	21
A. General .....	21
B. Vegetation .....	23
C. Soils .....	23
D. Runoff and Erosion .....	23
V. Methods .....	24
A. Data Collection .....	24
1. Meteorological Data .....	24
2. Runoff Data .....	25
3. Erosion Data .....	25
B. Model Parameterization .....	28
1. Geometric Parameters .....	28
2. Soil Related Parameters .....	34
3. Overall Watershed Parameters .....	38
C. Evaluation Procedure .....	39
1. Parameter Sensitivity .....	40
2. Calibration .....	42
3. Erosion Evaluation .....	48
VI. Results .....	48
A. Hydrologic Response .....	48
B. Erosion Response .....	59
C. Model Assessment .....	59
VII. Conclusions .....	67

## **I. Introduction**

The ability to predict soil losses has become essential for the purpose of making land management decisions. Continually increasing use and manipulation of the land by man is upsetting its natural interactions. (Foster and Meyer, 1977) The ability to predict soil losses is needed to help identify potential and real problems that are born from this intrusion and to aide in dealing with these problems effectively. Land uses that are of potential importance concerning the need to know what is happening with erosion are agricultural purposes, landfill cover integrity and other manifestations of man's existence such as urban developments and retention reservoirs.

Computer models have long been used for such erosion prediction purposes. Much of the work done in the past has been with simple, empirical models. These models are based on simple equations working off of huge data bases that have been established over the years. Empirical models, such as the Universal Soil Loss Equation and the Soil Conservation Service curve number method, have been found to work relatively well, but they lack the specificity to predict the effects of particular changes made in the watershed and its sensitivity to various physical factors and assumptions. (Loague et al., 1975) (Wilcox et al., 1990) This has largely been the impetus for the study of physically-based distributed models such as KINEROS. They are clearly superior to the simple, empirical models in that they are able to account for the uniqueness of each site.

There are two reasons why physically-based distributed models have the plausibility of being much more effective in predicting erosion. Since they are process-based models, they have the ability to take into account all the different processes going on in the watershed and the fact that they are distributed models enables them to calculate the processes to the extent that they actually happen. The other reason for their superiority is that the model parameters have physical meaning. That is to say, they can be estimated from a finite set of data. This allows model parameterization with limited calibration. This is important for the usefulness of models in being able to predict runoff and erosion from ungauged basins. Following along with this, the data base for the empirical equations is inherently restricted. There is no possible way that data can exist that fit the exact parameters of specific sites. (Kimberlin, 1977) This limits the applicability of empirical equations. This factor is especially significant in the western United States where there are often wide variations in rainfall, topography and climate.

The relative usefulness of the physically-based distributed models is offset, however, by the number of parameters that need to be estimated. The application of these models may be limited by the feasibility of taking the measurements needed to estimate parameters reliably. This also means that the model needs to be validated for each specific type of site. It is the site specific climate, soil, topography and soil surface conditions along with their interactions that are the major factors effecting erosion and sedimentation. (ASCE, 1975) These factors, and potentially their processes, can vary significantly from site to site. It is important to know that the important processes are being taken into account by the model. Indeed, the relative usefulness of physically-based models has been challenged. Bearing in mind the constraints placed upon them, physically-based models, in some cases, have not been found to work any better than simple empirical models. (Loague, 1975) (Wilcox, 1991)

Sediment yield, erosion less sedimentation throughout the watershed, is produced primarily by processes involving the detachment, transportation and deposition of sediment by raindrop impact and flowing water. (Foster and Meyer, 1977) Thus, the sediment yield prediction is a function of the hydrology. This makes it important foremost to understand the hydrologic processes of the watershed. In turn, both the sediment yield prediction and runoff prediction are functions of both the reliability of parameter estimations and their sensitivity in the model and of the model equations. How the model handles the parameters and the processes taken into account in the model equations are important to the creditability of model results.

Hence, focuses in the study of KINEROS are the importance of predicting runoff and erosion correctly through investigating the means by which they are calculated. This includes account for accurate estimates of parameters and investigation of the processes occurring on the watershed.

For use in Los Alamos county in northern New Mexico, this research is important to researchers studying environmental contaminants and how they could possibly spread. Since contaminants can sorb and travel with soil displaced by runoff, the process of erosion can dramatically affect the spread of contaminants. Models, such as the subject of this study, may help researchers determine which contaminated areas should be stabilized quickly or take precedence in preservation or remediation efforts. The research may also

help people in other areas in the southwest with similar vegetation understand changes in runoff and erosion. Of specific importance in the southwest are the effects of cattle grazing. (The New Mexican, 8/2/95)

Testing of models is one of many important steps in their development. It can help make models more powerful tools for use in prediction. Watershed studies, such as the Bandelier watershed study (Wilcox et al., in press), give modelers an opportune chance at testing how well models work. The importance of proving KINEROS a viable model with minimal calibration is important for it be able to be widely used confidently. (Wilcox, 1989) The goal of this study is to validate KINEROS for a semi-arid hillslope in the southwest United States with reference to both runoff and erosion. In the end, the conclusions are not going to necessarily state whether KINEROS works for the study area or not, but rather show the relative usefulness of the model in different hydrological situations (i.e. drizzling rain vs. intense rainstorms).

## **II. Background**

### **A. Physically-Based Models**

A physically-based model is one that has a theoretical basis and whose parameters and variables are measurable in the field. (Beven, 1983) It is based on physical laws such as the laws of conservation of energy and mass, and the law of thermodynamics. Model output provides specific information concerning the hydrograph and soil loss occurring at each point along the hillslope profile. This information allows the user to then experiment with alternative management systems, based on the spatial and temporal soil loss distribution estimates. The model can quickly assess the impact of the proposed systems for the site-specific information. (Nearing, 1990)

### **B. Erosion and Sedimentation - Current Technology and Limitations**

The current soil erosion prediction technology available is physically based on fundamentals of hydrologic and erosion science. As pointed out by Nearing et al. (1991), however, even though current prediction of soil erosion still rely on an understanding of the basic processes of detachment (i.e. the hydrodynamic forces induced by raindrop impact and surface flow and the interparticle bonding forces within the soils), this new

prediction technology is fundamentally different from the traditional empirical Universal Soil Loss Equation. The basic tenet of physically-based models is that they are specific enough to be able to account for more specific phenomena than have been able to have been taken into account in the past. Therefore, it carries with it a new set of research needs.

The literature sets forth specific voids in the current prediction equations for erosion. Specifically, methods are needed for predicting which soils seal and crust and to what degree these phenomena affect infiltration rates. Also, drying and cracking, which expedite infiltration of surface soils, are topics not that are still not currently addressed. It is important to note that these phenomena are present in the study area. Another deficiency discussed is the lack of representation of sediment size distributions. Differentiation of sediment from rill and interrill areas can be very important in estimating chemical transport associated with sediment. These gaps in current prediction equations can only add to the uncertainty under which erosion predictions are made.

An accurate estimate of sediment yield must also consider the entire watershed erosion-sedimentation system. This includes identifying major sources and sinks, determining the watershed's erosion and sedimentation history and examining the assumption of channel equilibrium. Possible significant sources include agricultural lands, construction sites, roadways, ditches, disturbed forest lands and natural geologic 'badlands'. Sinks are classified as anywhere deposition occurs because the flow's transport capacity is reduced below its sediment load. Some examples of possible sinks are concave slopes, strips of vegetation, fallen trees, flood plains and reservoirs.

Finally, models currently run on the assumption of channel equilibrium. This is a hard assumption to justify because most channels are dynamic, dropping sediment and changing their path as they flow. This is especially true in the region in which the study area subsides. After short, intense storms which are typical of northern New Mexico, many channels on the watershed have been found to have changed beds completely.

## C. Model Analysis

### 1. Validation



Validation of a model entails comparisons between model predictions and measured field data. Validation of physically-based models is necessary for two reasons. One reason being to prove the validity of a model's output. The other reason is to substantiate the cause of increasing the complexity of a model. A systematic analysis of a number of data sets must be used to evaluate the need for incorporation of a new set of information into the process-based technology.

## **2. Sensitivity Analysis**

Sensitivity analysis helps the modeler to identify the aspects of the overall erosion process which most influence accurate prediction and control of erosion and sediment yields. It is important to always take this into consideration because different management practices and field sites may experience varying sensitivity to the parameters involved. (Nearing et al., 1990)

Even though sensitivity analysis can be a helpful tool, there are two things a modeler should be on the lookout for. They are that 1) current knowledge dictates the model relationships and 2) results of sensitivity analysis for a given variable, or set of variables, are dependent on the values of the remaining variables. (Kitandis & Bras, 1980)

## **3. Evaluation of Confidence Limits**

Confidence limits are at issue when modeling any natural system. Natural processes are inherently highly variable. (Rosenbluth, 1975) It is important for a modeler to realize the constraints set upon him by the system.

# **III. Model description**

## **A. General description**

KINEROS, A Kinematic Runoff and Erosion Model, is an event-oriented, physically based model simulating the processes of interception, infiltration, surface runoff, and erosion. KINEROS is a child of KINGEN by Rovey et al. (1977), which used the kinematic wave approximation, with some simplifying assumptions. KINGEN employed a model that derived a computer solution for infiltration to simulate the production of runoff.

KINEROS is the modified version, most notable modifications being the inclusion of simulation of erosion and sediment transport, revision of the infiltration component, and inclusion of a pond element. The model uses partial differential equations to describe overland flow, channel flow, erosion and sediment transport. These equations are solved by finite difference techniques.

KINEROS is event oriented. The model can not maintain a hydrologic balance between storms. It does not take evapotranspiration or soilwater movement between storms into account due to the relatively short length of time that the model is simulating. KINEROS, therefore, is not appropriate for watersheds with significant subsurface flow components.

## B. Upland Hydrology

KINEROS simulates the major components of rangeland hydrology, including infiltration, Hortonian overland flow, soil water and storage. It is assumed that runoff is generated by the Hortonian mechanism and is calculated using the kinematic wave equations. When rainfall rates exceed the infiltration capacity the model produces overland flow. In other words, the amount of water that does not infiltrate is assumed to be runoff.

There are different situations under which infiltration can be taking place. At the beginning of a storm, infiltration is initially limited by rainfall intensity and  $F$ , the amount of rain already absorbed in the soil, is accumulated at the rate of rainfall. If the soil can absorb the rainwater faster than the rain is supplying it, it may be called a rain limited infiltration period. The maximum rate the water can enter the soil is called the infiltration capacity,  $f_c$ . The infiltration capacity can be described as a function of the initial water content,  $\theta_i$ , and the amount of rain already absorbed in the soil. Two parameters that are key to the infiltration model are the effective saturated hydraulic conductivity,  $K_s$ , and the effective net capillary drive,  $G$ .

The point at which the infiltration capacity becomes limiting is called ponding. At this stage, Eqn. 1, which is taken from Smith and Parlange (1978), defines the infiltration rate.

$$f_c = K_s \exp(F/B)/[\exp(F/B)-1] \quad \text{Eqn. 1}$$

where  $f_c$  is the infiltration capacity,  $K_s$  is the effective hydraulic conductivity and  $B$  is the saturation deficit of the soil, which is the difference between the volumetric water-holding capacity of the soil and its initial water content.

Infiltration continues after the rain ceases or falls to a rate below the infiltration capacity,  $f_c$ . Rain and flowing water still on the soil surface supply the infiltration process. The supply of infiltrating water from flowing water, however, cannot be assumed to be continuous over the surface. The kinematic treatment of the surface water flow used in KINEROS does not require the assumption of “sheet” flow. This allows KINEROS to take the microtopography of the watershed into account. The model asks for a surface microtopography parameter, RECS, that represents the local maximum average depth of surface water flow for which the surface is essentially completely covered by the water. As the average flowing water depth is reduced below this depth (RECS), the percentage of the surface covered with water declines in direct proportion to the depth. A very low value of RECS would represent a relatively smooth soil surface, while a large value would represent a very rough and rilled surface.

KINEROS also models the changes that take place in the soil moisture conditions between storms when a hiatus occurs in which part or all of the surface is free of water. After such a period, a subsequent rainfall will find a new and higher initial soil saturation,  $S_i$ . The change in relative saturation during such an event are based on an analytic estimate of the water content that the soil would attain for a steady unsaturated flow with a given rainfall rate,  $r$ , that is less than  $K_s$ . This relationship is based on a relation between soil flux (equal to a rain rate) and relative saturation at a constant rate,  $S(r)$ , by Brooks and Corey (1964) and others (Eqn. 2.):

$$S(r) = S_r + (S_{\max} - S_r) \{r/K_s\}^p ; (r < K_s) \quad \text{Eqn. 2}$$

where  $p$  is a constant on the order of 0.20 and  $S_{\max}$  is the maximum possible soil saturation.

KINEROS estimates the change in  $S_i$  during a hiatus in assuming that its value moves asymptotically towards the value of  $S(r)$  for when  $r < K_s$ .

Hortonian overland flow begins when the rainfall rate exceeds the infiltration capacity and sufficient water ponds on the surface to overcome surface tension effects and fill small

depressions. The calculations for overland flow are viewed as a one-dimensional flow process in which the flux is proportional to some power of storage per unit area:

$$Q = \alpha h^m \quad \text{Eqn. 3}$$

where  $Q$  = discharge per unit width

$h$  = storage of water per unit area

$\alpha, m$  = parameters related to slope, surface roughness and turbulence

Eqn. 3 is used in conjunction with the equation of continuity:

$$\delta h / \delta t + dQ / \delta x = q(x,t) \quad \text{Eqn. 4}$$

where  $t$  = time

$x$  = spatial coordinate

$q(x,t)$  = lateral inflow rate

If Eqn. 3 and Eqn. 4 are combined, the result is:

$$\delta h / \delta t + \alpha h^{m-1} \delta h / \delta x = q(x,t) \quad \text{Eqn. 5}$$

The kinematic wave equations are a simplification of the de Saint Venant equations and do not preserve all the properties of the more complex equations. Specifically, backwater cannot be accommodated and waves do not attenuate. The kinematic wave equations have been shown to provide an excellent approximation for most overland flow conditions.

In KINEROS the kinematic wave equations are solved numerically by a four-point implicit method. The finite difference equation is:

$$h^{i+1}_{j+1} - h^i_{j+1} + h^{i+1}_j + 2dt/dx \{ \theta_w [\alpha^{i+1}_{j+1} (h^m)^{i+1}_{j+1} - \alpha^{i+1}_j (h^m)^{i+1}_j] + (1-\theta_w) [\alpha^i_{j+1} (h^m)^i_{j+1} - \alpha^i_j (h^m)^i_j] \} - dt \{ q_{j+1} + q_j \} = 0 \quad \text{Eqn. 6}$$

where  $\theta_w$  is a weighting parameter for the x derivatives at the advanced time step.

A solution to this equation is obtained by Newton's method (sometimes referred to as the Newton-Raphson technique.)

Four options are available to the user for  $\alpha$  and m in Eqn. 5. They are the Manning hydraulic resistance law, a laminar law in combination with Manning's law, a laminar law in combination with the Chezy law and the Chezy law.

The hydraulic resistance parameters chosen, along with slope, slope length, rainfall intensity and infiltration characteristics, will control the overland flow response characteristics.

### C. Channel Phase

Open channel flow, or unsteady, free surface flow in channels, is also represented by the kinematic approximation to the equations of unsteady, gradually varied flow. Channel segments may receive distributed, time-varying lateral inflow from planes on either or both sides of the channel, from one or two channels at the upstream boundary, or from a plane at the upstream boundary. Rainfall on the channel is neglected.

The continuity equations for a channel with lateral inflow is:

$$\delta A / \delta t + \delta Q / \delta x = q_c(x,t) \quad \text{Eqn. 7}$$

where A is the cross sectional area, Q is the channel discharge, and  $q_c(x,t)$  is the net lateral inflow per unit length of channel.

The kinematic assumption is demonstrated in the relationship between channel discharge and cross-sectional area in:

$$Q = \alpha R^{m-1} A \quad \text{Eqn. 8}$$

where  $R$  is the hydraulic radius and  $m$  and  $\alpha$  are dictated by the hydraulic resistance law chosen. Channel cross-sections may be approximated as trapezoidal or circular.

The trapezoidal approximation does introduce a significant error in the channel area covered by low flow rates, however KINEROS has an empirical expression to estimate an “effective wetted perimeter” for infiltration:

$$p_e = \min [ h/(0.15 (BW)^{1/2}), 1.0 ] p \quad \text{Eqn. 9}$$

where  $p_e$  = the effective wetted perimeter for infiltration

$h$  = depth

$BW$  = bottom width

$p$  = channel wetted perimeter at depth  $h$

The effective wetted perimeter is used in calculating infiltration until a threshold depth is reached, at which point  $p = p_e$ .

The kinematic equations for channels are also solved by a four point implicit technique (Eqn. 10) using Newton’s method to solve for the unknown area.

$$A^{i+1}_{j+1} - A^i_{j+1} + A^{i+1}_j - A^i_j + 2dt/dx \{ \theta_w [dQ/dA^{i+1} (A^{i+1}_{j+1} - A^{i+1}_j)] + (1-\theta_w) [dQ/dA^i (A^i_{j+1} - A^i_j)] \} - 0.5dt \{ q_{cj+1}^{i+1} + q_{cj}^{i+1} + q_{cj+1}^i + q_{cj}^i \} = 0 \quad \text{Eqn. 10}$$

#### D. Erosion and Sediment Transport

KINEROS can simulate the movement of eroded soil along with the movement of surface water. The model accounts separately for erosion caused by raindrop energy and erosion caused by flowing water. Similar procedures are used to describe transport of sediment

within surface and channel elements. The simulation of erosion in KINEROS is based on work done by Smith (1978, 1981).

Upland erosion in KINEROS is described through a mass balance equation similar to that for kinematic water flow (Bennett, 1974):

$$\delta/\delta t(AC_s) + \delta/\delta x(QC_s) - e(x,t) = q_s(x,t) \quad \text{Eqn. 11}$$

where  $C_s$  = sediment concentration [ $L^3/L^3$ ]

$A$  = cross sectional area of flow [ $L^2$ ]

$e$  = rate of erosion of the soil bed [ $L^2/T$ ]

$q_s$  = rate of lateral sediment inflow for channels [ $L^3/T/L$ ]

Equation 11 is solved numerically at each time step used by the surface flow equations. A four-point implicit finite-difference scheme is used, however, so iteration is not necessary.

The rate of erosion,  $e$ , is composed of two components - the rain splash erosion rate,  $g_s$ , and the hydraulic erosion rate,  $g_h$ , which is due to the interplay between shear force of water on the loose soil bed and the tendency of soil particles to settle under the force of gravity.

The transport capacity is important in calculating hydraulic erosion. KINEROS provides the user with a choice of six different sediment transport relationships. Each of the relationships can be represented by a generalized relation of the type

$$q_m = c_{mx}Q = \omega S^\beta Q^\gamma r^i [1 - \tau_c/\tau_o]^\epsilon ; \tau_o \geq \tau_c \quad \text{Eqn. 12}$$

where  $q_m$  = transport capacity [ $L^2/T$ ]

$\tau_o$  = bed shear stress [ $L^2/T$ ]

$\tau_c$  = critical shear stress [ $L^2/T$ ]

$\omega$  = a coefficient

Exponents  $\beta$ ,  $\gamma$  and  $\epsilon$  have values of either 0 or between 1 and 2 and  $\iota$  varies from 0 to

-2.24. All transport relations use local hydraulic conditions , such as slope, velocity, or depth of flow. In addition, some use sediment specific gravity and mean particle size of the soil.

Sediment transport simulation for channels follows the same general approach as that for upland areas. The two significant differences are that splash erosion ( $g_s$ ) is neglected for channel flow and the term  $q_s$  represents lateral inflows.

#### E. Watershed Geometry

The watershed is represented by a cascade of planes and channels. Each plane may be described by its unique parameters, initial conditions, and precipitation inputs. Each channel may be described by its geometry. As a result, spatial and temporal variability of rainfall and infiltration, runoff, and erosion parameters can be accommodated. The user must be aware that the geometry of the model is only an approximation of the real watershed.

The dimensions of the planes are calculated to completely cover the watershed. The channels do not represent actual area in the watershed.

#### F. Parameter Estimation

Values for all of the parameters needed to run the hydrology component of KINEROS can be assigned based upon physical characteristics of a watershed. In theory, calibration should not be necessary to use the model.

The KINEROS manual states that although they do give guidelines for estimating parameters where information is available, where there is little or no information, runoff and erosion predictions may be subject to significant error if they are sensitive to the parameter in question.

See Table 1 for a complete listing of the parameters required for KINEROS. The parameters required for the pond simulation part of the model are not included because they



Table 1. KINEROS definitions of input variables and parameters used in this study.  
(note: some parameters available in the model are not included because they are not pertinent to this study.)

<u>Name</u>	<u>Definition</u>
BW	Channel bottom width - ft or m.
CF	Rainsplash parameter equation [35].
CG	Hydraulic erosion transfer coefficient rate - equation [37].
CH	Rainsplash erosion damping parameter - equation [36] - in or mm.
CLEN	Characteristic length of overland or channel flow. Use maximum of sum of lengths of cascading planes or longest channel - ft or m.
CO	Parameter in Kilinc and Richardson erosion relationship - equation [A.3].
CS	Parameter in tractive force erosion equation [A.1].
D	Accumulated rainfall depth at time (T) - in or mm.
D50	Median sediment particle diameter - ft or um.
DELT	Time increment to be used in calculations - estimate using equations [48] or [49].
DIAM	Conduit diameter - ft or m.
DINTR	Interception depth - in or mm.
FMIN	Saturated hydraulic conductivity. English - in/h. Metric - mm/h.
G	Effective net capillary drive - in or mm.
GAGE	Rain gage (1-20) for input to watershed element.
J	Element number.
LAW	Code for erosion law. 1      Tractive force - equation [A.1] 2      Unit stream power - equation [A.2] 3      Bagnold/Kilinc - equation [A.3] 4      Ackers and White - equation [A.4] 5      Yalin - equation [A.12] 6      Engelund and Hansen - equation [A.13]
MAXND	Maximum number of rainfall time-depth pairs - $MAXND \leq 100$ .
NCASE	Code for channel type: 1      Trapezoidal. 2      Circular.

NC1	Element number of first channel contributing at upstream boundary.
NC2	Element number of second channel contributing at upstream boundary.
ND	Number of rainfall time-depth pairs for specific rain gage - $ND \leq MAXND$ .
NELE	Number of plane and channel elements - $NELE \leq 60$ .
NEROS	Code for erosion option: 0,1 No erosion calculation. 2 Erosion option.
NGAGES	Number of rain gages $1 \leq NGAGES \leq 20$ .
NL	Element number of plane contributing to left side of channel.
NLOG(1)	Denotes order of calculation. Element corresponding to NLOG(1) will be calculated first, NLOG(2) will be calculated second, etc.
NPRINT	Code for detailed printout in auxiliary output file: 1 Do not print. 2 Print.
NR	Element number of plane contributing inflow to right side of channel.
NRES	Resistance law code: 1 Manning's Law. 2 Laminar - Manning. 3 Laminar - Chezy. 4 Chezy.
NRP	Code for printout of rainfall and intermediate runoff rates in the primary output file: 0 No print. 1 Print rainfall rates for this element. 2 Print intermediate runoff rates. 3 Print both rainfall and runoff rates.
NTIME	Code for time units: 1 Seconds. 2 Minutes.
NU	Element number of plane contributing to upstream boundary.
NUNITS	Code for units: 1 English. 2 Metric.
PAVE	Proportion of surface area covered with gravel. $PAVE = 1$ denotes a paved surface.
POR	Soil porosity.
R1	Manning's n for $NRES = 1$ or $2$ .

	Chezy C for NRES = 3 or 4.
R2	Laminar “k” for NRES = 2 or 3. Not required for NRES = 1 or 4.
RECS	Infiltration recession factor - in or mm.
RHOS	Specific gravity of sediment particles.
ROC	Volumetric rock content of soil - dimensionless.
S	Slope.
SI	Relative soil saturation - dimensionless $S_r < SI < 1.0$ .
SIGMAS	Standard deviation of sediment diameter - ft or um.
SMAX	Maximum relative saturation under imbibition - $SI < SMAX < 1.0$ .
T	Time for rainfall depth (D) - s or min.
TEMP	Temperature. If in English units, Fahrenheit; in metric, centigrade. Default value is 65°F if TEMP = -1.
TFIN	Duration of runoff computations.
THETA	Weighting factor in finite difference equations - $0.5 < THETA \leq 1.0$ .
W	Width of plane. If channel, W = 0 - ft or m.
WEIGHT	Multiplication factor to be applied to rainfall depths for GAGE to obtain rainfall pattern for specific element.
XL	Length of plane or channel - ft or m. If zero for a channel, the outflow will be the sum of the channel inflows.
ZL	Side slope of left side of trapezoidal channel.
ZR	Side slope of right side of trapezoidal channel.

were not used in this study. The table is based on the table of parameters in the KINEROS manual.

#### G. Previous Validation of KINEROS

Previous studies of KINEROS have generated generally positive results. (Goodrich et al., 1993) (Renard et al., 1993) (Woolhiser et al., 1990a) (Smith et al., 1994) Tests of the model have been done using data from constructed experimental runoff facilities and data from sites in Arizona and Mississippi. Specifically, KINEROS has been judged to be effective in simulating runoff, though there are a few studies that have found conflicting results. Michaud and Sorooshian (1992) conducted a test for large, flood-producing storms on large watersheds (~15,000 ha.) They found that KINEROS was “reasonably accurate in simulating time to peak, but provides poor simulations of peak flow and runoff volume.” Also, Smith et al. (1994) suggested a limited applicability of KINEROS concerning the uncertainty of measurements of smaller storms. There has been limited analysis of the erosion prediction capability of the model. In one of the few studies done examining erosion, Zevenbergen and Peterson (1988) found the tractive force transport relation to predict erosion extremely well (e.g. the computed coefficient of determination was 0.96.)

Model analysis has attributed model error to the selection of the optimization set (i.e. they were not inclusive of the whole range of possible storms), varying antecedent soil conditions and channel losses, poor rainfall estimation and poor prediction of infiltration. Renard et al. (1993) conclude model predictions of small changes in runoff from a modified watershed can be misleading if the parameters are estimated from a small subset of the pretreatment data. Goodrich and others (1990, 1993) specifically point out the importance of recognizing the limitations imposed by the assumption of spatially uniform rainfall, particularly when runoff is a result of thunderstorm rainfall. They found the outflow hydrographs to be more sensitive to the rainfall input and its spatial variability than the other parameters. The suite of studies on KINEROS, in general, have also displayed an extreme model sensitivity to two parameters: relative saturated hydraulic conductivity and Manning’s roughness coefficient.

Goodrich et al. (1994) emphasized the importance of the initial soil water content (SI) in their study on the effect of SI on model output. Two methods for estimating SI were

compared, remote sensing by satellite of soil moisture data and estimations derived from a simple daily water balance model. It was found for small watersheds that either of the measurement methods could be used to obtain reasonable runoff predictions. It was noted that changes in rainfall representation had a much greater impact on runoff simulation than changes in SI inputs. At the medium watershed scale, a basin-wide remotely sensed average SI was found to be sufficient.

Significant improvements are on the way in the next version of KINEROS, tentatively called KINEROS2. Modifications include small scale variability of saturated hydraulic conductivity within a model element, space-time rainfall interpolation method to utilize multiple raingage information and soil and sediment characterization by a distribution of up to 5 particle size classes. (Smith et al., 1994)

#### IV. Study site

##### A. General

The study area used in the test is on the Pajarito Plateau in northern New Mexico. The site is on a mesa top overlooking Frijoles Canyon in Bandelier National Monument. The Frijolito watershed is a semi-arid pinon-juniper woodland, characteristic of north-central New Mexico. It is one hectare (2.5 acre) and is situated on a hillslope with a gradient of 0.105 with an elevation range of 1969 to 1990 m. (Figure 1)

Average annual precipitation for the Los Alamos area is 46 cm. The breakdown of the precipitation along with average temperatures is in Table 2. (Bowen, 1990) The monthly averages show that the majority of the precipitation in the study area occurs during the summer monsoon season. The averages were calculated using a 30 year period.

Table 2.  
Average monthly precipitation (cm.) and temperature (°F).

	January	February	March	April	May	June
Precipitation	2.16	1.73	2.57	2.18	2.87	2.84
Temperature	29.1	32.2	37.6	45.6	54.9	65.1

	July	August	September	October	November	December
Precipitation	8.08	9.98	4.14	3.86	2.44	2.44
Temperature	68.2	65.8	60.2	50.3	37.9	30.8

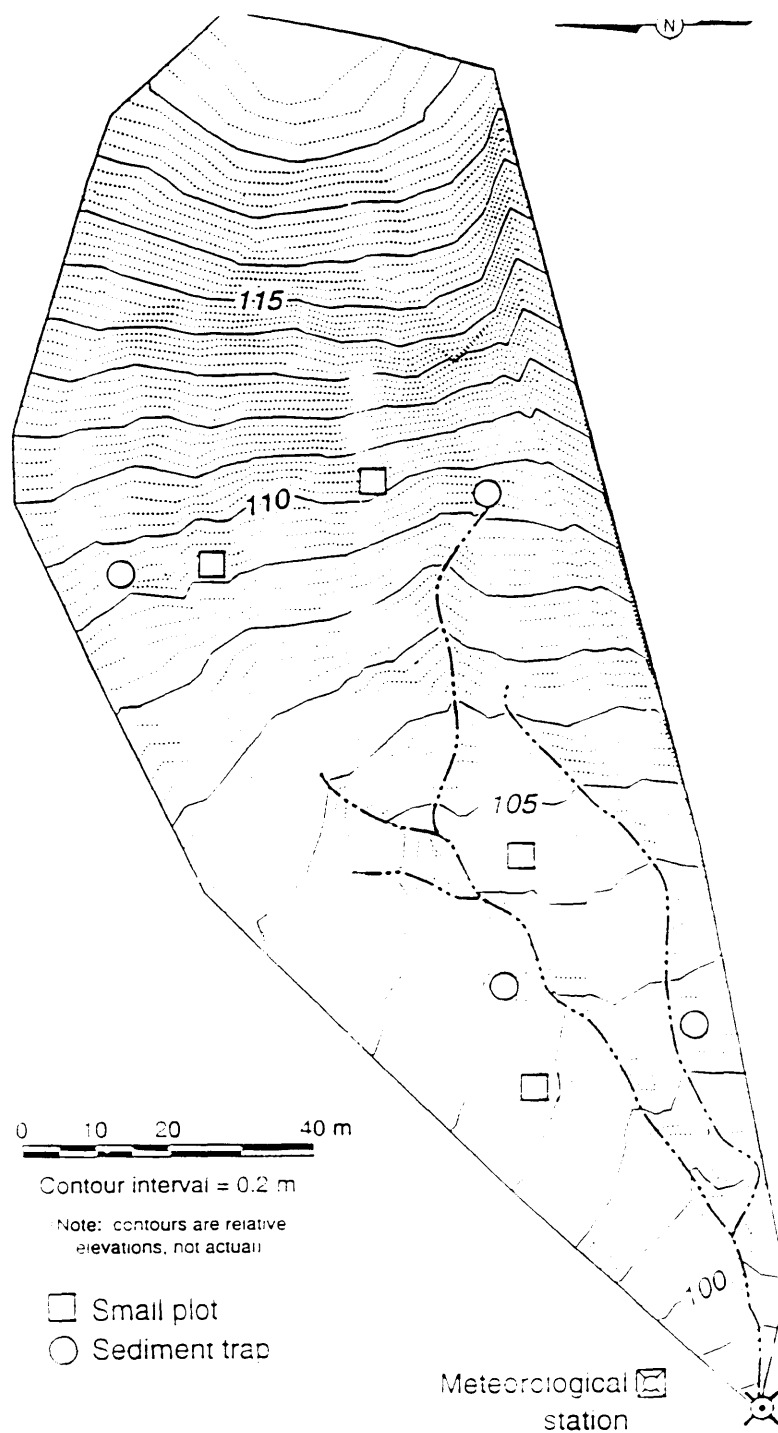


Figure 1. Countour map of the Frijolito watershed.

## B. Vegetation

The current species of flora in the watershed are predominantly pinon pine trees and juniper pine trees. The canopies of these trees make up about 45% of the watershed area. Clumps of grasses are scattered throughout the watershed, making up about 1% of basal cover. Intermittent patches of cryptogam also appear throughout the watershed and accounts for less than 1% of basal cover.

The vegetation has gone through drastic changes in the past 100 years. Local historic records, including fire records aerial photographs taken from 1935 to 1991, show that at one time the site was dominated by lowest-elevation ponderosa pine. They were driven out by a severe regional drought during the 1950s along with an associated outbreak of bark beetles and the invasion of the present pinon-juniper woodlands. The grass cover of the site was also greatly affected by a history of intensive grazing and fire suppression. Diminished grass cover has, in turn, triggered accelerated soil erosion.

## C. Soils

The surface soils in the watershed are texturally classified as sandy loam ( $D_{50} = 0.06$  mm), loamy sand ( $D_{50} = 0.10$  mm) and loam ( $D_{50} = 0.05$  mm). The predominant soil classification of the watershed is sandy loam. There are also patches of pumice which make up about 22% of the Frijolito watershed. The pumice patches are significant because pumice characteristically readily soaks up water and is very resistant to erosion. The characterization of the rest of the watershed is ~50% canopy and ~25% bare soil.

## D. Runoff & Erosion

The Frijolito watershed exhibits runoff characteristics typical of semiarid watersheds (Pilgrim et al., 1988) where infrequent runoff makes up a very small part of the annual water budget and is related to specific precipitation events or is “event based.” When runoff does occur, it is as overland flow.

The summer monsoon storms are typically short, intense storms. These storms are chosen to be modeled because they produce great amounts of runoff and erosion in very short

periods of time and are thought to be the major source of erosion for the plateau. Only once between 1993 and 1995 did runoff occur in the winter months (October 1994).

From July 1993 to October 1995, 17 runoff events occurred. Thirteen of those events were used in this model validation. The runoff in each of the events were the result of intense summertime thunderstorms. The peak flow was often quite high with a relative short duration of flow. The storms that are modeled in this study did exhibit a range in storm intensity and storm length, however. Each of the storms hyetographs and corresponding hydrographs are in Appendix A.

A possible difficulty in the erosion prediction is represented by the log dams interspersed throughout the watershed. The log dams have been built up over the years, effectively creating a sink for sediments eroding from the watershed. This sink is currently turning into a source, however. Stream channels are breaking through the dams either because the logs are rotting or the sediment built up on the upstream side of the logs has weakened enough for the streamflow to erode a path under the logs. This process is letting loose a volume of sediment that was heretofore in storage in the watershed, creating an irregularity within the system. It could be important to know the time scale on which such events happen in the watershed. This irregularity may or may not be part of the natural sediment erosion cycle of the system, hence it may or may not be altering the erosion data to produce misleading results.

## **V. Methods**

### **A. Data Collection**

Meteorological and runoff data have been collected year round at the Frijolito watershed since July 1993. Collection of erosion data began in spring of 1994 with the installation of the first sediment trap at the outflow point of the watershed. The erosion collection system was modified in July 1994 to increase the capacity for sediment collection.

#### **1. Meteorological Data**

Meteorological data are measured by a solar powered weather station. Data collected includes precipitation, wind speed, wind direction, ambient air temperature, solar radiation



and relative humidity. Data is collected regularly on 15 minute intervals. Accelerated precipitation data is taken every minute during a precipitation event. Precipitation measurements are taken using a heated tipping bucket rain gauge. Table 3 summarizes the event data collected.

## 2. Runoff Data

Flume flow is recorded every minute runoff occurs during and immediately after a precipitation event. The flume is located near the meteorological station at the outflow point of the watershed. (see Figure 1.) The design of the flume follows that of Replogle et al. (1990). The flume is constructed from a 4-m long piece of 38-cm PVC pipe. The floor of the pipe has a flat concrete sill that forces the flow to critical depth (Froude number = 1.0) as it exits the pipe. Water height in the flume is measured by a pressure transducer located in an adjacent stilling well.

## 3. Erosion Data

Sediment data has been collected since the beginning of the 1994 summer monsoon season. On a watershed scale, sediment is collected at the outflow of the watershed in a 0.4 m<sup>3</sup> sediment trap located immediately upstream from the flume. Four 1 m<sup>3</sup> sediment traps were installed in July of 1994 when it was discovered that the one previous sediment trap was insufficient to capture the erosion produced by the watershed. These four traps have contributing areas of ~1/12 of the total area of the watershed. The breakdown of the contributing areas are in Table 4. Figure 2 is a geographical representation of the contributing areas.

Table 4. Characteristics of the contributing areas for sediment traps (ST).

Catchment portion	Area (m <sup>2</sup> )	Slope
ST1	1046	0.1
ST2	308	0.063
ST3	308	0.188
ST4	1107	0.1
FLUME	10,000	0.105

The sediment traps are monitored after each precipitation event. Sediment collected in the traps is shoveled out into 5-gallon buckets and the number of buckets of sediment retrieved

Date	Precipitation			Runoff			Erosion
	Amount (in)	Duration (min)	Peak (in/hr)	Volume (ft <sup>3</sup> )	Duration (min)	Peak flow (CFS)	Catchment (lbs.)
July 28, 1993	1.32	41 + 15*	0.07	2520	33 + 20*	1.57	+
Aug. 20, 1993	0.21	18	0.02	73.5	13	0.21	+
Aug. 27, 1993	0.81	24	0.08	3076	32	2.21	+
Aug. 28, 1993	0.26	18 + 19*	0.03	1831	30 + 60*	0.3	+
Sept. 6, 1993	0.81	39	0.08	1402.6	31	1.5	+
Sept. 13, 1993	0.16	8	0.04	113.7	14	0.25	+
Aug. 2, 1994	0.22	21	0.04	536	15	0.81	+
Aug. 21, 1994	0.17	6	0.06	196.7	9	0.96	+
May 29, 1995	0.47	34	0.04	1829	41	2.39	1178
June 29, 1995	0.95	25	0.11	1187	19	2.17	3600
July 18, 1995	0.45	18 + 36*	0.02	1196	66	0.42	692.2
Aug. 13, 1995	0.39	22	0.04	422.2	17	0.91	671.8

\* indicates that rainfall and runoff occurred in two distinct phases

+ indicates that data was not yet being collected

Table 3. Summary of event data for the 1993-1995 seasons. (note: erosion data was not collected until the 1995 season)

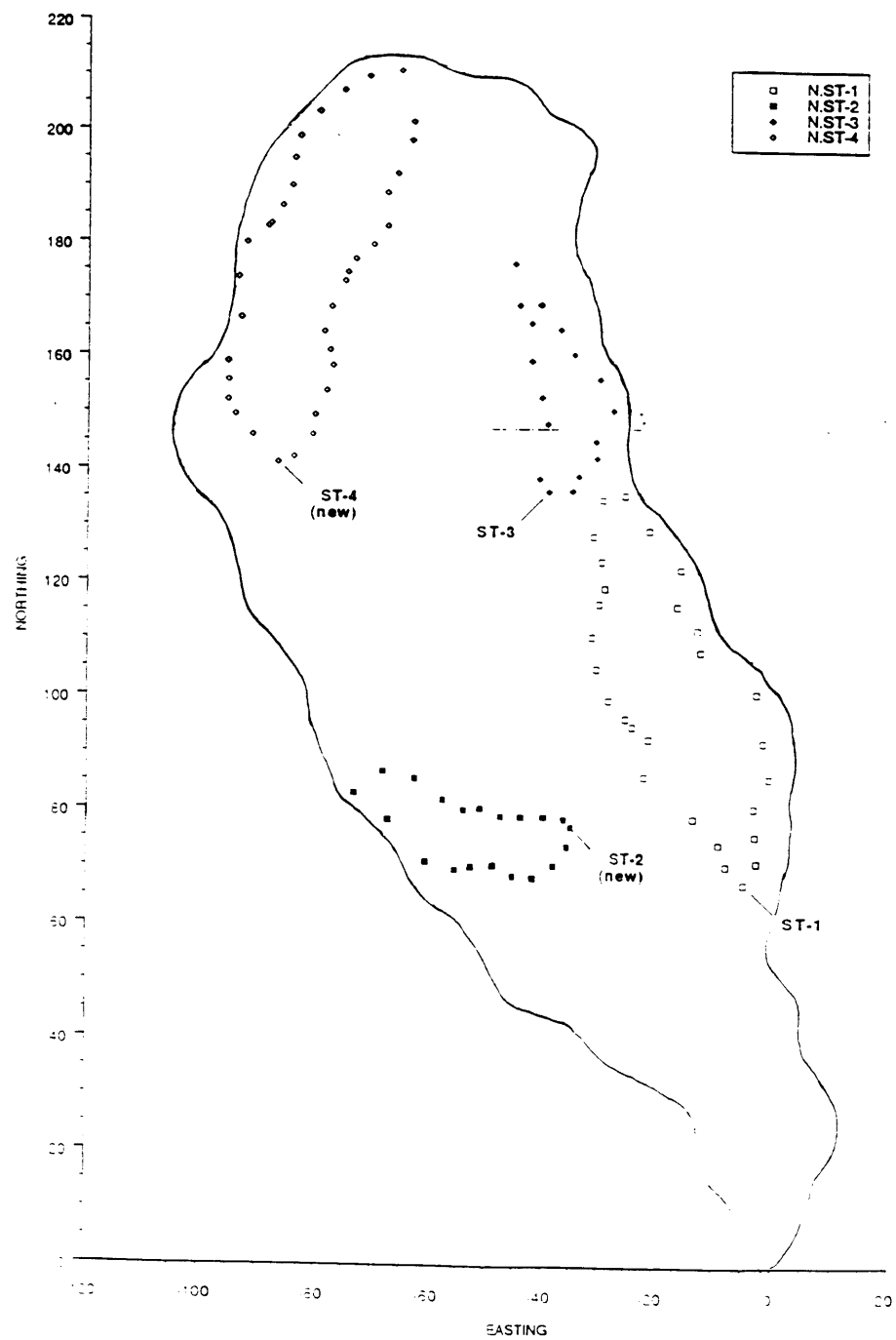


Figure 2. Contributing areas for sediment traps.

from the trap is recorded. Sediment samples from the traps collected after each storm are taken back to the lab where they are dried and sieved. From this information the bulk density and, therefore, the weight of the sediment eroded can be determined. Table 5 summarizes the erosion data collected during the 1995 monsoon season.

Table 5. Erosion data for summer 1995.

Pounds (lb.) of sediment transported with each storm, Summer 1995				
Trap	May 29	June 29	July 18	August 13
ST1	150.8	552.8	23.5	34.5
ST2	0	627.0	11.5	51.7
ST3	200.4	318.6	106.0	17.2
ST4	0	1205.8	137.0	68.9
FLUME	826.8	895.7	413.4	499.5
Total erosion	1178.0	3600.0	692.2	671.8

## B. Model Parameterization

KINEROS requires the identification of parameters concerning soil and hydraulic characteristics and watershed geometry. In some cases the parameters can be measured directly (e.g. taking soil corings and surveying.) In other cases in which parameters can not be explicitly measured, they can be estimated from related data and charts and tables provided in the KINEROS manual. Examples of the input files used in this study can be found in Appendix B.

### 1. Geometric Parameters

Two parameter files were made to represent the watershed. The first file made was done to fit the geometric characteristics of the model as closely as possible to the actual watershed. These characteristics include slope, stream density and pumice patches. Figure 3 depicts the stream network. Due to the density of stream channels and changes in gradient, these efforts resulted in a parameter file consisting of 42 elements. Figure 4 shows the resultant geographical representation of the elements in the parameter file and Figure 5 is a flow diagram of the watershed as the model sees the input. A second parameter file was made to test the efficaciousness of using the 42-element file. This parameter file consists of eight elements only. (Figures 6 and 7) The eight elements were based on significant changes in slopes and pumice fields in the watershed.

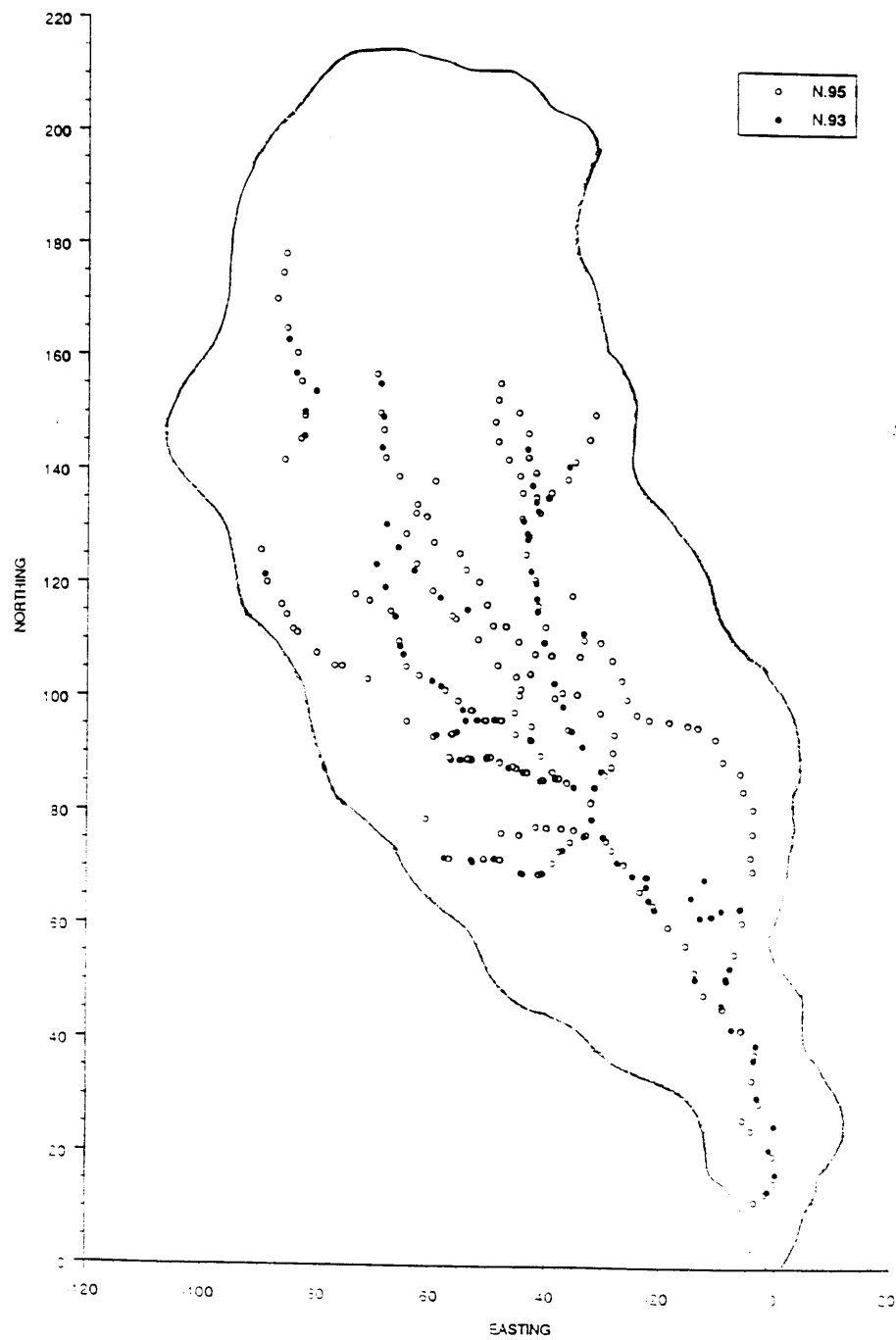


Figure 3. Channel network.

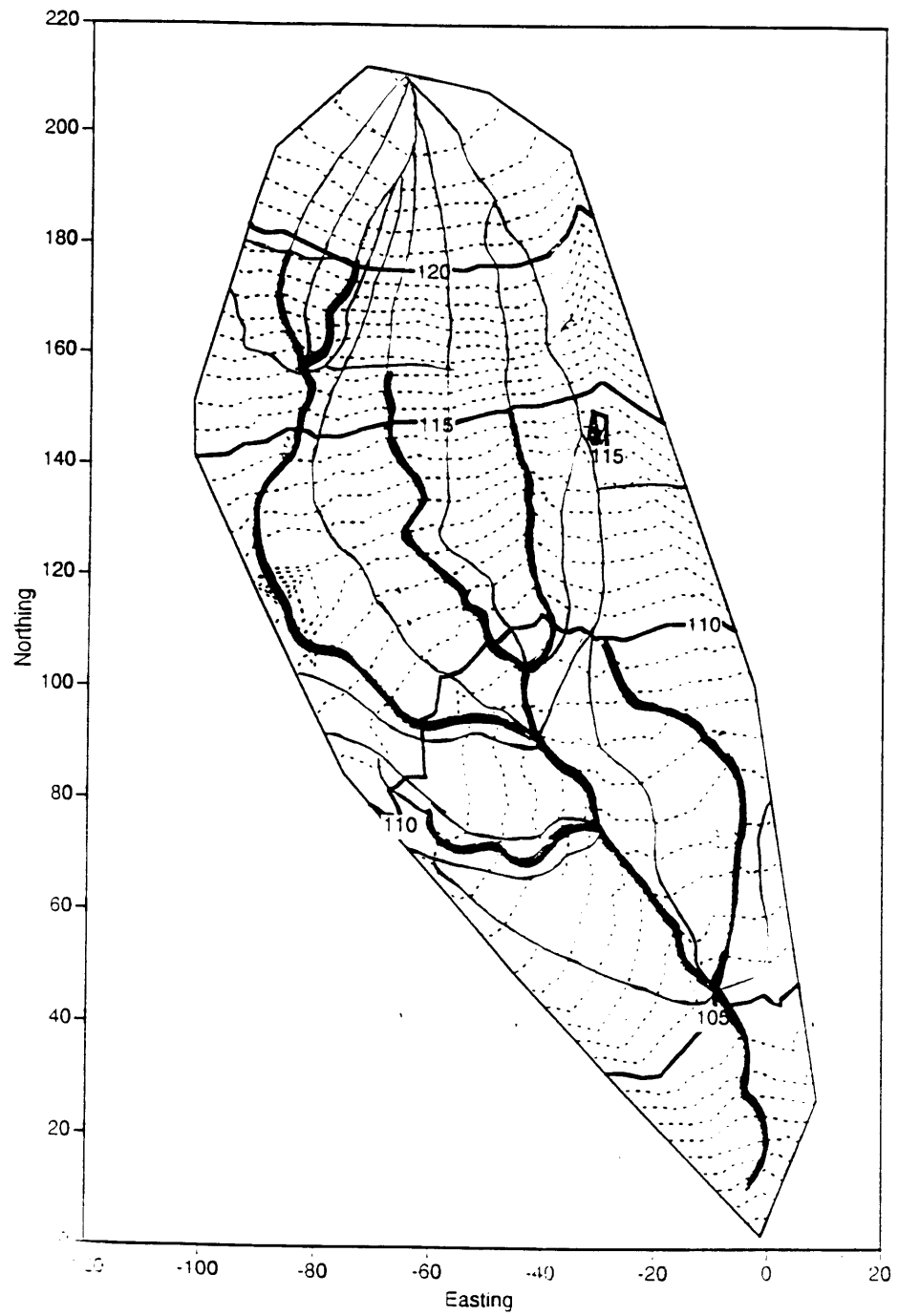


Figure 4. Geographical representation of the 42-element parameter file.

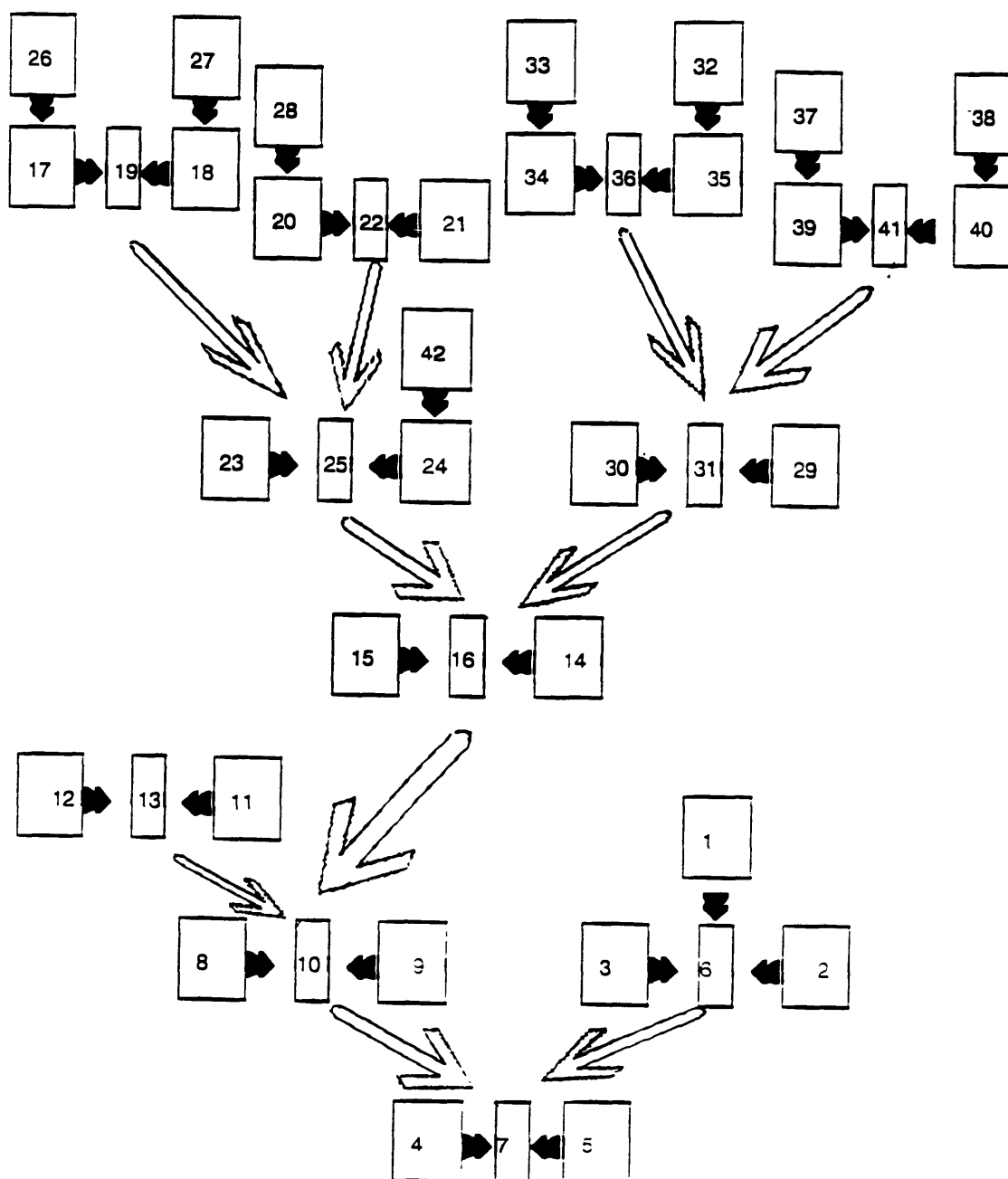


Figure 5. Flow diagram of the 42-element parameter file. The squares represent planes and the rectangles are channels. The hollow arrows depict upstream channels flowing into downstream channels and the small black arrows represent the flow from planes to planes and planes to channels.

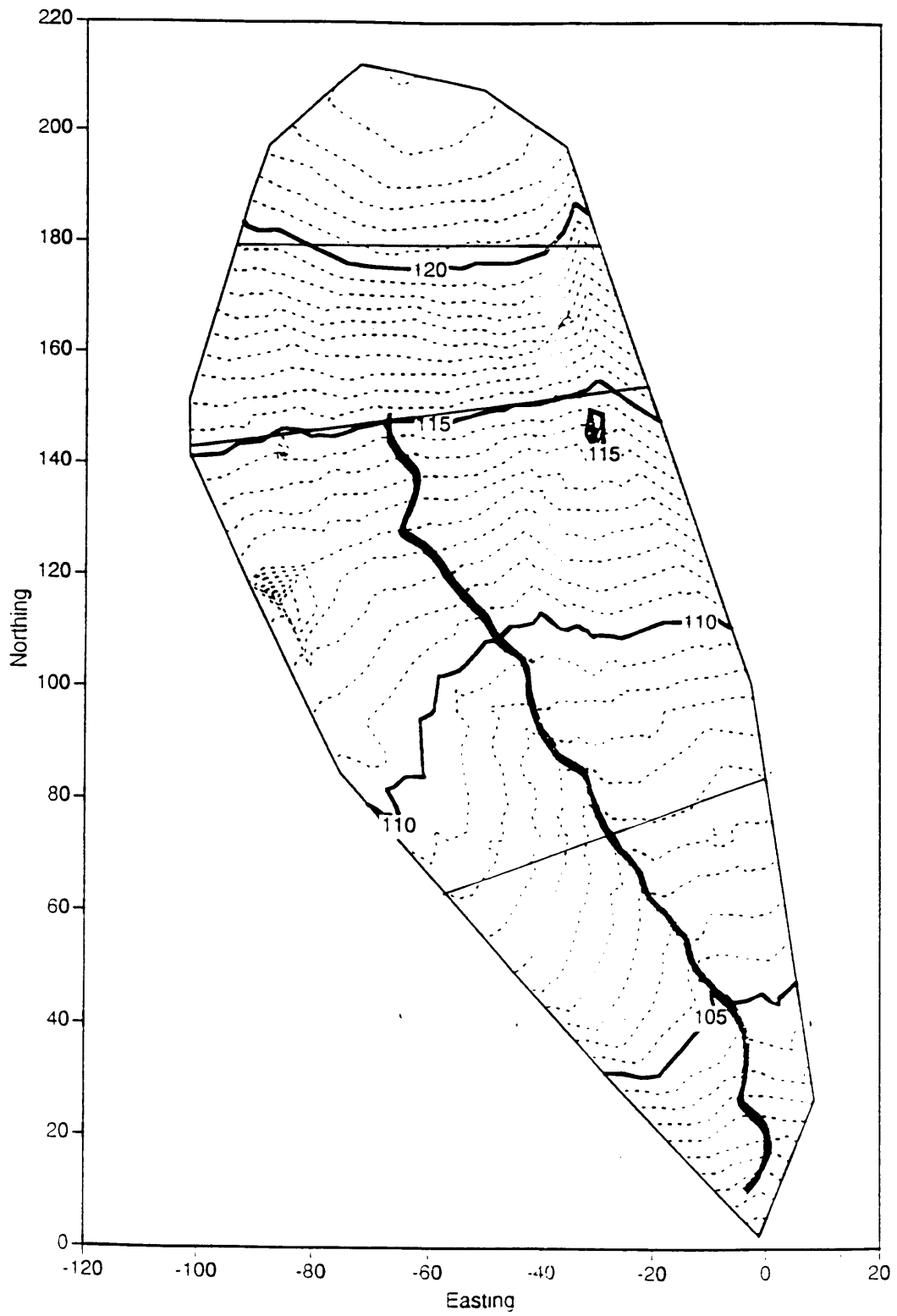


Figure 6. Geographical representation of the 8-element parameter file.



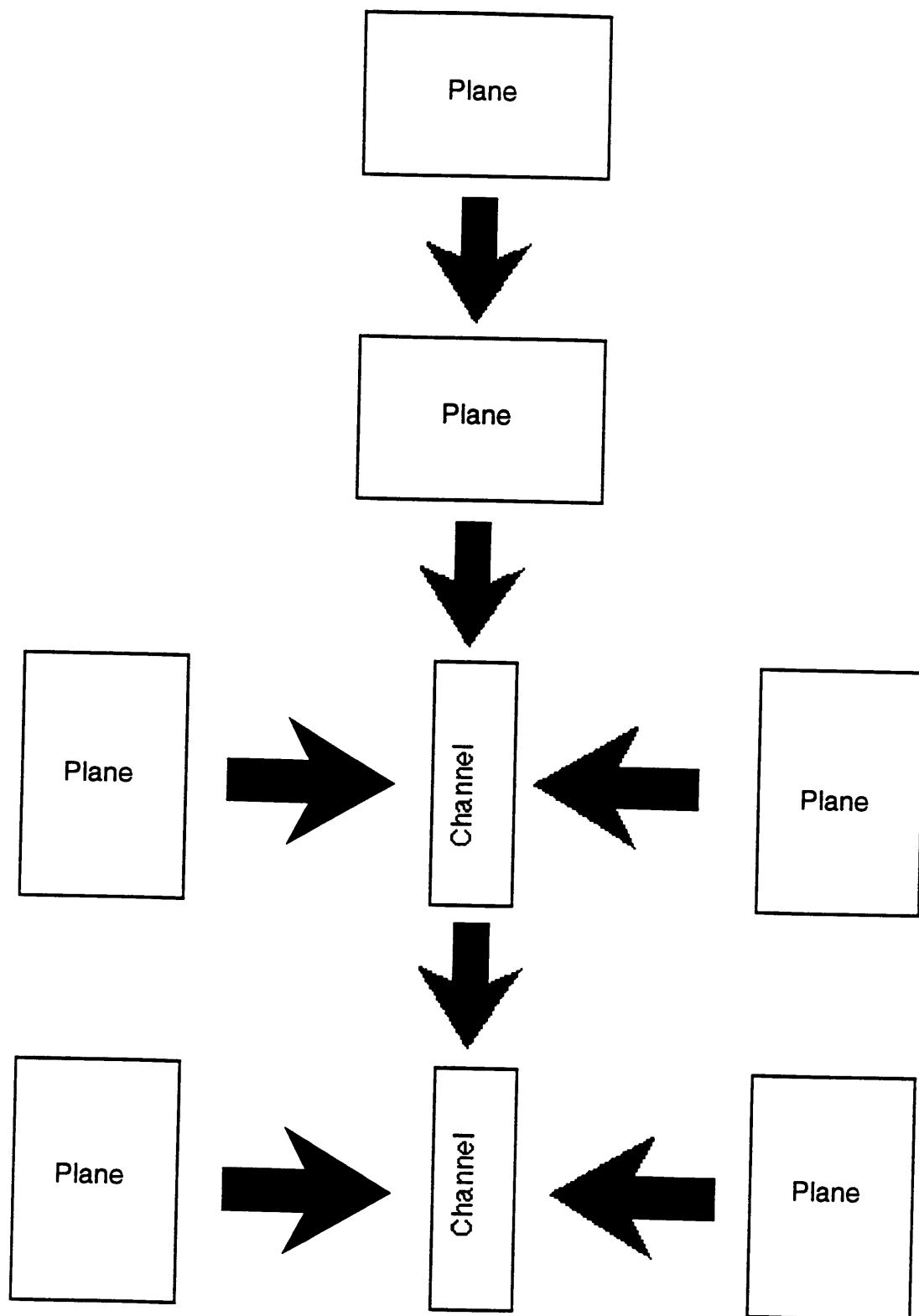


Figure 7. Flow diagram of the 8-element parameter file.

The set of geometric measurements are estimated from a topographical map of the watershed and from a walking survey of the watershed. These measurements include length, width and slope of the planes (S, W, XL), length and slope of the channels (BW, ZL, ZR) and the characteristic length (CLEN) of the watershed. Three classifications of width and depth for the channels were established to use as estimates throughout the watershed. See Table 6 and Table 7 for a comparison of the selected lengths and widths for the eight and 42 element parameter files and the actual areas of the planes that make up the watershed. As suggested by the KINEROS manual, the characteristic length was estimated using the longest stream channel in the watershed. It is estimated to be 200 ft. Channels do not represent actual area in the model because KINEROS does not include channels in the area over which it calculates rainfall and infiltration.

The proportion of the watershed considered impervious, represented by the parameter PAVE, is zero in this watershed.

## 2. Soil Related Parameters

Surface soil parameters were estimated by taking direct samples from the study site and using that data in conjunction with more extensive soils work that has been done on similar sites.

Table 8. Surface soil characteristics.

Soil Type	Mean Particle Diameter (mm)	Standard Deviation	Clay content (%)	K factor	C <sub>t</sub>
sandy loam	0.06	0.09	11.4	0.30	32.49
loamy sand	0.10	0.15	4.4	0.23	24.90
loam	0.05	0.07	17.5	0.31	33.76

The soil type in the Frijolito watershed is determined using soil corings. (Dave Davenport, 1994 personal communication). The watershed surface soils consists of sandy loam, loamy sand, loam and pumice. (Table 8) Mean particle diameter (D50) for the watershed was taken to be 0.0012 in. with a standard deviation (SIGMAS) of 0.0018. The area represented by pumice is calculated to be 22% of the watershed in the 8 element parameter file and 23% in the 42 element parameter file. There was no rock found in the soil column so the volumetric rock content (ROC) was taken as zero. Clay content of the soil was also

8 element parameter file element dimensions.						
Element #	Length (ft.)	Width (ft.)	Calculated area (ft <sup>2</sup> )	Actual area (ft <sup>2</sup> )	Slope	Element category
1	113.75	188.5	6597.5	6386.3	0.05	plane
2	227.5	97.5	6825.0	6955.0	0.12	plane
3	269.75	97.5	8092.5	8552.6	0.02	plane
4	243.75	130.0	9750.0	9578.9	0.03	plane
5	276.25	3.0*	--	--	0.06	channel
6	243.75	65.0	4875.0	5086.0	0.03	plane
						(pumice)
7	260	48.75	3900.0	3557.9	0.02	plane
						(pumice)
8	308.75	3.5*	--	--	1.5	channel
Total watershed area:			40040.0	40116.7		

\* The 'Width' values for channels represents the channel bottom width.

Table 6. Dimensions of the elements in the 8-element parameter file, both the calculated input for model and the actual area.

42 element parameter file element dimensions.						
Element #	Length (ft.)	Width (ft.)	Calculated area (ft^2)	Actual area (ft^2)	Slope	Element category
1	238.0	45.0	10710.0	10619.1	0.12	plane
2	302.0	33.0	9966.0	10477.6	0.21	plane (pumice)
3	208.0	30.0	6240.0	6513.1	0.04	plane
4	114.0	81.0	9234	10194.4	0.1	plane (pumice)
5	225.0	30.0	6750	2831.8	0.04	plane
6	235.0	0.98*	--	--	1.0	channel
7	146.0	1.5*	--	--	1.0	channel
8	55.0	110.0	6050.0	6442.3	0.085	plane (pumice)
9	96.0	16.0	1536.0	1939.8	0.0625	plane
10	105.0	3.25*	--	--	1.7	channel
11	125.0	10.0	1250.0	1274.3	0.1	plane (pumice)
12	170.0	10.0	1700.0	2194.6	0.035	plane (pumice)
13	105.0	3.25*	--	--	1.7	channel
14	150.0	24.0	3600.0	1798.2	0.035	plane
15	43.0	125.0	5375.0	6470.6	0.08	plane
16	65.0	3.25*	--	--	1.7	channel
17	72.0	22.0	1584.0	849.5	0.055	plane (pumice)
18	63.0	19.0	1197.0	849.5	0.03	plane (pumice)
19	81.0	3.25*	--	--	1.7	channel
20	63.0	12.0	756.0	707.9	0.03	plane (pumice)
21	85.0	9.8	833.0	566.4	0.14	plane
22	65.0	3.25*	--	--	1.7	channel
23	300.0	20.0	6000.0	1911.4	0.06	plane
24	276.0	28.0	7728.0	7929.0	0.0625	plane
25	333.0	2.0*	--	--	1.2	channel
26	120.0	26.0	3120.0	2761.0	0.09	plane
27	110.0	15.0	1650.0	1415.9	0.1	plane
28	100.0	20.0	2000.0	1699.1	0.09	plane
29	30.0	130.0	3900.0	2265.4	0.125	plane
30	24.0	96.0	2304	2320.0	0.1	plane
31	33.0	1.5*	--	--	1.0	channel
32	130.0	24.0	3120.0	1769.9	0.127	plane
33	130.0	12.0	1560.0	1486.7	0.117	plane
34	201.0	22.0	4422.0	4106.1	0.05	plane
35	185.0	23.0	4255.0	4247.7	0.01	plane
36	211.0	1.5*	--	--	1.0	channel
37	185.0	25.0	4625.0	3822.9	0.14	plane
38	120.0	17.0	2040.0	1557.5	0.175	plane
39	144.0	30.0	4320.0	4318.4	0.055	plane
40	136.0	20.0	2720.0	3185.7	0.08	plane
41	146.0	2.0*	--	--	1.4	channel
42	114.0	8.0	912.0	849.5	0.1	plane
Total watershed area:			121457	109375		

\* The 'Width' values for channels represents the channel bottom width.

Table 7. Dimensions of the elements in the 42-element parameter file, both the calculated input for model and the actual area.

estimated from the established soil type. Specific gravity (RHOS) of the soil particles was set at 2.5 due to the fact that they are mainly quartz particles. The K factors were taken from figures in the RUSLE manual according to soil type. (Renard et al., 1991)

The hydraulic characteristics of the watershed can also be either estimated from field data or charts based on soil types. For this study, an initial value of 0.2 in/hr for hydraulic conductivity (FMIN) is taken as the suggested hydraulic conductivity for pinon-juniper woodlands. Porosity (POR) and net capillary drive (G) were estimated from the KINEROS User's Manual table 5 (Woolhiser et al., 1990b). Values were taken from the table for sandy loam since that was found to be the predominant soil type in the watershed. POR was given a value of 0.453 and G was taken to be 5.0 in. Soil moisture conditions (SI) are estimated from field data from similar sites. The information used from other sites include neutron moisture probe measurements and data from a recent pinon-juniper woodland infiltrometer study. For the years 1994 and 1995, the SI values are based on soil moisture data available from a bare area in a nearby pinon-juniper study area. The SI values for the 1993 storms were estimated using the 1994/1995 soil moisture data along with a comparison of rainfall histories. (Table 9) Maximum relative saturation (S<sub>MAX</sub>) is a value ranging from SI and 1.0. In this study it is assumed to be 1.0.

Table 9. Values for relative initial soil saturation (SI).

Storm date	Relative initial soil saturation
July 28, 1993	0.3*
Aug. 20, 1993	0.3*
Aug. 26, 1993	0.2*
Aug. 27, 1993	0.75*
Aug. 28, 1993	0.75*
Sept. 6, 1993	0.3*
Sept. 13, 1993	0.2*
Aug. 2, 1994	0.4
Aug. 21, 1994	0.4
May 29, 1995	0.4
June 29, 1995	0.75
July 18, 1995	0.68
Aug. 13, 1995	0.75

\* denotes estimation

Rainsplash erodibility factors,  $C_r$  and  $C_h$ , are important in controlling the rate at which rainfall energy produces loose, transportable particles from the soil surface.  $C_h$  controls the effect of surface water depth on raindrop detachment, dictating the extent the kinetic energy of the raindrop is absorbed. This value can be calculated by  $2/dr$  (raindrop diameter) and may

be estimated by using an average raindrop diameter of 3mm without having a significant effect on the model. An average value of 7.99 in. is used for  $C_h$ .

$C_r$ , (Eqn. 13), is related to the susceptibility of the soils to erosion.

$$C_r = 422 K_{usle} (\Theta_r) \quad \text{Eqn. 13}$$

$\Theta_r$  is the fraction of the soil left exposed and is derived from a watershed topography study done by Bandelier National Monument ecologists. In their study, three transects across the watershed were characterized by groundcover. Again taking sandy loam to be the predominant soil type,  $C_r$  is calculated to be 32.49 for the Frijolito watershed. (see Table 8)

$C_g$ , the hydraulic erosion coefficient, represents the relative rate of erosion by flowing water when the hydraulic conditions for the selected transport capacity relation indicate a larger transport capacity than the local concentration.  $C_g$  is calculated through the set of equations:

$$C_g = 5.6 K_{usle} \Theta_r / a_T \quad \text{Eqn. 14}$$

$$\text{if } f_{cl} \leq 0.22, a_T = 188 - 468f_{cl} + 907f_{cl}^2 \quad \text{Eqn. 15}$$

$$\text{or } a_T = 130 \text{ if } f_{cl} > 0.22.$$

The KINEROS manual suggests either the Manning law or Chezy law for large watersheds where there are 'considerable distortions introduced by the geometric representation or where surfaces are hydraulically rough.' (Woolhiser et al., 1990b) Specifically, the manual recommends that Manning's law (option 1) be used for KINEROS unless the watershed to be modeled is very small and hydraulically smooth, in which case option 2 (Laminar-Manning) is recommended. The resistance law (LAW) chosen for this study is Manning's law. Manning's  $n$  (R1) is selected from charts available in the KINEROS manual. Classifying the watershed as having loamy soils with intermittent patches of grass and brush, a value of 0.11 is chosen for the planes and 0.01 is chosen for the channels.

### 3. Overall Watershed Parameters

The interception depth (DINTR) is estimated from Table 1 in the KINEROS User's Manual. Table 1 gives a range of values from 0.5 to 1.8 mm. Since there is no accurate description of the Frijolito watershed represented in the table, an estimate is made using the wide range of values given for this parameter along with groundcover information taken from the transect study done by Bandelier National Monument ecologists. Interception depth, though it may be highly significant in the annual water balance, is found to be relatively unimportant for flood-producing storms. (Woolhiser et al., 1990b) The estimate for the Frijolito watershed is 0.01 due to the fact that the soil is mostly bare because of previous extensive cattle grazing in the area.

The infiltration recession factor (RECS) is the local maximum average depth of surface water. The value for this factor was estimated from microtopography measurements taken throughout the year at eight erosion bridges within the watershed. The value of the RECS parameter for the Frijolito watershed is estimated to be 3 mm.

North-central New Mexico experiences a mild climate. The temperature during the summer is generally in the range of 70-75° F and the temperature typically decreases immediately before and during a storm. The temperature variable (TEMP) is given the default value of 65° F.

There is a formula available to calculate the maximum time step allowable (DELT) to effectively run the model. For this study, it is necessary to use the smallest time step possible due to the short-lived, high intensity hydrograph. Therefore, the calculation is not necessary for this test. A time step of one minute is used.

The model also asks for a weighting factor (THETA) for use in finite difference equations where  $0.5 < \text{THETA} \leq 1.0$ . The default value of 0.8 is chosen for this test.

### C. Evaluation Procedure

Complete model testing requires calibration of the model on part of the hydrologic record and evaluating the performance of the calibrated model on the record (Blackie and Eeles, 85). Since KINEROS is used to simulate the major processes that impact soil erosion by water, runoff being one of the more important ones, the storm hydrograph is what was used to calibrate the model. KINEROS was approximately calibrated using the hydrograph

on one summer monsoon storm and then validated against 12 other summer monsoon storms. The complete rainfall hyetographs were not used in running the model in some cases to ease the computational strain. In such cases, only the most intense portion of the storm was modeled. Both runoff and erosion data are used in evaluating the model.

### 1. Parameter Sensitivity

The first step in the evaluation of the model is to determine which parameters are the most sensitive, i.e. which parameters have the most effect on the output. Tests for significance were done on the parameters that had been estimated. Following in the same venue of previous studies, the only parameters that showed significant sensitivity to model output during model calibration were the relative saturated hydraulic conductivity (FMIN) and Manning's n (R1).

Figure 8 demonstrates the resulting effect on the hydrograph when using different saturated hydraulic conductivities. As is clearly shown, the model is very sensitive to the slightest changes in conductivities when the value of FMIN is very small and is not nearly as sensitive when the value of FMIN is larger.

Table 10. Simulated peak outflow and accumulative outflow produced by varying Manning's n for both planes and channels.

	Manning's n	Peak Outflow (CFS)	Accumulative flow (ft <sup>3</sup> )
Planes:	0.05	4.55	2631
	0.1	1.53	1240
	0.2	0.23	425
Channels:	0.01	1.63	1376
	0.02	1.60	1376
	0.03	1.55	1376
	0.035	1.52	1375
	0.04	1.50	1375

Increasing Manning's n also produced significant results in the peak of the hydrograph. Table 10 summarizes data concerning the peak outflow and accumulative flow produced when incrementally increasing Manning's n. An important point to be made is that changing Manning's n for the channel did not have any affect on the accumulative flume



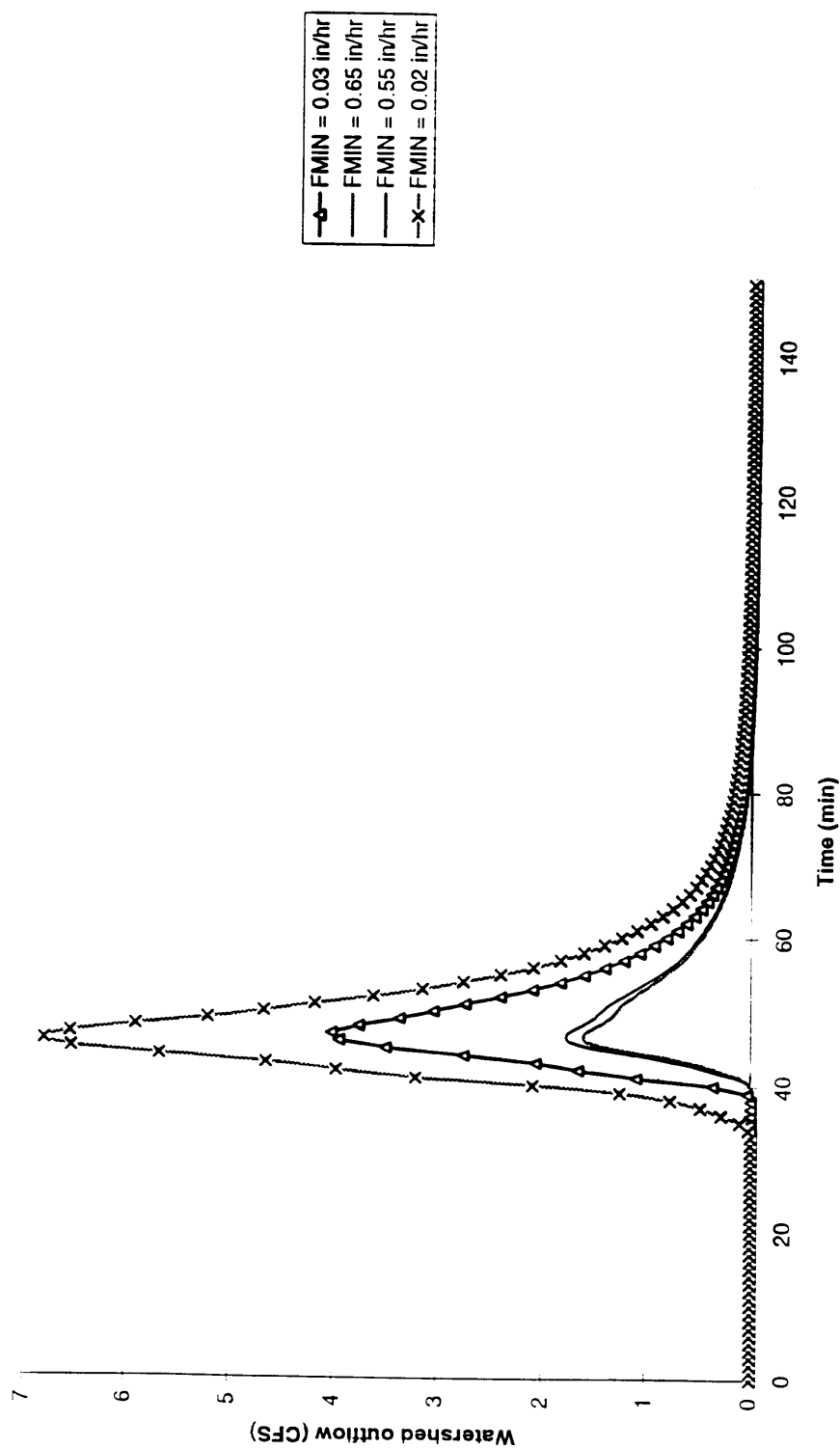


Figure 8. Comparison of different saturated hydraulic conductivities:  
September 6, 1993 simulated hydrographs.

flow produced by the model, only when adjusting Manning's  $n$  for the planes is this an issue.

Due to the uncertainty in the validity of the necessary extrapolation over time and space in estimated the initial soil saturation data, an analysis was also done on the sensitivity of this parameter as well. Based on soil characteristics, an initial estimate of SI for the Frijolito watershed was 0.2. This value was tested against the values for SI extrapolated from the soil saturation data from the nearby site. The results from a subset of the storms are found in Table 11. When the initial soil saturation of 0.2 was used, the model generally underpredicted the runoff. This trend is more visible when using a higher  $K_{sat}$ . When using  $K_{sat} = 0.2$ , the  $r^2$  increased from 0.66 to 0.80 when the extrapolated SI data were used and when using  $K_{sat} = 0.55$ , the  $r^2$  jumped from 0.80 to 0.89.

Table 11. Summary of data testing the significance of initial soil saturation (SI).

Peak flume flow (CFS)					
Storm Date	$K_{sat} = 0.2$ in/hr		$K_{sat} = 0.55$ in/hr		Observed peak
	SI = 0.2	SI variable	SI = 0.2	SI variable	
7/29/93	4.2	3.65	1.6	1.94	1.52
8/20/93	0	0	0	0	0.27
8/26/93	0.01	0.01	0	0	0.48
8/27/93	3.34	4.49	0.71	3.21	2.95
8/28/93	0	0	0	0	0.34
9/6/93	3.79	3.37	1.56	1.76	1.58
9/13/93	0	0	0	0	0.33
8/2/94	0	0	0	0	1.03
8/21/94	0	0.01	0	0	1.27
7/18/95	0.56	0.47	0	0	0.42
8/13/95	0.06	0.7	0	1.52	0.91
5/29/95	1.56	2.51	0.21	0.91	2.39

## 2. Calibration

At this point, the approach taken was to calibrate the hydrograph the model produced to the real data produced by the flume. Three characteristics of the hydrograph were examined during calibration of the hydrograph, time to peak flow, peak flow and accumulative flow. Time to peak flow was quickly found to be predicted accurately under all conditions tested so it was not continued to be used to calibrate the model. Accumulative flow was not used as the target in calibrating the model because that measurement was thought to be not reliable due to possible clogging of the flume during the recession of the hydrograph. The

hydrographs the flume produced were “corrected” to assume the fit of an expected hydrograph. Figure 9 shows an example of an original hydrograph and the “corrected” version of the same hydrograph. The integrity of the peak flume flow measurements is assumed to be preserved. The resultant decision was to calibrate the model to the peak flow of the hydrograph while fitting the model output as much as possible to the corrected flume hydrograph tail.

Initially, different hydraulic conductivities were tested in an attempt to reach a best fit without adjusting Manning’s  $n$ . The final suggested saturated hydraulic conductivity (0.55 in/hr) was reached when the resultant hydrograph produced a best fit for the September 6, 1993 storm. The storm hyetograph and hydrograph are shown in Fig. 10. This storm is chosen for the calibration because the hydrograph produced by KINEROS fit the storm hydrograph peak and had a tail that fit much better than the original data. (Fig. 11)

This hydraulic conductivity did not work well for all storms, however. There is a class of storms that characteristically exhibits smaller peaks (i.e. peak flow < 1.5 CFS) in which the model, when using a saturated hydraulic conductivity of 0.55 in/hr, calculated total infiltration of the runoff. The hydraulic conductivity was then adjusted to fit just this class of storms. There was not any one storm that seemed to work extremely well with any specific hydraulic conductivity tested so a hydraulic conductivity was chosen to represent the minimum variability among the small, less intense storms. The resultant hydraulic conductivity was 0.03 in/hr.

Manning’s  $n$  was also varied in an attempt to reach a best fit with the September 6, 1993 storm. First, the Manning’s  $n$  for the planes was modified in conjunction with decreasing the hydraulic conductivity in an attempt to more accurately model the accumulative flow. This resulted in raising the predicted peak flow. To remedy this, the next thing done was to vary Manning’s  $n$  for the channels. The Manning’s  $n$  for the channels was increased to bring the predicted peak flow back down to the observed peak flow. The resultant Manning’s  $n$  were 0.11 for the planes and 0.035 for the channels. This change in Manning’s  $n$  produced a statistically insignificant change in peak flow, but it did improve model prediction. The results of this modification are presented in Figure 12.

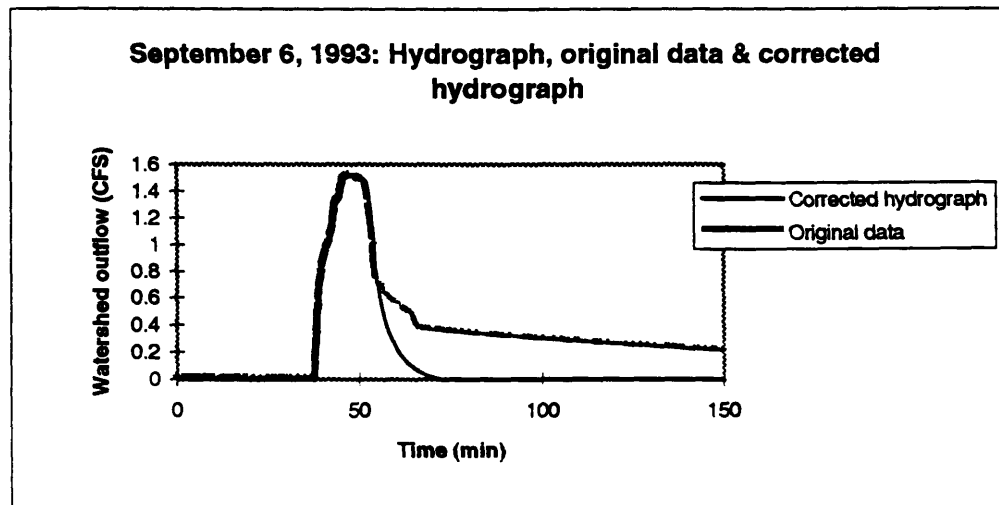
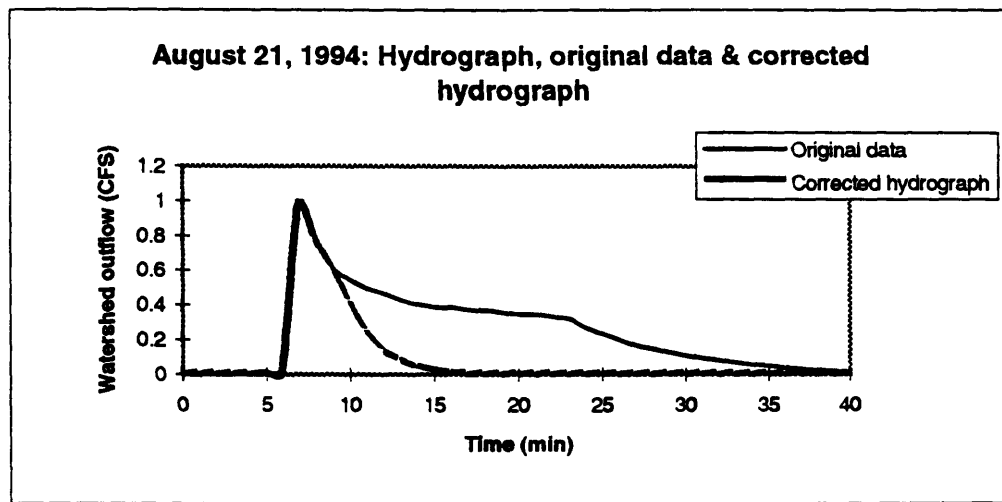


Figure 9. Examples of “correcting” the artificially high tail of the hydrographs produced during actual events.

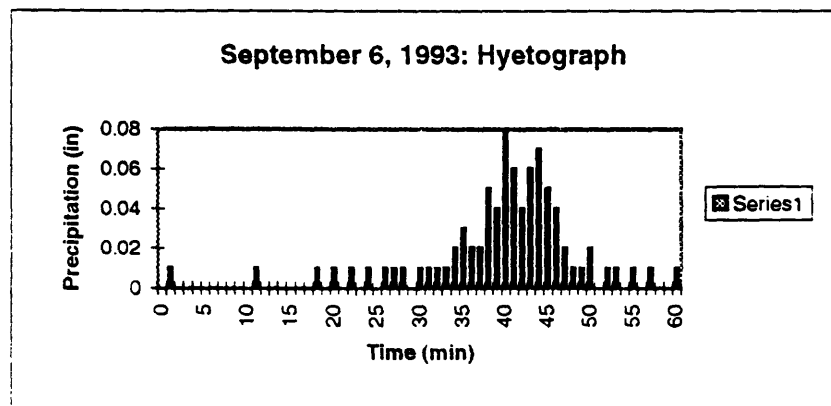
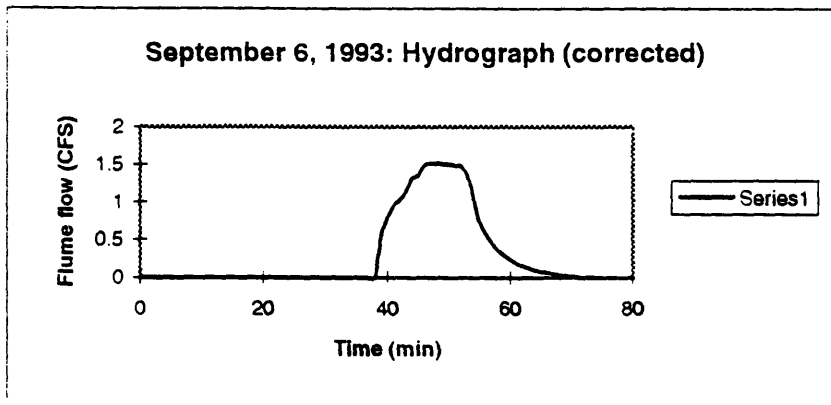


Figure 10. September 6, 1993 storm hydrograph and hyetograph.

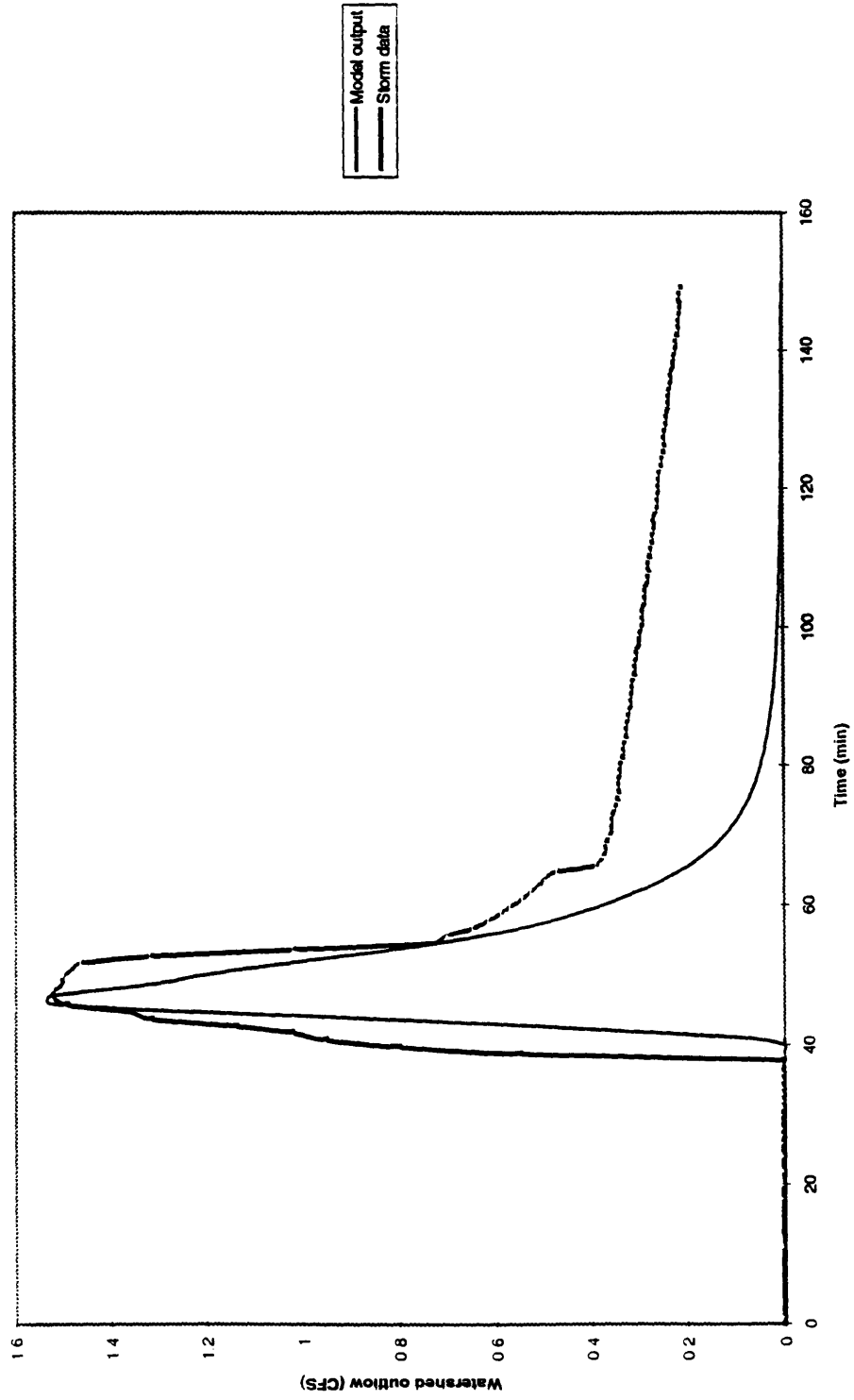


Figure 11. September 6, 1993 simulated and observed peak watershed outflow.

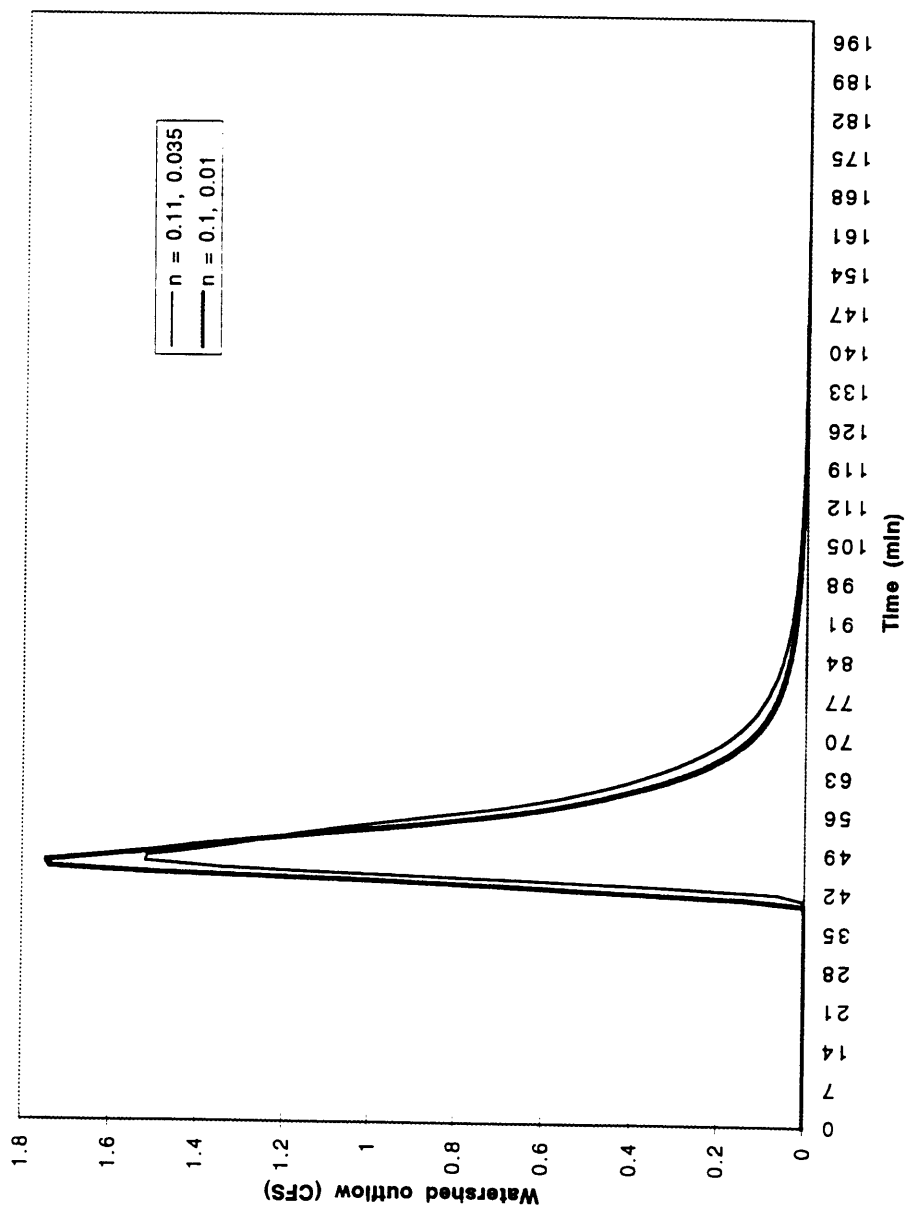


Figure 12. Results of the calibration of Manning's n for both planes and channels - September 6, 1993 storm.

### 3. Erosion Evaluation

This study also does a comparison of three of the six transport relationships available for calculating erosion in KINEROS, namely those relationships attributed to Yalin (1963), Ackers and White (1973) and Engelund and Hansen (1967). These transport relationships estimate transport capacity as a function of particle size, specific gravity, and water viscosity. The manual recommends some limitations in the use of these erosion laws per studies done by the authors. Yalin is shown to give high results in analysis done by the authors of the model, yet it has been the favored relationship of others. (Foster and Meyer, 1972) Ackers and White is recommended only for particles greater than 0.04 mm. Engelund and Hansen has been shown to be relatively accurate for a useful range of particles sizes and hydraulic conditions. The equations for each of these transport relationships are in the Appendix C.

Two of the methods not chosen were dismissed because they would have been dependent on estimations of additional parameters for which the information is not available for the Frijolito watershed. The other method not chosen was not considered due to the fact that it had not been validated for the mean particle diameter that is represented in the Frijolito watershed.

The resultant erosion produced by the model using each of the relationships was tested against the erosion data collected from the actual events.

## VI. RESULTS

### A. Hydrologic response

Examination of the hydrographs produced by the flume identified a problem with the runoff data collected. The flume was discovered to often not give a correct picture of the tail of the hydrograph for the storms modeled in this test. The flume sometimes became clogged or semi-blocked and would give a false picture of a longer, larger tail than what actually occurred, thereby giving a much higher volume than what actually flowed through the flume. Peak flow is not thought to be affected by this because the high flow rates would



hydrograph that sediments would settle in the flume. Also, sediments built up at the outflow of the pipe might cause a small amount of runoff to sit in the bottom of the flume for some time after runoff has stopped flowing. This also would result in the production of a hydrograph with an artificially high tail.

The calibration and testing of KINEROS was done using the 42-element parameter file rather than the 8-element parameter file due to the superior representation of the channel network. This decision was based on the concentration of channels in the watershed and the potential importance of channel processes in the resulting hydrograph. (Lane, 1982) A watershed with a high channel density will usually have a fast response to water runoff and a rapid, more complete transport of sediment from the area. (Onstad et al., 1977) Subject to the same conditions, neither parameter file performed consistently better than the other when comparing both peak watershed outflow and accumulative outflow to storm data. The most notable difference was that the 42-element file consistently estimated more runoff. Figures 13 and 14 graphically show the differences in results concerning peak flow and accumulative flow from using the 42-element file versus the 8-element file with both the hydraulic conductivities of 0.03 in/hr and 0.55 in/hr. Figure 15 depicts the difference in the average storm computed peak flow and accumulative flow using the two different conductivities with the parameter files.

Evaluation of the model results using the two sets of Manning's  $n$  data revealed that the suggested increase did not improve the accuracy of the overall model's predicted peak flow and did not increase the model's accuracy in predicting accumulative flume flow. Peak outflow and accumulative outflow produced by the model using the original estimation of Manning's  $n$  ( $n = 0.1, 0.01$ ) used with a hydraulic conductivity of 0.55 in/hr and the calibrated Manning's  $n$  ( $n = 0.11, 0.035$ ) used with a hydraulic conductivity of 0.5 in/hr are shown in Table 12.

Even though the adjusted parameters produced a better fit for the September 6, 1993 storm (see Figure 12), the subset of storms analyzed in Table 12 did not show an increase in the efficiency of the model. In most cases, the modified Manning's  $n$  and hydraulic conductivity did worse than the original estimates of the parameters in predicting peak flow. Accumulative flow was predicted better but not by a factor greater than the confidence limits put on the storm data. Due to the small adjustments that were actually made from the original estimations of Manning's  $n$  and the insignificance of these changes

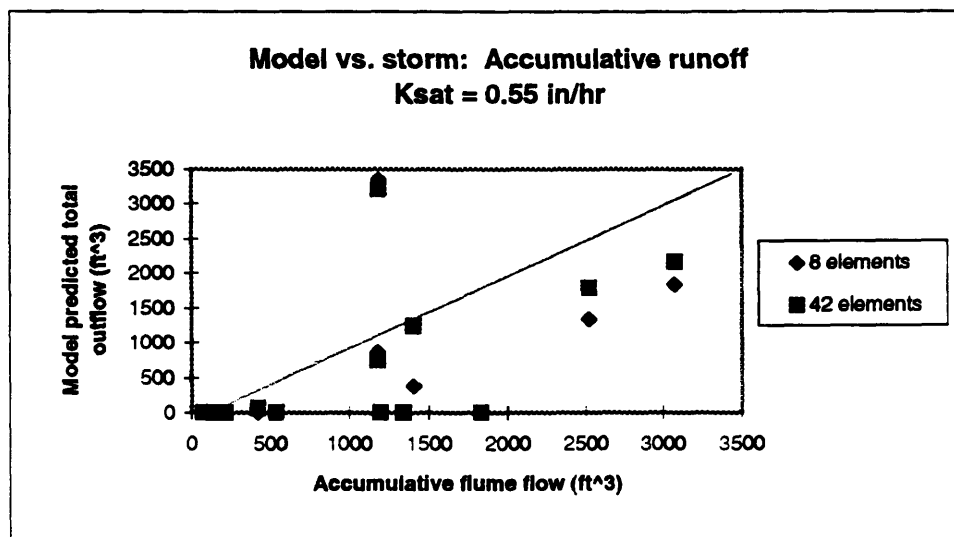
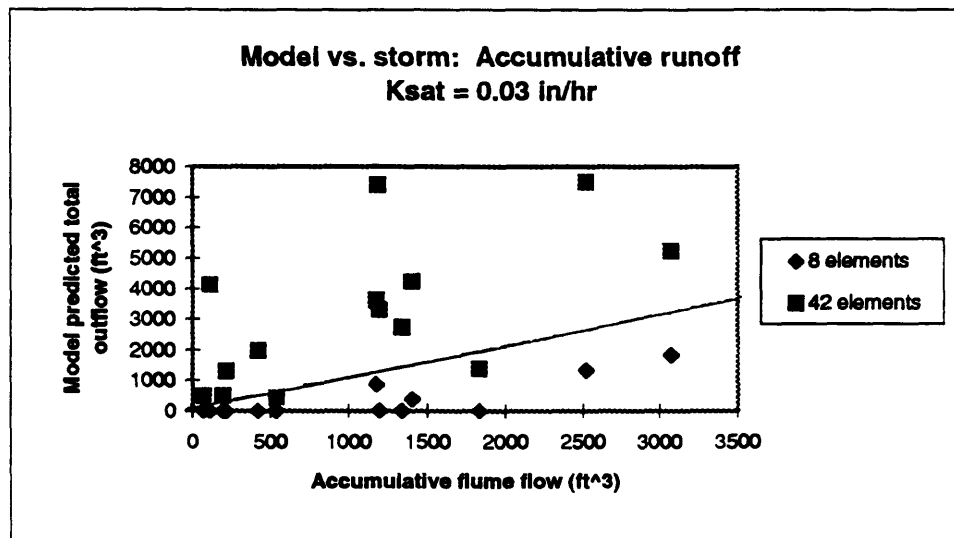


Figure 13. Simulated versus observed accumulative watershed outflow, data for 8- and 42-element parameter files.

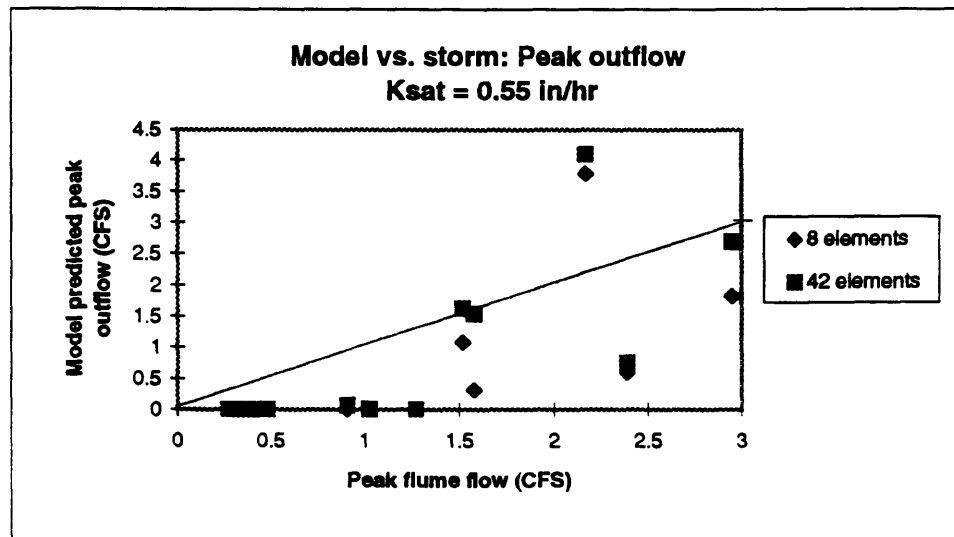
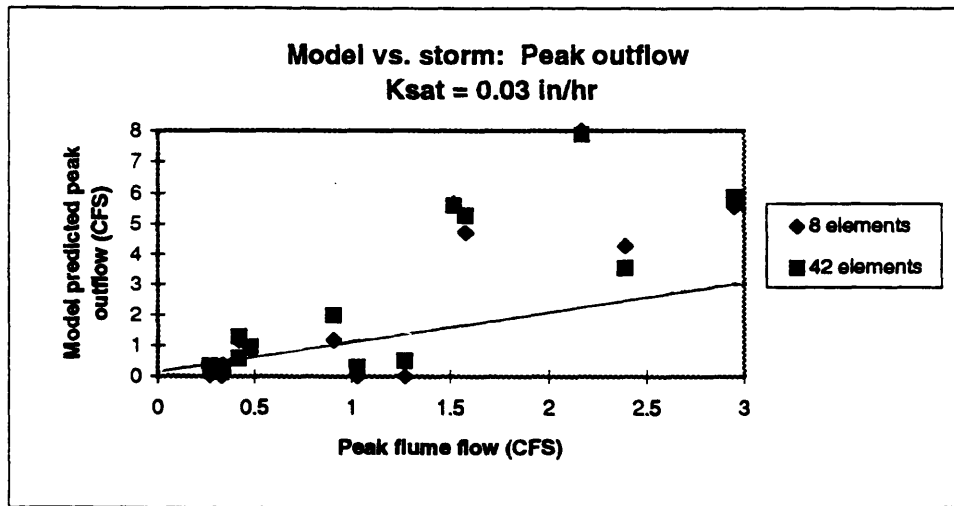


Figure 14. Simulated versus observed peak watershed outflow, data for 8- and 42-element parameter files.

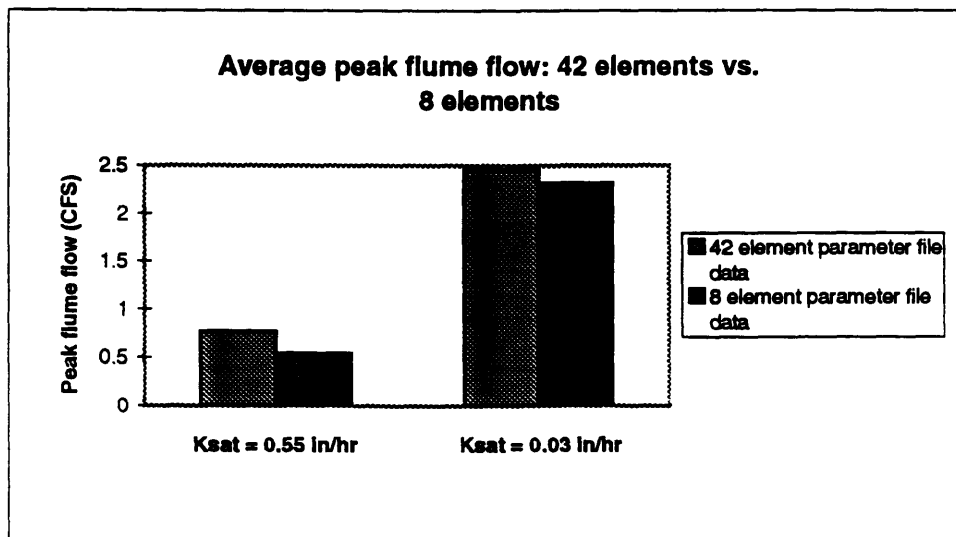
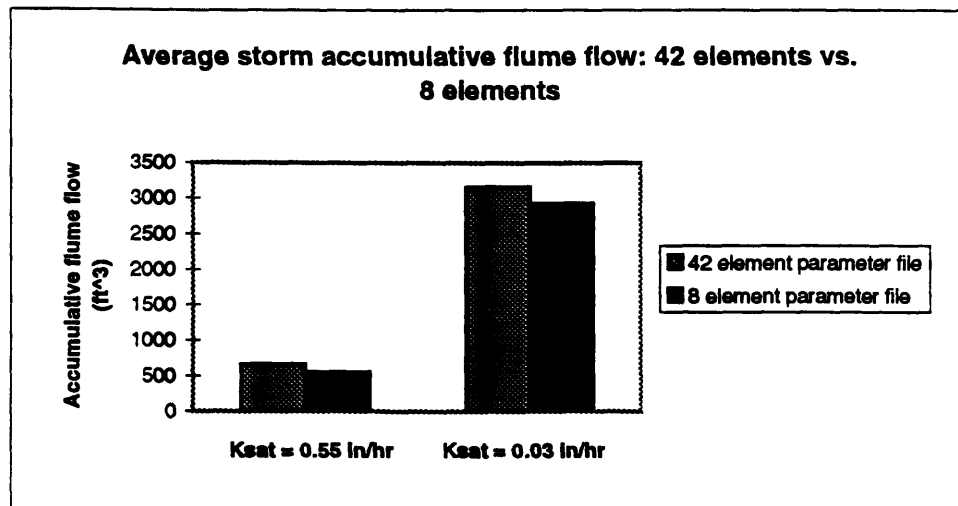


Figure 15. Average accumulative and peak flume flow for the complete set of storms, data for 8- and 42-element parameter files.

when examining the complete set of storms, no further analysis was done and the original estimates for Manning's  $n$  were used for the rest of the study.

Table 12. Peak outflow and accumulative outflow from the watershed predicted by the model using the initial estimates of Manning's  $n$  (0.1, 0.01) with a hydraulic conductivity of 0.55 in/hr and the calibrated Manning's  $n$  (0.11, 0.035) with a hydraulic conductivity of 0.5 in/hr and the observed data.

Storm Date	Peak Watershed Outflow (CFS)			Accumulative Watershed Outflow (ft <sup>3</sup> )		
	$n = 0.1,$ 0.01	$n = 0.11,$ 0.035	Observed	$n = 0.1,$ 0.01	$n = 0.11,$ 0.035	Observed
7/28/93	1.62	1.77	1.52	1778	2056	2520
8/27/93	2.69	2.63	2.95	2162	2310	3076
9/6/93	1.53	1.52	1.58	1240	1375	1402
5/29/95	0.74	0.81	2.39	748	881	1829
8/13/95	0.06	0.06	0.91	65	99	422

Three different scenarios were run on the complete suite of storm data for the 13 storms. The first run was done using the original estimate of saturated hydraulic conductivity for the watershed ( $F_{MIN} = 0.2$  in/hr.) The second run was done using the calibrated  $F_{MIN}$  of 0.55 in/hr. The third run used the  $F_{MIN}$  of 0.03 in/hr calibrated for the small, less intense storms. A comparison of predicted and observed runoff for each of the thirteen storms for each  $F_{MIN}$  tested is given in Appendix D.

The characteristics of the hydrograph analyzed in each situation to determine the viability of the chosen parameters were time to peak flow, peak flume flow and accumulative watershed outflow. Tables 13, 14 and 15 summarize the results of these characteristics for each run. Figures 16, 17 and 18 show the correlation of the predicted time to peak, peak flume flow and accumulative outflow with the observed data. The time to peak predicted by the model was right on target for the majority of the simulations. Changing the hydraulic conductivity to fit the height of the peak and the volume of flow affected this result very little. The other two characteristics of the hydrograph, peak flow and accumulative flow, did not produce as good a fit with storm data. Peak flow and accumulative flow were both heavily dependent on the final estimate of hydraulic conductivity. In general, an increase in the estimate of hydraulic conductivity was readily associated with a decrease in runoff. Runoff generated using a file with  $F_{MIN} = 0.03$

Time to peak. (min.)							
Storm date	K <sub>sat</sub> = 0.03 in/hr, x = 42 <sup>a</sup>	K <sub>sat</sub> = 0.2 in/hr, x = 42	K <sub>sat</sub> = 0.55 in/hr, x = 42	K <sub>sat</sub> = 0.03 in/hr, x = 8	K <sub>sat</sub> = 0.2 in/hr, x = 8	K <sub>sat</sub> = 0.55 in/hr, x = 8	Observed peak
29-Jul-93	28	31	33	30	33	37	28
20-Aug-93	35	n/a <sup>b</sup>	n/a	94	n/a	n/a	36
26-Aug-93	39	n/a	n/a	48	n/a	n/a	39
27-Aug-93	14	15	16	16	17	18	10
28-Aug-93	186	n/a	n/a	194	n/a	n/a	215
6-Sep-93	46	47	47	48	48	49	48
13-Sep-93	9	n/a	n/a	n/a	n/a	n/a	9
2-Aug-94	11	n/a	n/a	24	n/a	n/a	13
21-Aug-94	7	13	n/a	16	n/a	n/a	7
29-May-95	72	73	73	74	75	76	73
29-Jun-95	128	129	130	129	130	133	126
18-Jul-95	212	218	n/a	218	220	n/a	184
13-Aug-95	22	22	22	25	25	47	22

a. 'x' refers to the number of elements in the paramter file.

b. 'n/a' is used when the model did not produce runoff.

Table 9. Summary of the predicted and observed time to peak.

Peak watershed outflow. (CFS)							
Storm date	K <sub>sat</sub> = 0.03 in/hr, x = 42 <sup>a</sup>	K <sub>sat</sub> = 0.2 in/hr, x = 42	K <sub>sat</sub> = 0.55 in/hr, x = 42	K <sub>sat</sub> = 0.03 in/hr, x = 8	K <sub>sat</sub> = 0.2 in/hr, x = 8	K <sub>sat</sub> = 0.55 in/hr, x = 8	Observed peak
29-Jul-93	5.59	3.65	1.62	5.65	3.64	1.08	1.52
20-Aug-93	0.33	n/a <sup>b</sup>	n/a	0.03	n/a	n/a	0.27
26-Aug-93	0.94	0.01	n/a	0.88	n/a	n/a	0.48
27-Aug-93	5.87	4.49	2.69	5.56	3.75	1.82	2.95
28-Aug-93	0.28	n/a	n/a	0.36	n/a	n/a	0.34
6-Sep-93	5.26	3.37	1.53	4.7	1.93	0.31	1.58
13-Sep-93	0.13	n/a	n/a	n/a	n/a	n/a	0.33
2-Aug-94	0.29	n/a	n/a	<0.01	n/a	n/a	1.03
21-Aug-94	0.5	0.01	n/a	0.01	n/a	n/a	1.27
29-May-95	3.54	2.51	0.74	4.27	1.73	0.59	2.39
29-Jun-95	7.88	6.3	4.1	8.0	6.17	3.79	2.17
18-Jul-95	0.59	0.47	n/a	1.13	0.38	n/a	0.42
13-Aug-95	1.96	0.7	0.06	1.17	0.21	<0.01	0.91

a. 'x' refers to the number of elements in the paramter file used.

b. 'n/a' is used when the model did not produce runoff.

Table 10. Summary of the predicted and observed peak watershed outflow.

Accumulative watershed outflow. (ft <sup>3</sup> )							
Storm date	K <sub>sat</sub> = 0.03 in/hr, x = 42 <sup>a</sup>	K <sub>sat</sub> = 0.2 in/hr, x = 42	K <sub>sat</sub> = 0.55 in/hr, x = 42	K <sub>sat</sub> = 0.03 in/hr, x = 8	K <sub>sat</sub> = 0.2 in/hr, x = 8	K <sub>sat</sub> = 0.55 in/hr, x = 8	Observed peak
29-Jul-93	7486	4545	1778	7839	4635	1332	2520
20-Aug-93	476	n/a <sup>b</sup>	n/a	176	n/a	n/a	73.5
26-Aug-93	2722	35	n/a	2530	n/a	n/a	1341
27-Aug-93	5224	3649	2162	5173	3431	1828	3076
28-Aug-93	1384	n/a	n/a	1099	n/a	n/a	1831
6-Sep-93	4216	2555	1240	4234	1994	378	1402.6
13-Sep-93	4114	n/a	n/a	n/a	n/a	n/a	113.7
2-Aug-94	450	n/a	n/a	29	n/a	n/a	536
21-Aug-94	506	17	n/a	24	na/	n/a	196.6
29-May-95	3614	2120	748	6803	1978	856	1829
29-Jun-95	7395	5002	3206	7872	5487	3345	1187
18-Jul-95	3299	740	n/a	2721	794	n/a	1196
13-Aug-95	1983	782	65	1543	422	2	422.2

a. 'x' refers to the number of elements in the paramter file.

b. 'n/a' is used when the model did not produce runoff.

Table 11. Summary of the predicted and observed accumulative watershed outflow.

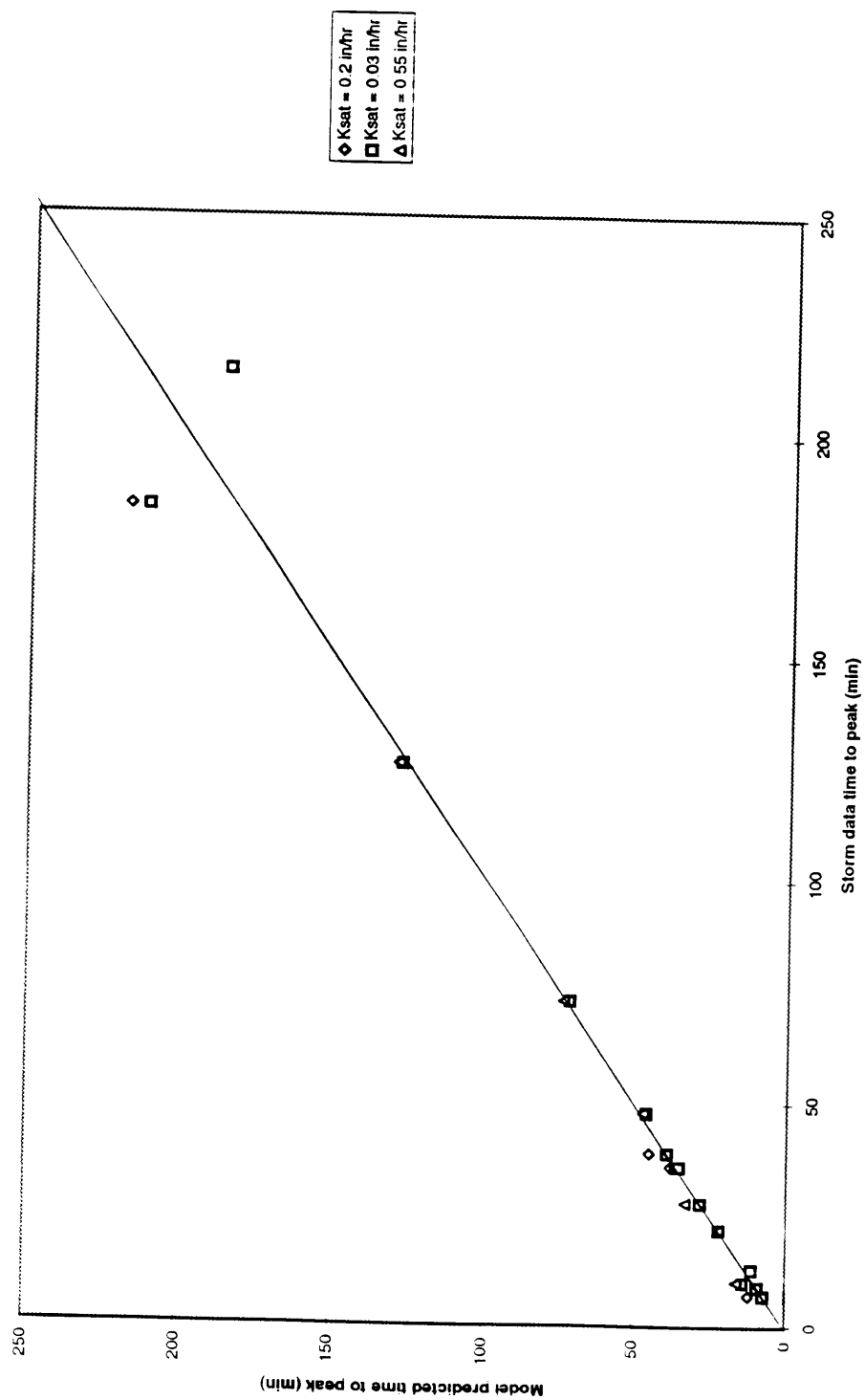


Figure 16. Simulated versus observed time to peak.



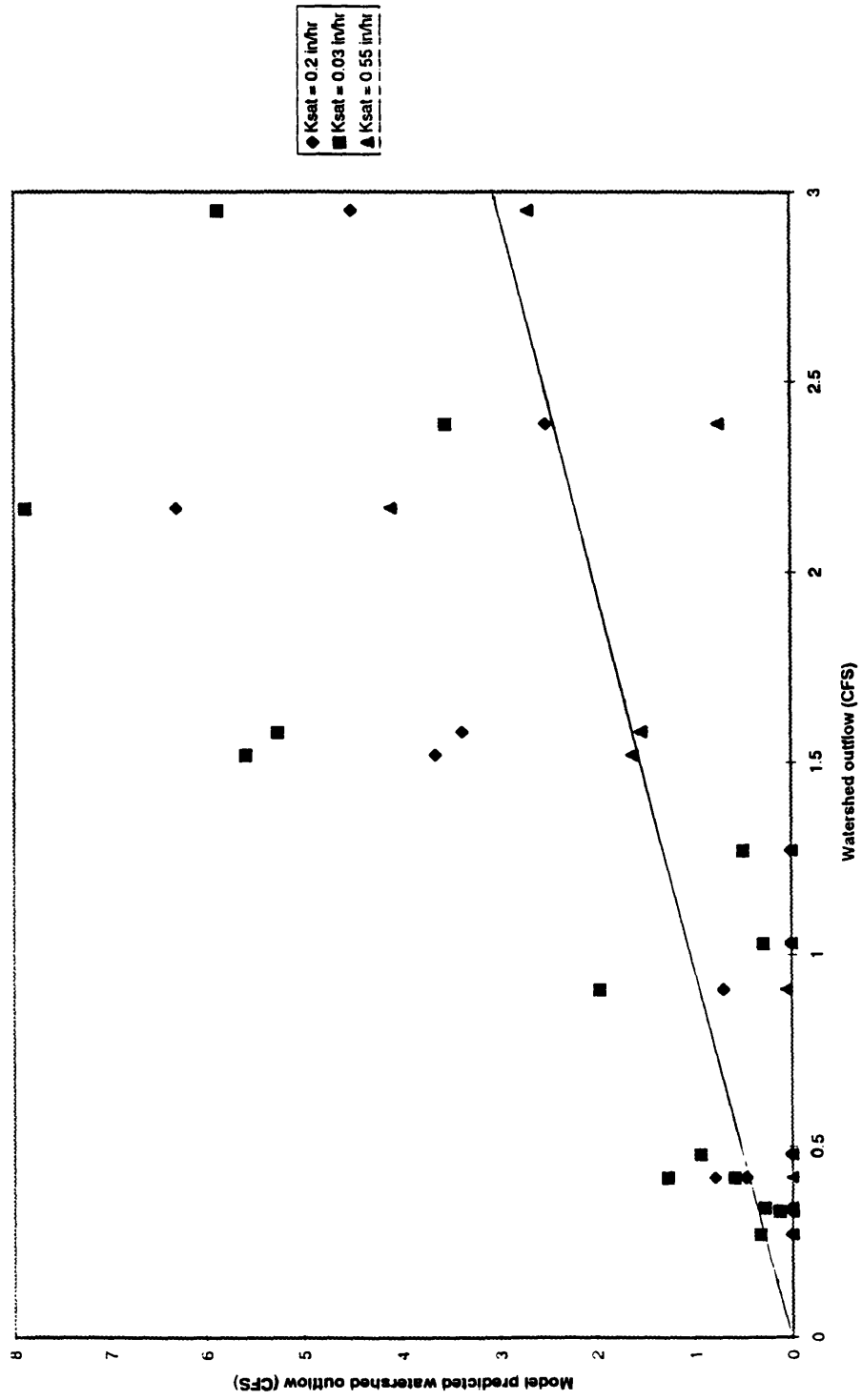


Figure 17. Simulated versus observed peak watershed outflow.

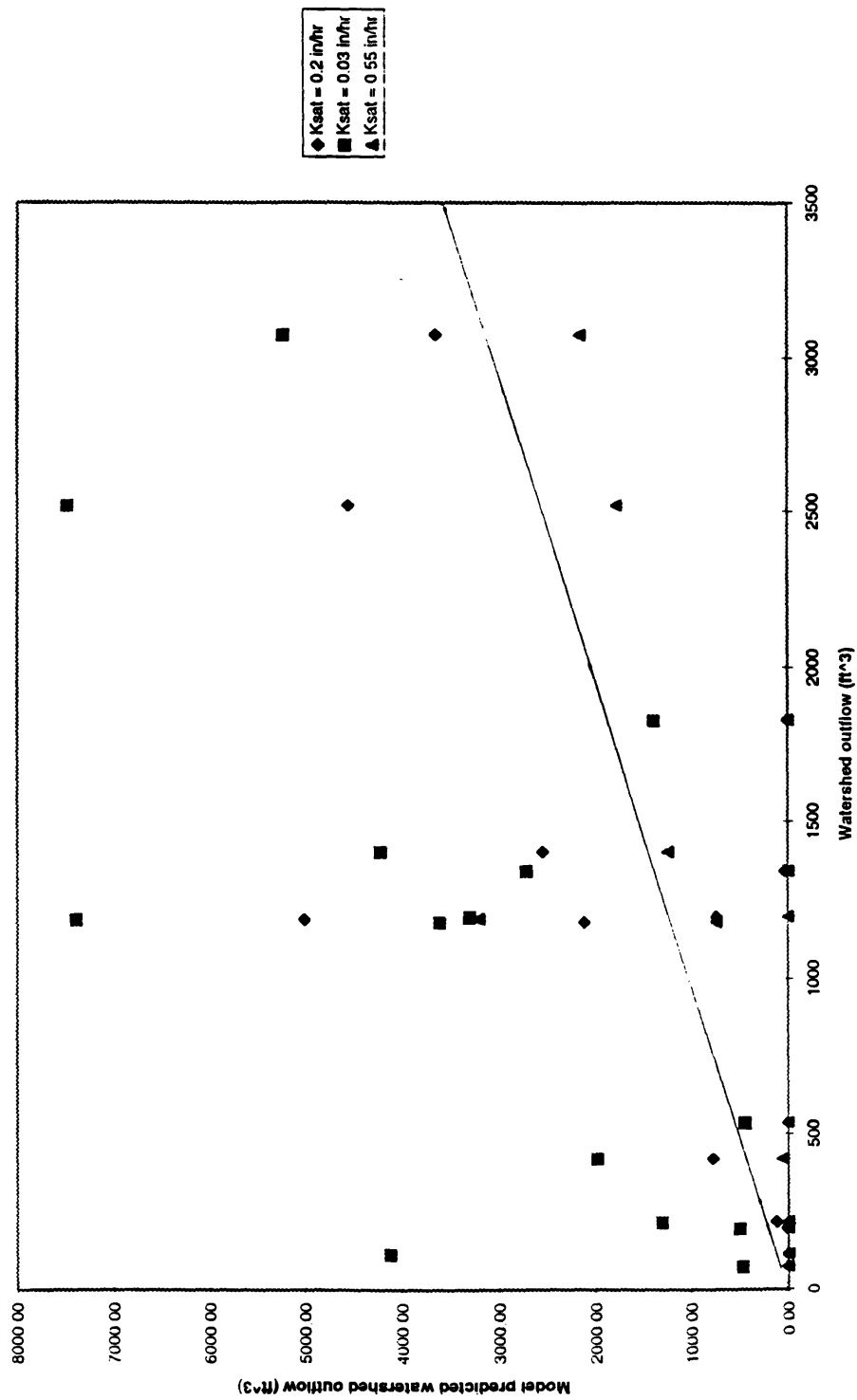


Figure 18. Simulated versus observed accumulative watershed outflow.

in/hr was always greater than when using  $F_{MIN} = 0.2$  in/hr, which, in turn, always produced more runoff than when  $F_{MIN} = 0.55$  in/hr was used.

## B. Erosion Response

Table 16 summarizes the erosion data produced by KINEROS using each of the three erosion laws with the recommended relative saturated hydraulic conductivity ( $F_{MIN} = 0.55$  in/hr) and using a slightly smaller conductivity (0.5 in/hr.) Law 4 (Ackers and White, 1973) and Law 6 (Engelund and Hansen, 1967) drastically underestimated the erosion. Law 5 (Yalin, 1963) predicted the erosion within one order of magnitude.

The data show that erosion is also extremely sensitive to the user's choice of relative saturated hydraulic conductivity. Decreasing  $F_{MIN}$  from 0.55 in/hr to 0.5 in/hr greatly increased the amount of sediment eroded. In some cases erosion doubled, while in other cases the predicted erosion more than quadrupled.

The erosion data for each channel segment outflow point within the watershed also showed trends that the different erosion laws followed. Laws 4 and 6, though they gave similar end results, did not produce erosion in the same manner. The erosion produced in Law 4 was almost completely due to erosion occurring in the channels, almost no erosion occurred on the planes. Law 6, on the other hand, did produce erosion from the planes. The amount of erosion from the planes was less than the erosion from the channels, but it was still on the order of 25 - 30% of the erosion produced by the channels. Law 5 produced erosion from planes and channels of the same order of magnitude.

## C. Model Assessment

Model performance was evaluated using the Nash and Sutcliffe (1970) efficiency criterion (E) along with an  $r^2$  analysis. The coefficient of efficiency was selected for model evaluation because it is dimensionless and easily interpreted. If the model predicts observed runoff with perfection,  $E = 1$ . If  $E < 0$ , the models predictive power is worse than simply taking the average of observed runoff. E is computed by

$$E = 1 - [\sum (Y_{obs} - Y_{pred})^2 / \sum (Y_{obs} - Y_{mean})^2] \quad \text{Eqn. 16}$$

Total Erosion (lbs.) (FMIN = 0.5 in/hr)				
Storm Date	Law 4	Law 5	Law 6	Actual Data
July 28, 1993	154.9	8083	104.1	*
August 27, 1993	183.2	8280	135.8	*
Sept 6, 1993	103.3	5523	66.7	*
May 29, 1995	59.3	4050	34.5	1178
June 29, 1995	276.8	10907	230	3600
August 13, 1995	1.7	605	1.5	671

Total Erosion (lbs.) (FMIN = 0.55 in/hr)				
Storm Date	Law 4	Law 5	Law 6	Actual Data
July 28, 1993	607.7	2019	62.8	*
August 27, 1993	753.4	2439	92.5	*
Sept 6, 1993	427.7	1467	42.9	*
May 29, 1995	24.7	922	20.5	1178
June 29, 1995	1115.9	3400	160	3600
August 13, 1995	9.3	44.3	0.8	671

\*Erosion data was not yet being collected at the time of the event.

Table 16. Total erosion produced by the model when using two different saturated hydraulic conductivities (FMIN = 0.5 and 0.55 in/hr) and the total observed erosion during each storm.

where  $Y_{obs}$  is the observed runoff,  $Y_{pred}$  is model predicted runoff, and  $Y_{mean}$  is the mean of the observed runoff.

$R^2$  is computed by squaring the “r” calculated by

$$r = \Sigma Y_{obs} Y_{pred} / [ (\Sigma Y_{pred}^2) (\Sigma Y_{obs}^2) ]^{1/2} \quad \text{Eqn. 17}$$

The model was evaluated with respect to three elements of the hydrograph. These were time to peak, peak flow and accumulative flow.

Calculations of E and  $r^2$  were done for each hydraulic conductivity tested using all of the storms. The same calculations were also made for distinctive subsets of the group of storms: short duration, long duration, low intensity and high intensity storms. Figures 19 (a) and (b) graph the complete set of storms according to duration and intensity, respectively. The cutoff for the subset of short duration storms was 30 min. The subset of low intensity storms included the storms with peak rainfall intensity equal to or less than 0.04 in/hr. The results of the  $r^2$  analysis done on the complete set of storms are given in Table 17 and the E and  $r^2$  calculations for the subsets of the storms are given in Tables 18 and 19.

The model was right on target for time to peak of the hydrograph for all categories of storms for each hydraulic conductivity with an average  $r^2$  of 0.98. Figure 16 demonstrated the high correlation between observed and simulated time to peak.

The peak flow and accumulative flow data do not give such a good fit, however, and a more complex analysis of the data is required. The  $r^2$  for peak flow ranged from 0.69 to 0.82 and the  $r^2$  for accumulative flow ranged from 0.69 to 0.84.

The coefficient of efficiency (E) data showed a number of trends. The high negative numbers for the run with FMIN set at 0.03 in/hr indicate that the model does not predict well the small, weak storms targeted with this estimate of conductivity. Even analyzing only the short storms and the less intense storms separately, E calculations still produced negative numbers. This goes along with the fact that the relatively large amount of runoff

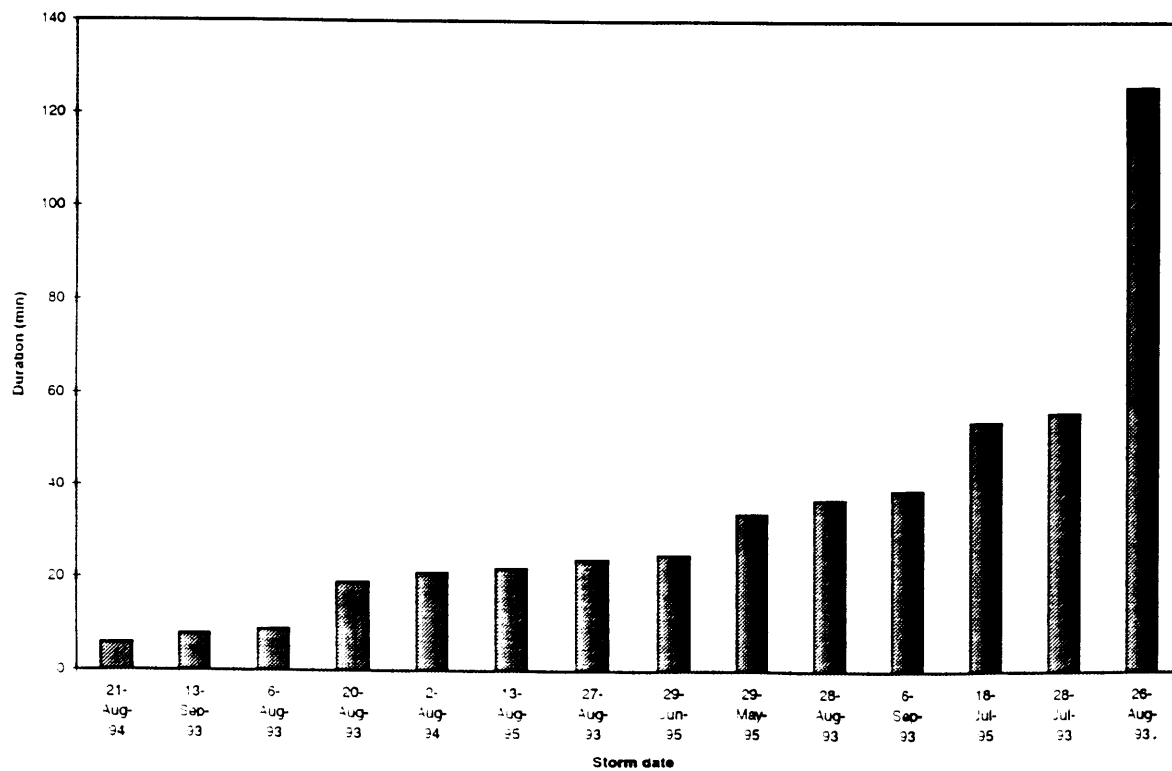
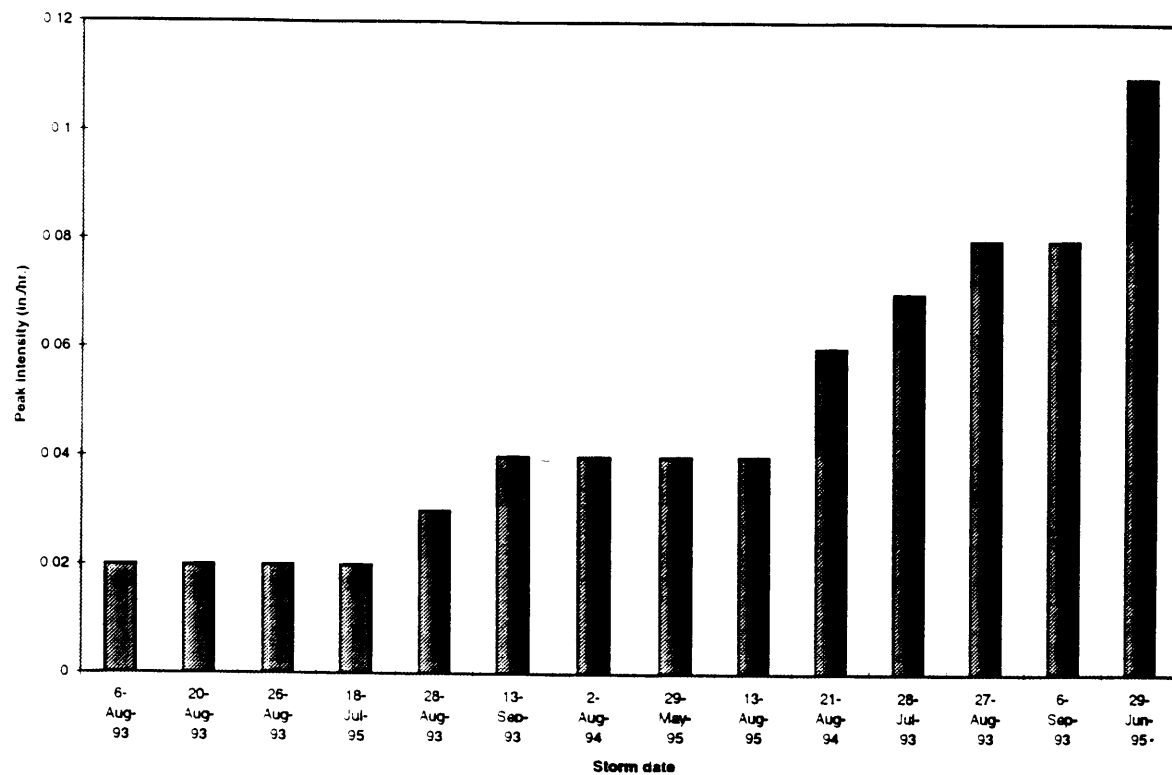


Figure 19. Storms graphed by (a) peak rainfall intensity and (b) length of rainfall.

$K_{sat}$	$t_{pk}$	$r^2$	
		$Q_p$	$Q_t$
0.03	0.98	0.82	0.78
0.2	0.98	0.79	0.73
0.31	0.98	0.75	0.72
0.5	0.98	0.73	0.72
0.55	0.98	0.71	0.72
0.03, x=8	0.94	0.80	0.84
0.2, x=8	0.98	0.73	0.73
0.55, x=8	0.96	0.69	0.69

Table 17. Correlation coefficient squared ( $r^2$ ) for event data time to peak ( $t_{pk}$ ), peak flow ( $Q_p$ ) and volume ( $Q_t$ ) for all storms with the model's predictions using the corresponding hydraulic conductivity ( $K_{sat}$ ).

a. $r^2$ - observed vs. predicted peak flume flow					
Storm subset	$K_{sat} = 0.03$ in/hr	$K_{sat} = 0.2$ in/hr	$K_{sat} = 0.31$ in/hr	$K_{sat} = 0.5$ in/hr	$K_{sat} = 0.55$ in/hr
all	<b>0.82</b>	<b>0.79</b>	<b>0.75</b>	0.73	0.71
short duration	<b>0.84</b>	<b>0.76</b>	0.73	0.70	0.70
long duration	<b>0.85</b>	<b>0.85</b>	<b>0.80</b>	<b>0.75</b>	<b>0.73</b>
low intensity	<b>0.87</b>	<b>0.79</b>	<b>0.77</b>	0.71	0.71
high intensity	<b>0.85</b>	<b>0.86</b>	<b>0.86</b>	<b>0.89</b>	<b>0.89</b>

b. $r^2$ - observed vs. predicted accumulative flume flow					
Storm subset	$K_{sat} = 0.03$ in/hr	$K_{sat} = 0.2$ in/hr	$K_{sat} = 0.31$ in/hr	$K_{sat} = 0.5$ in/hr	$K_{sat} = 0.55$ in/hr
all	<b>0.78</b>	0.73	0.72	0.72	0.72
short duration	0.64	<b>0.93</b>	<b>0.93</b>	<b>0.92</b>	<b>0.92</b>
long duration	<b>0.88</b>	0.65	0.62	0.60	0.59
low intensity	0.55	0.30	0.24	0.17	0.17
high intensity	<b>0.92</b>	<b>0.94</b>	<b>0.95</b>	<b>0.97</b>	<b>0.97</b>

Table 18.  $r^2$  data of observed versus predicted (a) peak flume flow and (b) accumulative flume flow for different saturated hydraulic conductivities tested.  $r^2$  analysis was done on varying subsets of the complete set of storm that were differentiated by storm characteristics.



a. E - observed vs. predicted peak flume flow					
Storm subset	$K_{sat} = 0.03$ in/hr	$K_{sat} = 0.2$ in/hr	$K_{sat} = 0.31$ in/hr	$K_{sat} = 0.5$ in/hr	$K_{sat} = 0.55$ in/hr
all	-3.96	-0.54	-0.04	<b>0.26</b>	<b>0.19</b>
short duration	-1.22	-0.04	<b>0.20</b>	<b>0.28</b>	<b>0.26</b>
long duration	-2.60	<b>0.08</b>	<b>0.44</b>	<b>0.69</b>	<b>0.63</b>
low intensity	-0.08	<b>0.51</b>	<b>0.33</b>	-0.28	-0.47
high intensity	-8.36	-1.80	-0.58	<b>0.57</b>	<b>0.60</b>

b. E - observed vs. predicted accumulative flume flow					
Storm subset	$K_{sat} = 0.03$ in/hr	$K_{sat} = 0.2$ in/hr	$K_{sat} = 0.31$ in/hr	$K_{sat} = 0.5$ in/hr	$K_{sat} = 0.55$ in/hr
all	-5.64	-0.21	<b>0.18</b>	<b>0.21</b>	<b>0.14</b>
short duration	-2.62	<b>0.84</b>	<b>0.90</b>	<b>0.80</b>	<b>0.75</b>
long duration	-32.51	-7.62	-4.88	-4.09	-4.46
low intensity	-9.09	-1.06	-1.05	-1.23	-1.27
high intensity	-8.79	-0.60	<b>0.46</b>	<b>0.71</b>	<b>0.54</b>

Table 19. Coefficient of efficiency (E) data of observed versus predicted (a) peak flume flow and (b) accumulative flume flow for different saturated hydraulic conductivities tested.  $r^2$  analysis was done on varying subsets of the complete set of storm that were differentiated by storm characteristics.

that occurs during the larger storms allows the model a larger margin of error in runoff prediction. This margin of error may be too big to accurately predict the smaller storms that occur in the watershed (i.e. storms with a peak flow less than 1.5 CFS.)

In general, the E data for the runs with FMIN set at 0.55 and 0.5 gave the most positive results. The results point out that these conductivities do not do well with low intensity storms. This is because the high hydraulic conductivity allows the soil to absorb all the precipitation. This may be an indicator that the estimate of FMIN is too high.

It is interesting to note that, had calibration not been possible, the initial suggested saturated hydraulic conductivity of 0.2 in/hr. produced an  $r^2 > 0.75$  for the complete set of storms and all the sub-sets of the storms evaluated. The  $r^2$  analysis also justifies the decision to focus on the 42-element parameter file. Comparing the data for corresponding hydraulic conductivities when used in the 42-element parameter file and the 8-element parameter file, the  $r^2$  for the 42-element parameter file was always greater. (Table 17)

Examination of Figure 17 shows what appears to be a reasonable fit for the larger class of storms (peak flow > 1.5 CFS) when using FMIN = 0.55 in/hr. The coefficient of efficiency data also support this fit. The E data for peak flume flow of the long duration and high intensity storms are relatively high, positive numbers. This trend concurs with the fact that the storms with smaller peaks can not be confidently estimated due to the margin of error. However, for the purpose of estimating erosion, this is not a problem because the storms that do not produce high flows also do not seem to be producing any significant erosion.

Two storms in the region of observed high flows have predicted outflow that significantly deviates from the observed outflow, however. The storm that the model seemed to over predict, June 1995, was believed to have bad flume data. The flume for that particular storm had become completely clogged and there was evidence that water had been flowing over the top of the flume during the storm. It is thought that the storm produced a peak much higher than what the flume recorded, similar to the peak flow predicted by the model. This is one instance that shows an explicit positive correlation between the results from modeling the watershed and what actually happened during the storm.

The underestimation of the other storm (May 1995) in the larger class of storms reveals another problem, the difficulty in establishing the initial soil saturation (SI). The role that SI plays in this problem can be clarified in comparing the July 1993 storm, where the model predicted peak flow almost perfectly, to the May 1995 storm in which the peak flow was underpredicted. Both storms experienced approximately 20 minutes of steady rainfall. The May storm produced less precipitation than the storm in July, yet the May storm still produced significantly greater runoff. That is to say, the May peak flow was recorded as ~2.4 CFS while the peak flow in July was only ~1.5 CFS. The estimates of SI in the model were 0.3 and 0.4 for July and May, respectively. A potential cause of this situation might be that the watershed had a significantly higher initial soil saturation before the May storm than it did before the July storm. Had this difference in SI been reflected in the model input, the calculated peak flow for May may have been higher. The possible error in the SI estimate for this study could have been caused by spatial variability between the site where the SI measurement was taken and the Frijolito watershed or it could have been due to error in extrapolation of data or other intricacies that are not as obvious. As presented in the background section, possible solution to this problem would be to employ a simple daily water balance model or, if reasonable, remote sensing of initial soil water content. A theory that could come from this scenario is that the model works for the larger, more intense storms - provided that the correct initial soil saturation is chosen.

The erosion data is also problematic. The problem stems from the differences in the way the erosion laws calculate erosion. The laws produce varying results and seem to get to these results through different mechanisms, i.e. erosion also originating from planes versus solely coming from the channels. Since limited recommendations are found in the literature as to which transport law is most suited for overland flow, it is up to the modeler to determine which transport equation is most suitable for their watershed. The erosion laws dependence on hydraulic conductivity complicates things even further. The total sediment loss of the watershed is very sensitive to the conductivity of the soils. This only emphasizes the importance in correctly estimating the relative saturated hydraulic conductivity.

## **VII. Conclusions**

Semi-arid watersheds are highly heterogeneous and thus difficult to hydrologically model. (Wilcox, 1989) KINEROS was designed to incorporate some of this variability through

the ability to divide the watershed up into several elements. In this respect, KINEROS is a breakthrough. The modeler is able to input small changes into his watershed (i.e. a clump of trees or a parking lot) and see what affect that will have on the runoff and erosion produced. The problem, however, stems from the numerous inputs the model requires. It is advantageous to be able to model the change in slope, for example, but for the model to work there has to be an accurate account of the slope on the scale being examined to start with. Some parameters (i.e. D50, POR, R1) are relatively easy to estimate from tables in the manual with the use of just a few measurements taken in the field. Other parameters are not as easy to estimate. The practical applicability may be limited if reliable estimates of the necessary parameters are not easily obtained.

The problems that occurred with the calibration of the model concerning the saturated hydraulic conductivity of the soil could be due to the spatial heterogeneity of the watershed. Spatial variability is often found to be a major limitation in the applicability of models. (Blackburn, 1975) The infiltration capacity is extremely variable between the pine needle beds under the canopy and the interspace area. Even distributed models, such as KINEROS, cannot, without great difficulty, incorporate such small scale variability.

A prime example of the difficulty in obtaining estimates of parameters is the case that came up in this study concerning the initial soil saturation (SI.) Even with weekly soil moisture profiles taken using a neutron soil moisture probe from a nearby site, evidence suggested that this study's estimates were not always on the mark. Most sites do not have the capability of taking soil moisture measurements. An improvement to the model would be if KINEROS could take the rainfall history immediately preceding the event being modeled into account and calculate the expected initial soil saturation for the user. Since it is relatively easy to obtain precipitation measurements, this would make the model much easier to use effectively, especially for the novice hydrologist.

One of the biggest faults that came to be noticed in this study is the extreme dependence on the relative saturated hydraulic conductivity. It is hard to determine from this one study if this dependence is a function of the model or the study area. The erodible soil surface in the watershed is mostly flat, bare soils with a few intermittent clumps of grass suggesting that the saturated hydraulic conductivity could well be an overriding factor for this watershed. If it is the case, however, that, in general, the conductivity of the soil dominates the hydrograph produced, than KINEROS is not any better than other, less

physically-based models. KINEROS needs to be studied further, both against a larger number of storms in the semi-arid Frijolito watershed and against storm data from other types of watersheds.

It is hard to come to a definite conclusion concerning the erosion estimation ability of KINEROS, though it is encouraging that this test found Law 5 to produce estimates of erosion on the order of magnitude of the data collected from the watershed. This study did not have enough erosion data to come to any statistically relevant conclusion. A few broad statements, however, can be made. There is a good chance, as was found in this study, that one of the erosion laws will suit the watershed under investigation. The problem is finding the right erosion law to use with the watershed. The manual itself says that there is an “...absence of a clearly superior relations for shallow surface runoff...” (Woolhiser et al., 1990b) There is a paucity of guidance, besides the mean particle size limits, in the manual or the literature in choosing which erosion law to use. This study found that the difference in pounds of erosion produced could be off by as much as two orders of magnitude. If no data exists from a site being studied, there is no way of knowing if the correct erosion law was chosen. Hence, there is no way to tell of the accuracy of the data produced. Further research needs to go into the guidance of the use of the erosion laws.

Part of the uncertainty in the erosion prediction can also be portioned to other problems. One possible cause for error could be the inherent spatial heterogeneity of the watershed that is not captured by the model. Instead of allowing differential flows across the planes, as the spatial heterogeneity of the saturated hydraulic conductivity in the watershed would dictate, the model forces the flow to act homogenous across each element. This stipulates homogenous erosion where, in actuality, there is a range of flows occurring in each element producing differential erosion. Areas of higher flows could possibly produce more erosion than is otherwise predicted by the model.

There is also the question of the applicability of the erosion laws to this particular watershed. Most of the transport equations available for use have been “...developed and/or validated based on data for flow of noncohesive particles in small laboratory flumes or natural channels....” with mildly sloping flow conditions. (Smith, 1978) These conditions are far from being close to those that flow experiences in the field where flows are often very shallow, slopes are often high and cohesive forces of soils are significant in

resisting erosion. This is a manifestation of the fact that little is known about upland sediment transport. (Woolhiser et al., 1990b)

It is encouraging to be able to say that this study did indicate that KINEROS can work under certain conditions. The model did work relatively well for storms with peak flow of 1.5 CFS or greater and it did predict erosion within an order of magnitude. For the purpose of predicting erosion, this prediction capability is sufficient due to the fact that the small, weak storms that the model did not accurately predict were not erosion producing storms. It is hard to say that the apparent shortcomings of the model that appeared in this study are definite problems. Nearing et al. (1991) pointed out that validation studies like this need to be carried out for many sites so that consistent model deficiencies may be identified. Only at that point can trends be established and model improvements made.

## BIBLIOGRAPHY

Ackers, P., and W.R. White. 1973. Sediment transport: New approach and analysis. *Journal of the Hydraulics Division, American Society of Civil Engineers* 99(HY11):2041-2060.

American Society of Civil Engineers (ASCE). 1975. *Sedimentation engineering*. Amer. Soc. of Civ. Engr. New York, NY. 745 p.

Bennett, J.P. 1974. Concepts of mathematical modeling of sediment yield. *Water Resources Research* 10(3):485-492.

Beven, K. 1989. Changing ideas in hydrology - the case of physically-based models. *Journal of Hydrology*, 105:157-172.

Blackburn, W.H. 1975. Factors influencing infiltration and sediment production on semiarid rangelands in Nevada. *Water Resour. Res.* 11:929-937.

Blackie, J. R. and C. W. O. Eeles. 1985. Lumped catchment models. In *Hydrological Forecasting*, eds. M. G. Anderson and T. P. Burt, 311-346. New York: John Wiley & Sons, Inc.

Bowen, B.M. 1990. *Los Alamos Climatology*. Los Alamos National Laboratory Report LA-11735-MS, Los Alamos, NM. 254 p.

Engelund, F., and E. Hansen. 1967. *A monograph on sediment transport in alluvial streams*. 62 pp. Teknisk Vorlag, Copenhagen.

Foster, G.R. 1982. Modeling the erosion process. In C.T. Haan, H.P. Johnson, and D.L. Brakensiek, eds., *Hydrologic modeling of small watersheds*, ASAE Monograph 5, pp. 297-380, American Society of Agricultural Engineers, St. Joseph, MO.

Foster, G.R. and D.L. Meyer. 1972. Transport of soil particles by shallow flow. *Transactions of the American Society of Agricultural Engineers* 15(1):99-102.

Foster, G.R. and D.L. Meyer, 1977. Soil Erosion and Sedimentation by Water - an Overview. from *Proceedings of the National Symposium on Soil Erosion and Sedimentation by Water*, Palmer House, Chicago, Illinois, Dec 12-13, p. 14-23.

Goodrich, D.C., T.J. Schumugge, T.J. Jackson, C.L. Unkrich, T.O. Keefer, R. Parry, L.B. Bach, and S.A. Amer. 1994. Runoff simulation sensitivity to remotely sensed initial soil water content. *Water Resources Research* 30(5):1393-1405.

Goodrich, D.C., D.A. Woolhiser, and C.L. Unkrich. 1990. Rainfall-Sampling Impacts on Runoff. from *Proceedings of Int'l Symposium: Hydraulics/Hydrology of Arid Lands*, Hydraulics Division, American Society of Civil Engineers, San Diego, CA p. 519-524.

Goodrich, D.C., J.J. Stone, and R. van der Zweep. 1993. Validation strategies based on model application objectives. from *Proceedings of the Federal Interagency Workshop on Hydrologic Modeling Demands for the 90's*, Fort Collins, CO, June 6-9, p. 8.1-8.8.

Kimberlin, L.W. and W.C. Moldenhauer, 1977. Predicting soil erosion. from Proceedings of the National Symposium on Soil Erosion and Sedimentation by Water, Palmer House, Chicago, Illinois, Dec 12-13, p. 31-42.

Kitandis, P. K. and R. L. Bras. 1980. Real-time forecasting with a conceptual hydrologic model. 2. applications and results. *Water Resources Research* 16(6):1034-1044.

Lane, L.J., 1982. Distributed model for small semiarid watersheds. *J. of Hydraulics Div., ASCE*, 108(HY10):1114-1131.

Loague, K. M., and R. A. Freeze. 1975. A comparison of rainfall-runoff modeling techniques on small upland catchments. *Water Resources Res.* 21: 229-248.

Michaud, J.D., and S. Sorooshian, 1992. Rainfall-runoff modeling of flash floods in semi-arid watersheds. Univ. of Arizona, Dept. of Hydrology and Water Resources Tech. Rep. No. HWR 92-030, 319 p.

Nash, J.E., and J.V. Sutcliffe. 1970. River flow forecasting through conceptual models, Part 1- A discussion of principles. *J. Hydrol.* 10(3):282-290.

Nearing, M. A., L. J. Lane, E. E. Alberts, and J. M. Laflen. 1990. Prediction technology for soil erosion by water: status and research needs. *Soil Sci. Soc. Amer. J.* 54:1702-1711.

Onstad, C.A., C.K. Mutchler and A.J. Bowie. 1977. Predicting sediment yields. from Proceedings of the National Symposium on Soil Erosion and Sedimentation by Water, Palmer House, Chicago, Illinois, Dec 12-13, p. 43-58.

Pilgrim, D. H., T. G. Chapman, and D. G. Doran. 1988. Problems of rainfall-runoff modeling in arid and semiarid regions. *Hydrol. Sci. J.* 33: 379-400.

Renard, K.G., G.R. Foster, G.A. Waists, and J.P. Porter. 1991. RUSLE Revised Universal Soil Loss Equation. *J. of Soil and Water Cons.* 46(1):30-33

Renard, K.G., L.J. Lane, J.R. Simanton, W.E. Emmerich, J.J. Sone, M.A. Wertz, D.C. Goodrich, and D.S. Yakowitz. 1993. Agricultural impacts in an arid environment: Walnut Gulch studies. *Hydrological Science and Technology.* 9(1-4):145-190.

Replogle, JH. A., A. J. Clemmens, M. G. Bos. 1990. Measuring irrigation water. In Hoffman, G. J., T. A. Howell, and K. H. Solomon (eds.) *Management of Farm Irrigation Systems.* ASAE Monograph, American Society of Agricultural Engineers, St. Joseph, MI. p. 345-351.

Rosenblueth, E. 1975. Point estimates for probability moments. *Proc. Natl. Acad. Sci. (USA)* 72:3812-3814.

Rovey, E.W., and D.A. Woolhiser. 1977. Urban storm runoff model. *Journal of the Hydraulics Division, American Society of Civil Engineers* 103(HY11):1339-1351.

Smith, R.E. 1981. A kinematic model for surface mine sediment yield. *Transactions of the American Society of Agricultural Engineers* 24(6):1508-1514.



- Smith, R.E., D.C. Goodrich, D.A. Woolhiser, and C.L. Unkrich. 1994. KINEROS - A kinematic runoff and erosion model, *In* Computer Models of Watershed Hydrology, ed. V.P. Singh, p. 697-732. Water Resources Publications.
- Smith, R.E., and J. Y. Parlange. 1978. A parameter-efficient hydrologic infiltration model. *Water Resources Research* 14(3):533-538.
- Wilcox, B. P., C. L. Hanson, J. R. Wight, and W. H. Blackburn. 1989a. Sagebrush rangeland hydrology and evaluation of the SPUR hydrology model. *Water Resources Bull.* 25: 653-666.
- Wilcox, B. P., K. R. Cooley, and C. L. Hanson. 1989b. Predicting snowmelt runoff on sagebrush rangeland using a calibrated SPUR hydrology model. *Trans., ASAE* 32: 1,351-1,357.
- Wilcox, B. P., W. J. Rawls, D L. Brakensiek, and J. R. Wight. 1990. Predicting runoff from rangelands: A comparison of two models. *Water Resources Res.*
- Wilcos, B.P., 1994. Runoff and erosion in intercanopy zones of pinyon-juniper woodlands. *J. Range Manage.* 47:285-295.
- Wilcox, B. P., J. Pitlick, C. Allen, D. Davenport (in press). Runoff and erosion from a rapidly eroding pinyon-juniper hillslope. In M. G. Anderson and S. Brooks (eds.) *Advances in Hillslope Processes*, John Wiley and Sons, New York.
- Woolhiser, D.A., D.C. Goodrich, W.E. Emmerich, and T.O. Keefer. 1990a. Hydrologic Effects of Brush to Grass Conversion. from *Watershed Planning and Analysis in Action Symposium Proceeding of IR Conference Watershed Mgt/IR Div/ASCE Durango, CO, July 9-11*, p.293-302.
- Woolhiser, D.A., Smith, R.E., and D.C. Goodrich, 1990b. KINEROS, A kinematic runoff and erosion model: Documentation and user manual. ARS-77, U.S. Dept. of Agric., Agric. Res. Svc., Washington, D.C., 130 pp.
- Yalin, Y.S. 1963. An expression for bed-load transportation. *Journal of the Hydraulics Division, Proceedings of the American Society of Civil Engineers* 89(HY3):221-250.
- Zevenbergen, L.W. and M.R. Peterson, 1988. Evaluation and testing of storm-event hydrologic models. *Proc. ASCE Nat. Conf. on Hydraulic Engr., Colo. Springs, CO, Aug. 6-12.*, p. 467-472.

## **Appendices.**

## **Appendices.**

### **Appendix A.**

Storm Hyetographs and Hydrographs.

### **Appendix B.**

KINEROS Input Parameter Files.

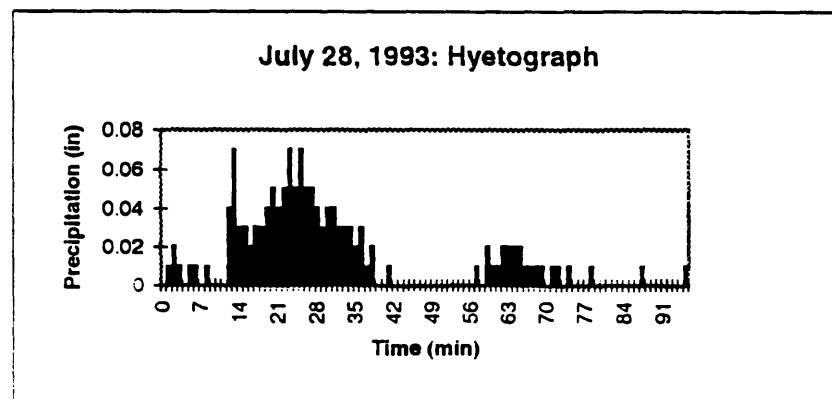
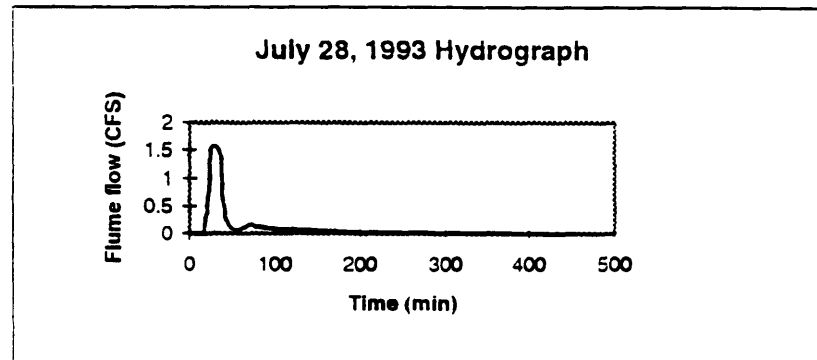
### **Appendix C.**

Sediment Transport Capacity Relations.

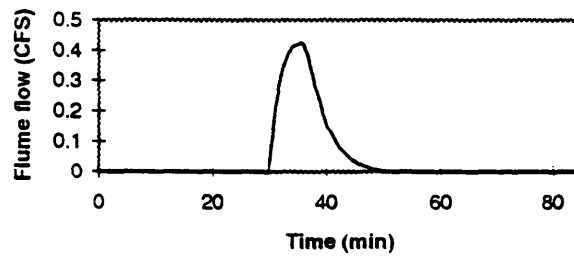
### **Appendix D.**

Model vs. Storm Hydrographs for  $K_{sat} = 0.03, 0.2$  and  $0.55$  in/hr.

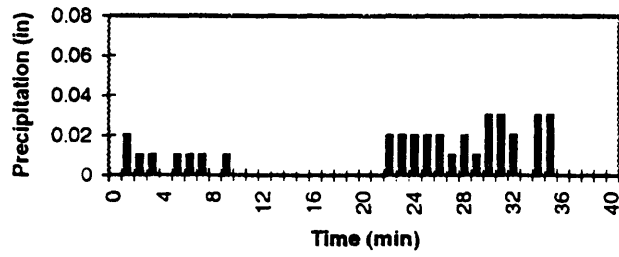
## Appendix A. Storm Hyetographs and Hydrographs



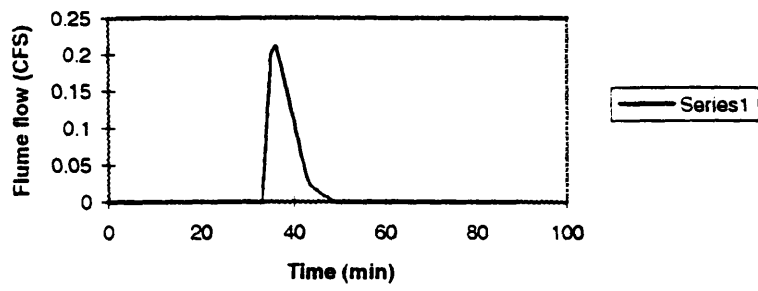
August 6, 1993: Hydrograph (corrected)



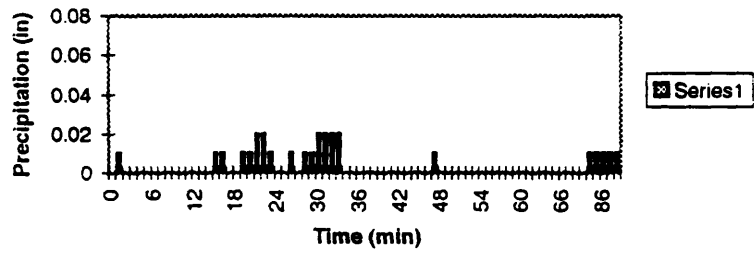
August 6, 1993: Hyetograph

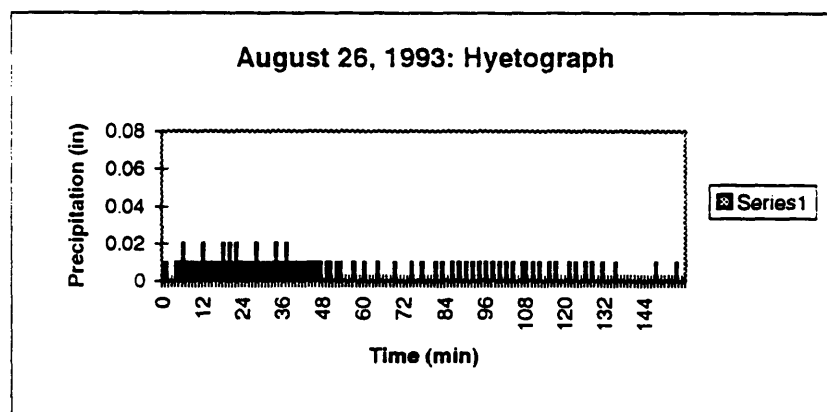
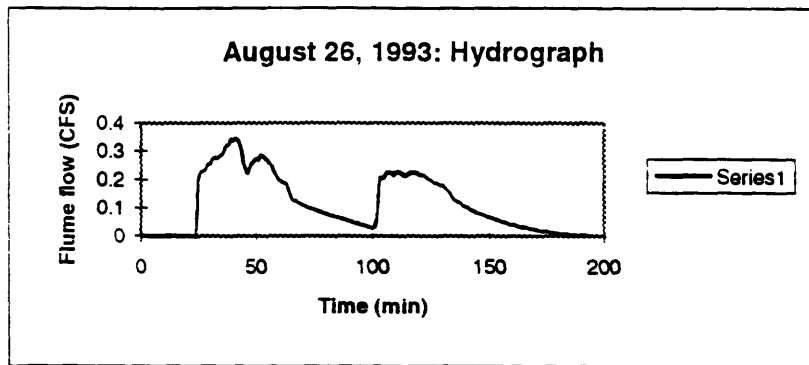


August 20, 1993: Hydrograph (corrected)

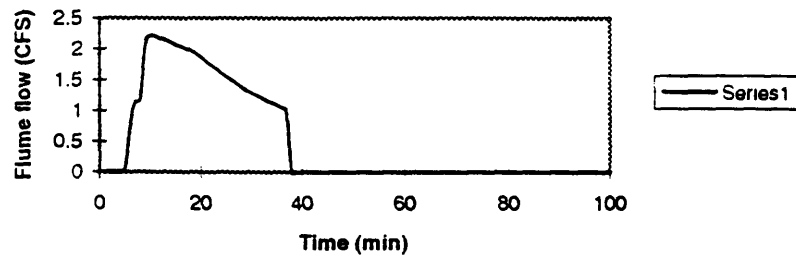


August 20, 1993: Hyetograph

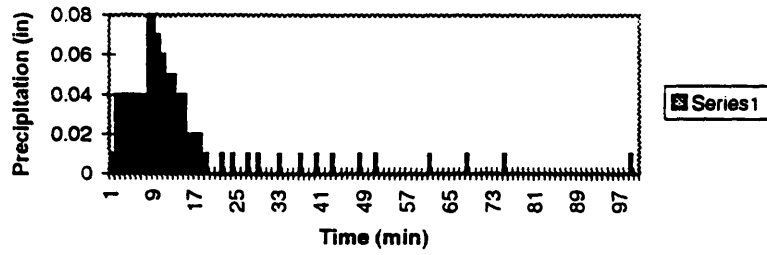




August 27, 1993: Hydrograph (corrected)

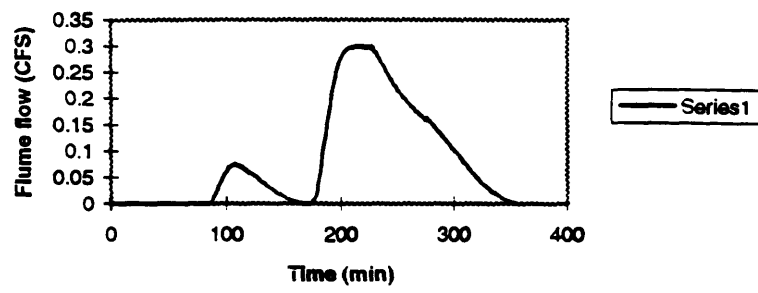


August 27, 1993: Hyetograph

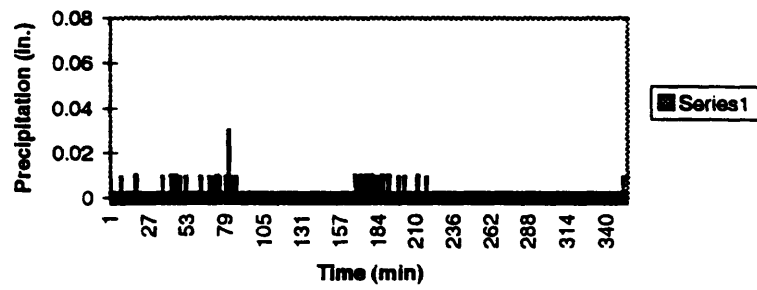




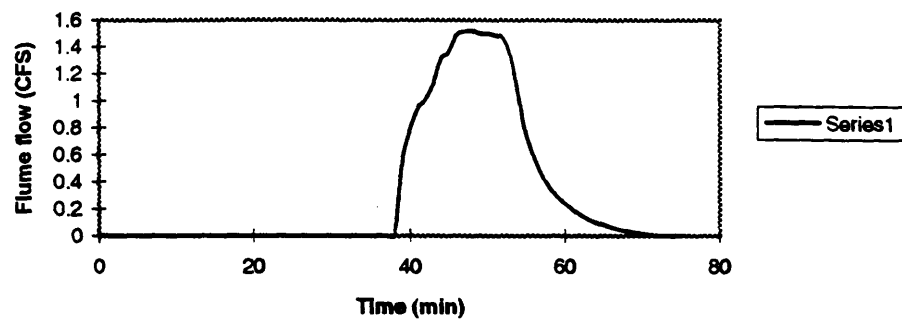
**August 28, 1993: Hydrograph**



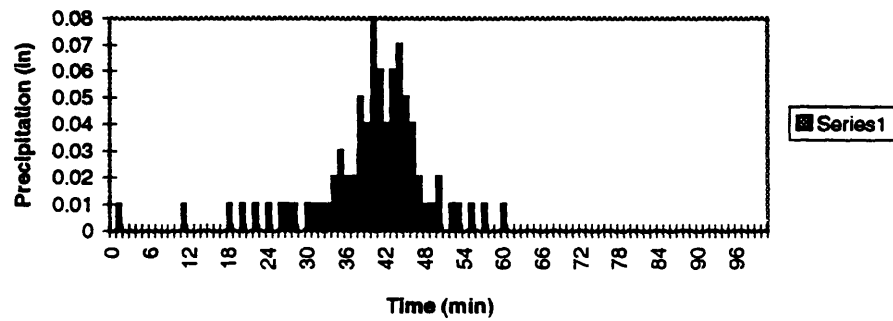
**August 28, 1993: Hyetograph**



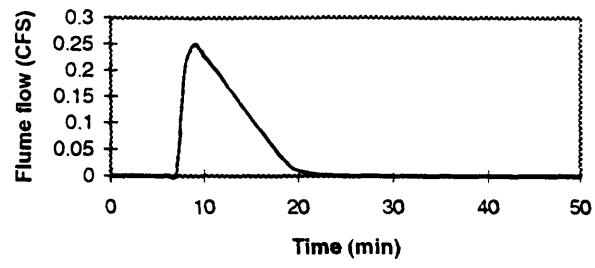
**September 6, 1993: Hydrograph (corrected)**



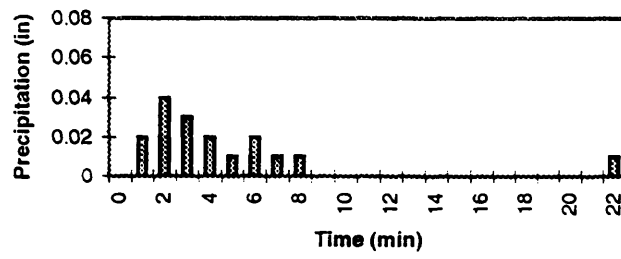
**September 6, 1993: Hyetograph**

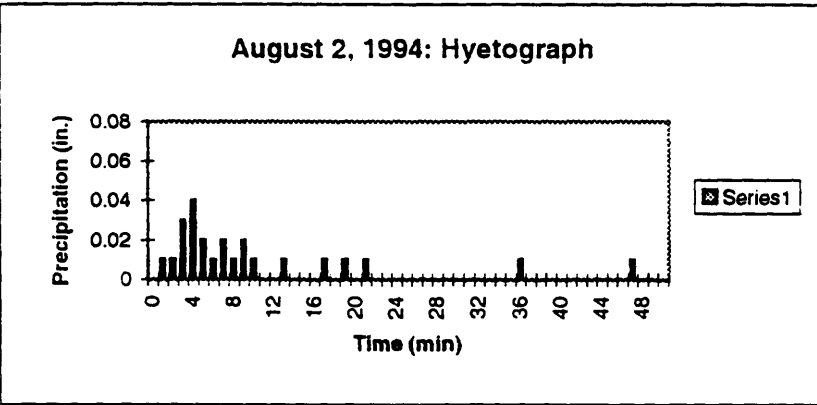
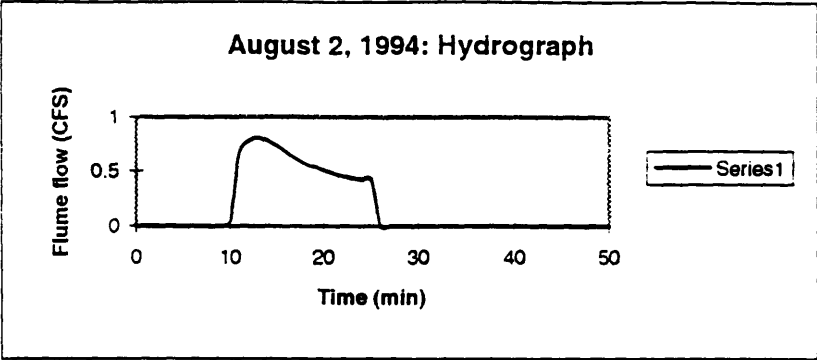


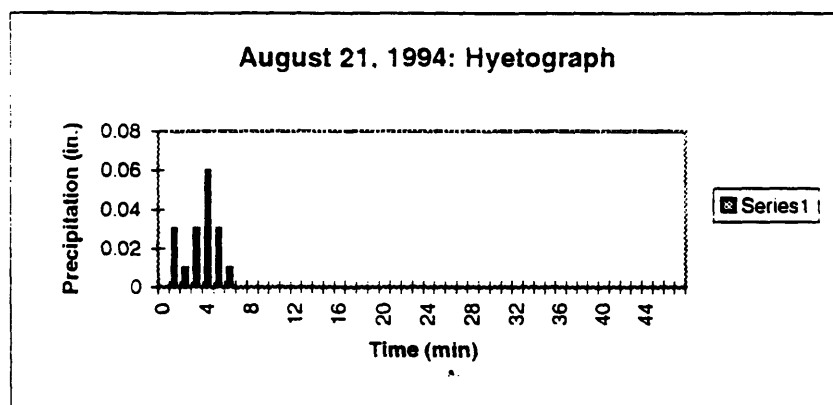
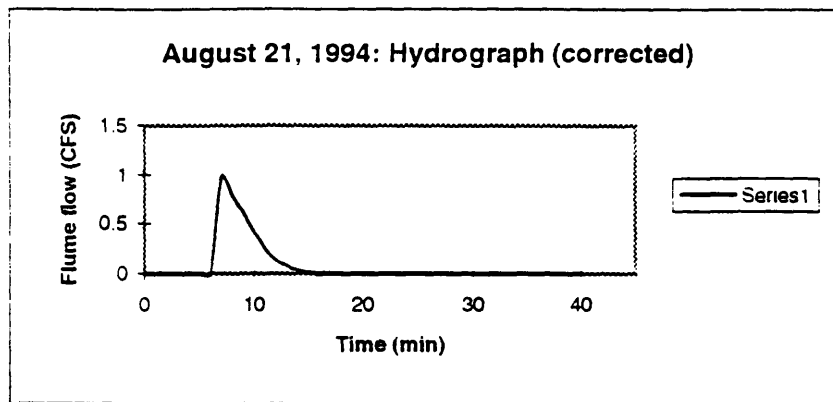
September 13, 1993: Hydrograph (corrected)



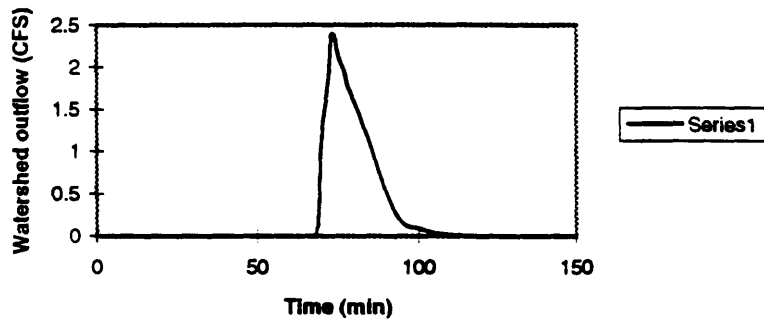
September 13, 1993: Hyetograph



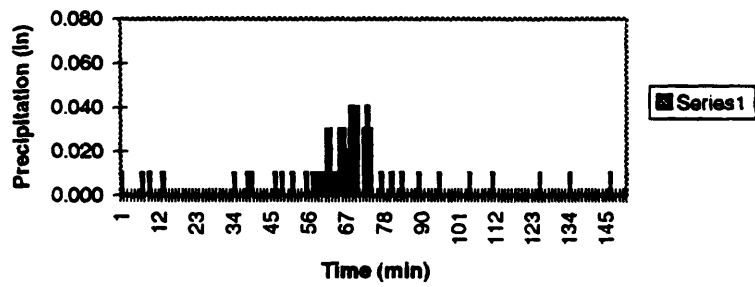




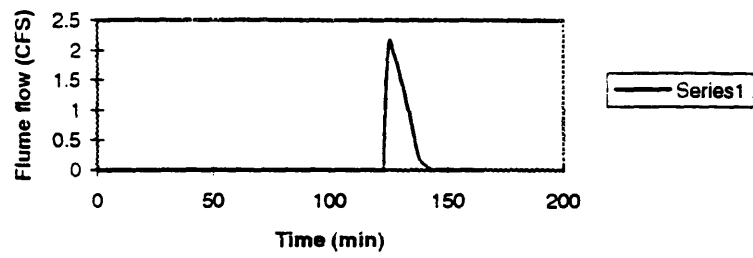
**May 29, 1995: Hydrograph (corrected)**



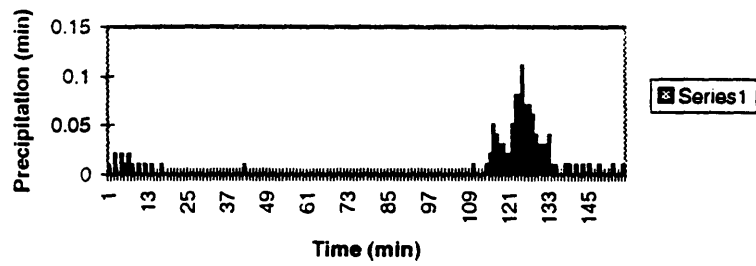
**May 29, 1995: Hyetograph**



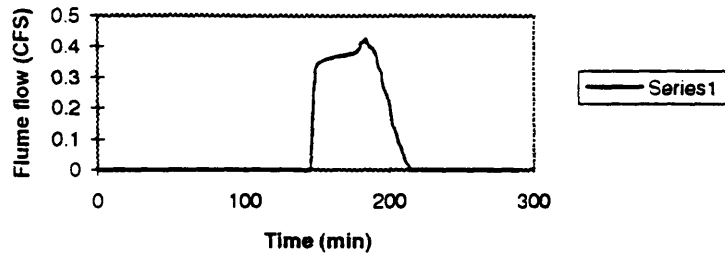
June 29, 1995: Hydrograph



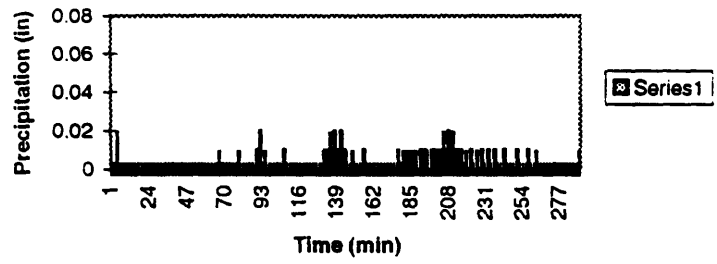
June 29, 1995: Hyetograph



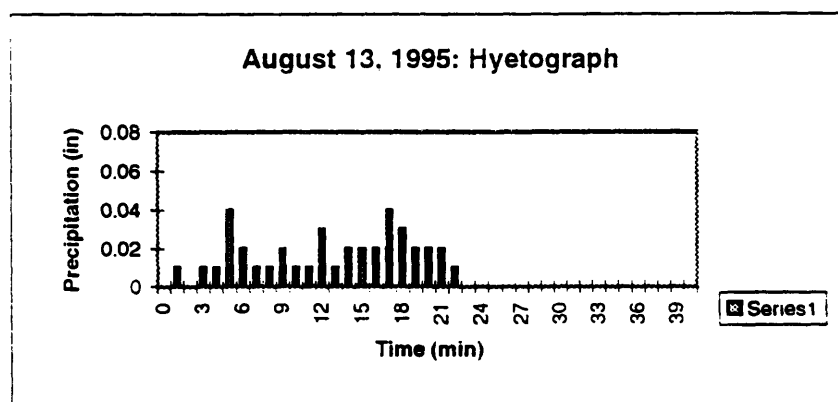
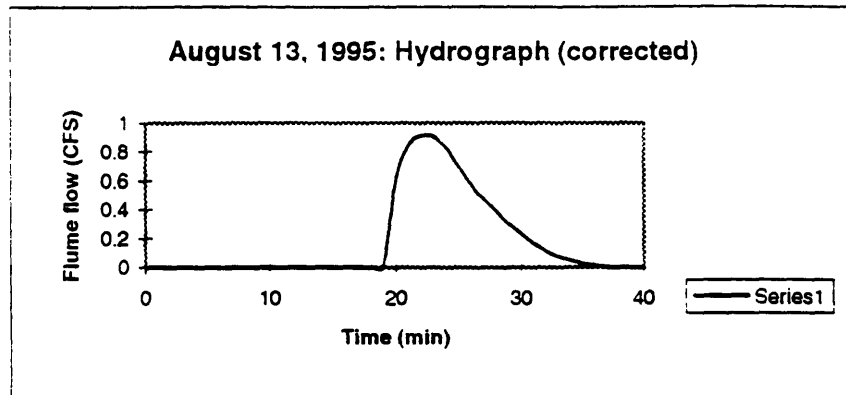
July 18, 1995: Hydrograph



July 18, 1995: Hyetograph







## Appendix B. KINEROS Input Parameter Files

### KINEROS Parameter Input File

```
#
*****
***** SYSTEM *****
*****
* NELE NRES NPART CLEN TFIN DELT THETA TEMP
  42  1  0  200.0 250.0 1.0  0.8  -1.
```

```
#
*****
***** OPTIONS *****
*****
NTIME NUNITS NEROS
  2    1    2
```

```
#
*****
**** COMPUTATION ORDER ****
*****
```

There must be NELE elements in the list. NLOG  
must be sequential. ELEMENT NUM. need not be.

```
#
COMP. ORDER  ELEMENT
(NLOG)      NUM. (J)
```

-----	-----
1	1
2	37
3	32
4	33
5	42
6	28
7	27
8	26
9	17
10	18
11	19
12	20
13	21
14	22
15	23
16	24
17	25
18	34
19	35
20	36
21	38
22	40
23	39
24	41
25	29
26	30
27	31
28	11

29	12
30	13
31	15
32	14
33	16
34	8
35	9
36	10
37	2
38	3
39	6
40	4
41	5
42	7

#

\*\*\*\*\*

\*\*\*\*\* ELEMENT-WISE INFO \*\*\*\*

\*\*\*\*\*

There must be NELE sets of the ELEMENT-WISE prompts and data records; duplicate records from \* to \* for each element. The elements may be entered in any order.

\*

J	NU	NR	NL	NC1	NC2	NCASE	NPRINT	NPNT	NRP
1	0	0	0	0	0	0	1	0	0

XL	W	S	ZR	ZL	BW	DIAM	R1	R2
238	45.0	0.12	0.0	0.0	0.0	0.0	0.1	0.0

FMIN	G	POR	SI	SMAX	ROC	RECS	DINTR
0.5	5.0	0.49	0.9	1.0	0.0	0.6	0.01

LAW	CF	CG	CH	CO-CS	D50	RHOS	PAVE	SIGMAS
2	32.49	0.001	7.99	0.0	0.0012	2.5	0.0	0.0018

\*

\*

J	NU	NR	NL	NC1	NC2	NCASE	NPRINT	NPNT	NRP
2	0	0	0	0	1	1	0	0	

XL	W	S	ZR	ZL	BW	DIAM	R1	R2
302.0	33.0	0.21	0.0	0.0	0.0	0.0	0.1	0.0

FMIN	G	POR	SI	SMAX	ROC	RECS	DINTR
29.0	5.0	0.453	0.9	1.0	0.0	0.6	0.01

LAW	CF	CG	CH	CO-CS	D50	RHOS	PAVE	SIGMAS
2	32.49	0.001	7.99	0.0	0.0012	2.5	0.0	0.0018

\*

\*

J	NU	NR	NL	NC1	NC2	NCASE	NPRINT	NPNT	NRP
3	0	0	0	0	1	1	0	0	

XL	W	S	ZR	ZL	BW	DIAM	R1	R2
208.0	30.0	0.04	0.0	0.0	0.0	0.0	0.1	0.0

-----										
	FMIN	G	POR	SI	SMAX	ROC	RECS	DINTR		
	0.5	5.0	0.453	0.9	1.0	0.0	0.6	0.01		
-----										
	LAW	CF	CG	CH	CO-CS	D50	RHOS	PAVE	SIGMAS	
	2	32.49	0.001	7.99	0.0	0.0012	2.5	0.0	0.0018	
*										
*	J	NU	NR	NL	NC1	NC2	NCASE	NPRINT	NPNT	NRP
	4	0	0	0	0	1	1	0	0	
-----										
	XL	W	S	ZR	ZL	BW	DIAM	R1	R2	
	114.0	81.0	0.1	0.0	0.0	0.0	0.0	0.1	0.0	
-----										
	FMIN	G	POR	SI	SMAX	ROC	RECS	DINTR		
	29.0	5.0	0.453	0.9	1.0	0.0	0.6	0.01		
-----										
	LAW	CF	CG	CH	CO-CS	D50	RHOS	PAVE	SIGMAS	
	2	32.49	0.001	7.99	0.0	0.0012	2.5	0.0	0.0018	
*										
*	J	NU	NR	NL	NC1	NC2	NCASE	NPRINT	NPNT	NRP
	5	0	0	0	0	1	1	0	0	
-----										
	XL	W	S	ZR	ZL	BW	DIAM	R1	R2	
	225.0	30.0	0.04	0.0	0.0	0.0	0.0	0.1	0.0	
-----										
	FMIN	G	POR	SI	SMAX	ROC	RECS	DINTR		
	0.5	5.0	0.453	0.9	1.0	0.0	0.6	0.01		
-----										
	LAW	CF	CG	CH	CO-CS	D50	RHOS	PAVE	SIGMAS	
	2	32.49	0.001	7.99	0.0	0.0012	2.5	0.0	0.0018	
*										
*	J	NU	NR	NL	NC1	NC2	NCASE	NPRINT	NPNT	NRP
	6	1	2	3	0	0	1	1	0	0
-----										
	XL	W	S	ZR	ZL	BW	DIAM	R1	R2	
	235.0	0.0	0.06	1.0	1.0	0.98	0.3	0.01	0.0	
-----										
	FMIN	G	POR	SI	SMAX	ROC	RECS	DINTR		
	0.0	0.0	0.0	0.0	0.0	0.0	0.6	0.00		
-----										
	LAW	CF	CG	CH	CO-CS	D50	RHOS	PAVE	SIGMAS	
	2	32.49	0.001	7.99	0.0	0.0012	2.5	0.0	0.0018	
*										
*	J	NU	NR	NL	NC1	NC2	NCASE	NPRINT	NPNT	NRP
	7	0	4	5	10	6	1	1	0	3
-----										
	XL	W	S	ZR	ZL	BW	DIAM	R1	R2	
	146.0	0.0	0.11	1.0	1.0	1.5	0.3	0.01	0.0	
-----										

FMIN	G	POR	SI	SMAX	ROC	RECS	DINTR
0.0	0.0	0.0	0.0	0.0	0.0	0.6	0.00

LAW	CF	CG	CH	CO-CS	D50	RHOS	PAVE	SIGMAS
2	32.49	0.001	7.99	0.0	0.0012	2.5	0.0	0.0018

\*

\*

J	NU	NR	NL	NC1	NC2	NCASE	NPRINT	NPNT	NRP
8	0	0	0	0	1	1	0	0	

XL	W	S	ZR	ZL	BW	DIAM	R1	R2
55.0	110.0	0.088	0.0	0.0	0.0	0.0	0.1	0.0

FMIN	G	POR	SI	SMAX	ROC	RECS	DINTR
29.0	5.0	0.453	0.9	1.0	0.0	0.6	0.01

LAW	CF	CG	CH	CO-CS	D50	RHOS	PAVE	SIGMAS
2	32.49	0.001	7.99	0.0	0.0012	2.5	0.0	0.0018

\*

\*

J	NU	NR	NL	NC1	NC2	NCASE	NPRINT	NPNT	NRP
9	0	0	0	0	1	1	0	0	

XL	W	S	ZR	ZL	BW	DIAM	R1	R2
96.0	16.0	0.0625	0.0	0.0	0.0	0.0	0.1	0.0

FMIN	G	POR	SI	SMAX	ROC	RECS	DINTR
0.5	5.0	0.453	0.9	1.0	0.0	0.6	0.01

LAW	CF	CG	CH	CO-CS	D50	RHOS	PAVE	SIGMAS
2	32.49	0.001	7.99	0.0	0.0012	2.5	0.0	0.0018

\*

\*

J	NU	NR	NL	NC1	NC2	NCASE	NPRINT	NPNT	NRP
10	0	9	8	16	13	1	1	0	0

XL	W	S	ZR	ZL	BW	DIAM	R1	R2
105.0	0.0	0.06	1.7	1.7	3.25	0.3	0.01	0.0

FMIN	G	POR	SI	SMAX	ROC	RECS	DINTR
0.0	0.0	0.0	0.0	0.0	0.0	0.6	0.00

LAW	CF	CG	CH	CO-CS	D50	RHOS	PAVE	SIGMAS
2	32.49	0.001	7.99	0.0	0.0012	2.5	0.0	0.0018

\*

\*

J	NU	NR	NL	NC1	NC2	NCASE	NPRINT	NPNT	NRP
11	0	0	0	0	0	1	1	0	0

XL	W	S	ZR	ZL	BW	DIAM	R1	R2
125.0	10.0	0.1	0.0	0.0	0.0	0.0	0.1	0.0

FMIN	G	POR	SI	SMAX	ROC	RECS	DINTR
------	---	-----	----	------	-----	------	-------

29.0	5.0	0.453	0.9	1.0	0.0	0.6	0.01		
------	-----	-------	-----	-----	-----	-----	------	--	--

---

LAW	CF	CG	CH	CO-CS	D50	RHOS	PAVE	SIGMAS
2	32.49	0.001	7.99	0.0	0.0012	2.5	0.0	0.0018

\*

\*

J	NU	NR	NL	NC1	NC2	NCASE	NPRINT	NPNT	NRP
12	0	0	0	0	1	1	0	0	

---

XL	W	S	ZR	ZL	BW	DIAM	R1	R2
170.0	10.0	0.035	0.0	0.0	0.0	0.0	0.1	0.0

---

FMIN	G	POR	SI	SMAX	ROC	RECS	DINTR
29.0	5.0	0.453	0.9	1.0	0.0	0.6	0.01

---

LAW	CF	CG	CH	CO-CS	D50	RHOS	PAVE	SIGMAS
2	32.49	0.001	7.99	0.0	0.0012	2.5	0.0	0.0018

\*

\*

J	NU	NR	NL	NC1	NC2	NCASE	NPRINT	NPNT	NRP
13	0	11	12	0	0	1	1	0	0

---

XL	W	S	ZR	ZL	BW	DIAM	R1	R2
105.0	0.0	0.06	1.7	1.7	3.25	0.3	0.01	0.0

---

FMIN	G	POR	SI	SMAX	ROC	RECS	DINTR
0.0	0.0	0.0	0.0	0.0	0.0	0.6	0.00

---

LAW	CF	CG	CH	CO-CS	D50	RHOS	PAVE	SIGMAS
2	32.49	0.001	7.99	0.0	0.0012	2.5	0.0	0.0018

\*

\*

J	NU	NR	NL	NC1	NC2	NCASE	NPRINT	NPNT	NRP
14	0	0	0	0	0	1	1	0	0

---

XL	W	S	ZR	ZL	BW	DIAM	R1	R2
150.0	24.0	0.035	0.0	0.0	0.0	0.0	0.1	0.0

---

FMIN	G	POR	SI	SMAX	ROC	RECS	DINTR
0.5	5.0	0.453	0.9	1.0	0.0	0.6	0.01

---

LAW	CF	CG	CH	CO-CS	D50	RHOS	PAVE	SIGMAS
2	32.49	0.001	7.99	0.0	0.0012	2.5	0.0	0.0018

\*

\*

J	NU	NR	NL	NC1	NC2	NCASE	NPRINT	NPNT	NRP
15	0	0	0	0	0	1	1	0	0

---

XL	W	S	ZR	ZL	BW	DIAM	R1	R2
43.0	125.0	0.08	0.0	0.0	0.0	0.0	0.1	0.0

---

FMIN	G	POR	SI	SMAX	ROC	RECS	DINTR
0.5	5.0	0.453	0.9	1.0	0.0	0.6	0.01

```

-----
LAW  CF  CG  CH CO-CS  D50 RHOS  PAVE SIGMAS
  2 32.49 0.001 7.99 0.0 0.0012 2.5 0.0 0.0018
*
*
J  NU  NR  NL  NC1  NC2 NCASE NPRINT  NPNT  NRP
16  0  14  15  25  31  1  1  0  0
-----
XL  W  S  ZR  ZL  BW  DIAM  R1  R2
65.0 0.0 0.06 1.7 1.7 3.25 0.3 0.01 0.0
-----
FMIN  G  POR  SI  SMAX  ROC  RECS  DINTR
0.0 0.0 0.0 0.0 0.0 0.0 0.6 0.00
-----
LAW  CF  CG  CH CO-CS  D50 RHOS  PAVE SIGMAS
  2 32.49 0.001 7.99 0.0 0.0012 2.5 0.0 0.0018
*
*
J  NU  NR  NL  NC1  NC2 NCASE NPRINT  NPNT  NRP
17  26  0  0  0  0  1  1  0  0
-----
XL  W  S  ZR  ZL  BW  DIAM  R1  R2
72.0 22.0 0.055 0.0 0.0 0.0 0.0 0.1 0.0
-----
FMIN  G  POR  SI  SMAX  ROC  RECS  DINTR
29.0 5.0 0.453 0.9 1.0 0.0 0.6 0.01
-----
LAW  CF  CG  CH CO-CS  D50 RHOS  PAVE SIGMAS
  2 32.49 0.001 7.99 0.0 0.0012 2.5 0.0 0.0018
*
*
J  NU  NR  NL  NC1  NC2 NCASE NPRINT  NPNT  NRP
18  27  0  0  0  0  1  1  0  0
-----
XL  W  S  ZR  ZL  BW  DIAM  R1  R2
63.0 19.0 0.03 0.0 0.0 0.0 0.0 0.1 0.0
-----
FMIN  G  POR  SI  SMAX  ROC  RECS  DINTR
29.0 5.0 0.453 0.9 1.0 0.0 0.6 0.01
-----
LAW  CF  CG  CH CO-CS  D50 RHOS  PAVE SIGMAS
  2 32.49 0.001 7.99 0.0 0.0012 2.5 0.0 0.0018
*
*
J  NU  NR  NL  NC1  NC2 NCASE NPRINT  NPNT  NRP
19  0  18  17  0  0  1  1  0  0
-----
XL  W  S  ZR  ZL  BW  DIAM  R1  R2
81.0 0.0 0.12 1.7 1.7 3.25 0.3 0.01 0.0
-----
FMIN  G  POR  SI  SMAX  ROC  RECS  DINTR
0.0 0.0 0.0 0.0 0.0 0.0 0.6 0.00
-----

```

LAW CF CG CH CO-CS D50 RHOS PAVE SIGMAS  
 2 32.49 0.001 7.99 0.0 0.0012 2.5 0.0 0.0018

\*

\*

J NU NR NL NC1 NC2 NCASE NPRINT NPNT NRP  
 20 28 0 0 0 0 1 1 0 0

XL W S ZR ZL BW DIAM R1 R2  
 63.0 12.0 0.03 0.0 0.0 0.0 0.0 0.1 0.0

FMIN G POR SI SMAX ROC RECS DINTR  
 29.0 5.0 0.453 0.9 1.0 0.0 0.6 0.01

LAW CF CG CH CO-CS D50 RHOS PAVE SIGMAS  
 2 32.49 0.001 7.99 0.0 0.0012 2.5 0.0 0.0018

\*

\*

J NU NR NL NC1 NC2 NCASE NPRINT NPNT NRP  
 21 0 0 0 0 0 1 1 0 0

XL W S ZR ZL BW DIAM R1 R2  
 85 9.8 0.14 0.0 0.0 0.0 0.0 0.1 0.0

FMIN G POR SI SMAX ROC RECS DINTR  
 0.5 5.0 0.453 0.9 1.0 0.0 0.6 0.01

LAW CF CG CH CO-CS D50 RHOS PAVE SIGMAS  
 2 32.49 0.001 7.99 0.0 0.0012 2.5 0.0 0.0018

\*

\*

J NU NR NL NC1 NC2 NCASE NPRINT NPNT NRP  
 22 0 21 20 0 0 1 1 0 0

XL W S ZR ZL BW DIAM R1 R2  
 65.0 0.0 0.06 1.7 1.7 3.25 0.3 0.01 0.0

FMIN G POR SI SMAX ROC RECS DINTR  
 0.0 0.0 0.0 0.0 0.0 0.0 0.6 0.00

LAW CF CG CH CO-CS D50 RHOS PAVE SIGMAS  
 2 32.49 0.001 7.99 0.0 0.0012 2.5 0.0 0.0018

\*

\*

J NU NR NL NC1 NC2 NCASE NPRINT NPNT NRP  
 23 0 0 0 0 0 1 1 0 0

XL W S ZR ZL BW DIAM R1 R2  
 300.0 20.0 0.06 0.0 0.0 0.0 0.0 0.1 0.0

FMIN G POR SI SMAX ROC RECS DINTR  
 0.5 5.0 0.453 0.9 1.0 0.0 0.6 0.01

LAW CF CG CH CO-CS D50 RHOS PAVE SIGMAS



2 32.49 0.001 7.99 0.0 0.0012 2.5 0.0 0.0018

\*

\*

J	NU	NR	NL	NC1	NC2	NCASE	NPRINT	NPNT	NRP
24	42	0	0	0	1	1	0	0	

XL	W	S	ZR	ZL	BW	DIAM	R1	R2
276.0	28.0	0.065	0.0	0.0	0.0	0.0	0.1	0.0

FMIN	G	POR	SI	SMAX	ROC	RECS	DINTR
0.5	5.0	0.453	0.9	1.0	0.0	0.6	0.01

LAW	CF	CG	CH	CO-CS	D50	RHOS	PAVE	SIGMAS
2	32.49	0.001	7.99	0.0	0.0012	2.5	0.0	0.0018

\*

\*

J	NU	NR	NL	NC1	NC2	NCASE	NPRINT	NPNT	NRP
25	0	24	23	19	22	1	1	0	0

XL	W	S	ZR	ZL	BW	DIAM	R1	R2
333.0	0.0	0.11	1.2	1.2	2.0	0.3	0.01	0.0

FMIN	G	POR	SI	SMAX	ROC	RECS	DINTR
0.0	0.0	0.0	0.0	0.0	0.0	0.6	0.00

LAW	CF	CG	CH	CO-CS	D50	RHOS	PAVE	SIGMAS
2	32.49	0.001	7.99	0.0	0.0012	2.5	0.0	0.0018

\*

\*

J	NU	NR	NL	NC1	NC2	NCASE	NPRINT	NPNT	NRP
26	0	0	0	0	0	1	1	0	0

XL	W	S	ZR	ZL	BW	DIAM	R1	R2
120.0	26.0	0.09	0.0	0.0	0.0	0.0	0.1	0.0

FMIN	G	POR	SI	SMAX	ROC	RECS	DINTR
0.5	5.0	0.453	0.9	1.0	0.0	0.6	0.01

LAW	CF	CG	CH	CO-CS	D50	RHOS	PAVE	SIGMAS
2	32.49	0.001	7.99	0.0	0.0012	2.5	0.0	0.0018

\*

\*

J	NU	NR	NL	NC1	NC2	NCASE	NPRINT	NPNT	NRP
27	0	0	0	0	0	1	1	0	0

XL	W	S	ZR	ZL	BW	DIAM	R1	R2
110.0	15.0	0.1	0.0	0.0	0.0	0.0	0.1	0.0

FMIN	G	POR	SI	SMAX	ROC	RECS	DINTR
0.5	5.0	0.453	0.9	1.0	0.0	0.6	0.01

LAW	CF	CG	CH	CO-CS	D50	RHOS	PAVE	SIGMAS
2	32.49	0.001	7.99	0.0	0.0012	2.5	0.0	0.0018

\*

\*

J	NU	NR	NL	NC1	NC2	NCASE	NPRINT	NPNT	NRP
28	0	0 0	0	0	1	1	0	0	

XL	W	S	ZR	ZL	BW	DIAM	R1	R2
100.0	20.0	0.09	0.0	0.0	0.0	0.0	0.1	0.0

FMIN	G	POR	SI	SMAX	ROC	RECS	DINTR
0.5	5.0	0.453	0.9	1.0	0.0	0.6	0.01

LAW	CF	CG	CH	CO-CS	D50	RHOS	PAVE	SIGMAS
2	32.49	0.001	7.99	0.0	0.0012	2.5	0.0	0.0018

\*

\*

J	NU	NR	NL	NC1	NC2	NCASE	NPRINT	NPNT	NRP
29	0	0 0	0	0	1	1	0	0	

XL	W	S	ZR	ZL	BW	DIAM	R1	R2
30.0	130.0	0.125	0.0	0.0	0.0	0.0	0.1	0.0

FMIN	G	POR	SI	SMAX	ROC	RECS	DINTR
0.5	5.0	0.453	0.9	1.0	0.0	0.6	0.01

LAW	CF	CG	CH	CO-CS	D50	RHOS	PAVE	SIGMAS
2	32.49	0.001	7.99	0.0	0.0012	2.5	0.0	0.0018

\*

\*

J	NU	NR	NL	NC1	NC2	NCASE	NPRINT	NPNT	NRP
30	0	0 0	0	0	1	1	0	0	

XL	W	S	ZR	ZL	BW	DIAM	R1	R2
24.0	96.0	0.1	0.0	0.0	0.0	0.0	0.1	0.0

FMIN	G	POR	SI	SMAX	ROC	RECS	DINTR
0.5	5.0	0.453	0.9	1.0	0.0	0.6	0.01

LAW	CF	CG	CH	CO-CS	D50	RHOS	PAVE	SIGMAS
2	32.49	0.001	7.99	0.0	0.0012	2.5	0.0	0.0018

\*

\*

J	NU	NR	NL	NC1	NC2	NCASE	NPRINT	NPNT	NRP
31	0	29 30	36	41	1	1	0	0	

XL	W	S	ZR	ZL	BW	DIAM	R1	R2
33.0	0.0	0.1	1.0	1.0	1.5	0.0	0.01	0.0

FMIN	G	POR	SI	SMAX	ROC	RECS	DINTR
0.0	0.0	0.0	0.0	0.0	0.0	0.6	0.00

LAW	CF	CG	CH	CO-CS	D50	RHOS	PAVE	SIGMAS
2	32.49	0.001	7.99	0.0	0.0012	2.5	0.0	0.0018

\*

\*

J	NU	NR	NL	NC1	NC2	NCASE	NPRINT	NPNT	NRP
32	0	0	0	0	0	1	1	0	0

XL	W	S	ZR	ZL	BW	DIAM	R1	R2
130.0	24.0	0.127	0.0	0.0	0.0	0.0	0.1	0.0

FMIN	G	POR	SI	SMAX	ROC	RECS	DINTR
0.5	5.0	0.453	0.9	1.0	0.0	0.6	0.01

LAW	CF	CG	CH	CO-CS	D50	RHOS	PAVE	SIGMAS
2	32.49	0.001	7.99	0.0	0.0012	2.5	0.0	0.0018

\*

\*

J	NU	NR	NL	NC1	NC2	NCASE	NPRINT	NPNT	NRP
33	0	0	0	0	0	1	1	0	0

XL	W	S	ZR	ZL	BW	DIAM	R1	R2
130.0	12.0	0.117	0.0	0.0	0.0	0.0	0.1	0.0

FMIN	G	POR	SI	SMAX	ROC	RECS	DINTR
0.5	5.0	0.453	0.9	1.0	0.0	0.6	0.01

LAW	CF	CG	CH	CO-CS	D50	RHOS	PAVE	SIGMAS
2	32.49	0.001	7.99	0.0	0.0012	2.5	0.0	0.0018

\*

\*

J	NU	NR	NL	NC1	NC2	NCASE	NPRINT	NPNT	NRP
34	33	0	0	0	0	1	1	0	0

XL	W	S	ZR	ZL	BW	DIAM	R1	R2
201.0	22.0	0.05	0.0	0.0	0.0	0.0	0.1	0.0

FMIN	G	POR	SI	SMAX	ROC	RECS	DINTR
0.5	5.0	0.453	0.9	1.0	0.0	0.6	0.01

LAW	CF	CG	CH	CO-CS	D50	RHOS	PAVE	SIGMAS
2	32.49	0.001	7.99	0.0	0.0012	2.5	0.0	0.0018

\*

\*

J	NU	NR	NL	NC1	NC2	NCASE	NPRINT	NPNT	NRP
35	32	0	0	0	0	1	1	0	0

XL	W	S	ZR	ZL	BW	DIAM	R1	R2
185.0	23.0	0.01	0.0	0.0	0.0	0.0	0.1	0.0

FMIN	G	POR	SI	SMAX	ROC	RECS	DINTR
0.5	5.0	0.453	0.9	1.0	0.0	0.6	0.01

LAW	CF	CG	CH	CO-CS	D50	RHOS	PAVE	SIGMAS
2	32.49	0.001	7.99	0.0	0.0012	2.5	0.0	0.0018

\*

\*

J	NU	NR	NL	NC1	NC2	NCASE	NPRINT	NPNT	NRP
36	0	35	34	0	0	1	1	0	0

XL	W	S	ZR	ZL	BW	DIAM	R1	R2
211.0	0.0	0.12	1.0	1.0	1.5	0.0	0.01	0.0

FMIN	G	POR	SI	SMAX	ROC	RECS	DINTR
0.0	0.0	0.0	0.0	0.0	0.0	0.6	0.00

LAW	CF	CG	CH	CO-CS	D50	RHOS	PAVE	SIGMAS
2	32.49	0.001	7.99	0.0	0.0012	2.5	0.0	0.0018

\*

\*

J	NU	NR	NL	NC1	NC2	NCASE	NPRINT	NPNT	NRP
37	0	0	0	0	0	1	1	0	0

XL	W	S	ZR	ZL	BW	DIAM	R1	R2
185.0	25.0	0.14	0.0	0.0	0.0	0.0	0.1	0.0

FMIN	G	POR	SI	SMAX	ROC	RECS	DINTR
0.5	5.0	0.453	0.9	1.0	0.0	0.6	0.01

LAW	CF	CG	CH	CO-CS	D50	RHOS	PAVE	SIGMAS
2	32.49	0.001	7.99	0.0	0.0012	2.5	0.0	0.0018

\*

\*

J	NU	NR	NL	NC1	NC2	NCASE	NPRINT	NPNT	NRP
38	0	0	0	0	0	1	1	0	0

XL	W	S	ZR	ZL	BW	DIAM	R1	R2
120.0	17.0	0.175	0.0	0.0	0.0	0.0	0.1	0.0

FMIN	G	POR	SI	SMAX	ROC	RECS	DINTR
0.5	5.0	0.453	0.9	1.0	0.0	0.6	0.01

LAW	CF	CG	CH	CO-CS	D50	RHOS	PAVE	SIGMAS
2	32.49	0.001	7.99	0.0	0.0012	2.5	0.0	0.0018

\*

\*

J	NU	NR	NL	NC1	NC2	NCASE	NPRINT	NPNT	NRP
39	0	0	0	0	0	1	1	0	0

XL	W	S	ZR	ZL	BW	DIAM	R1	R2
144.0	30.0	0.055	0.0	0.0	0.0	0.0	0.1	0.0

FMIN	G	POR	SI	SMAX	ROC	RECS	DINTR
0.5	5.0	0.453	0.9	1.0	0.0	0.6	0.01

LAW	CF	CG	CH	CO-CS	D50	RHOS	PAVE	SIGMAS
2	32.49	0.001	7.99	0.0	0.0012	2.5	0.0	0.0018

\*

\*

J	NU	NR	NL	NC1	NC2	NCASE	NPRINT	NPNT	NRP
---	----	----	----	-----	-----	-------	--------	------	-----

40 38 0 0 0 0 1 1 0 0

---

XL	W	S	ZR	ZL	BW	DIAM	R1	R2
136.0	20.0	0.08	0.0	0.0	0.0	0.0	0.1	0.0

---

FMIN	G	POR	SI	SMAX	ROC	RECS	DINTR
0.5	5.0	0.453	0.9	1.0	0.0	0.6	0.01

---

LAW	CF	CG	CH	CO-CS	D50	RHOS	PAVE	SIGMAS
2	32.49	0.001	7.99	0.0	0.0012	2.5	0.0	0.0018

---

\*

\*

J	NU	NR	NL	NC1	NC2	NCASE	NPRINT	NPNT	NRP
41	37	40	39	0	0	1	1	0	0

---

---

XL	W	S	ZR	ZL	BW	DIAM	R1	R2
146.0	0.0	0.12	1.4	1.4	2.0	0.0	0.01	0.0

---

FMIN	G	POR	SI	SMAX	ROC	RECS	DINTR
0.0	0.0	0.0	0.0	0.0	0.0	0.6	0.00

---

LAW	CF	CG	CH	CO-CS	D50	RHOS	PAVE	SIGMAS
2	32.49	0.001	7.99	0.0	0.0012	2.5	0.0	0.0018

---

\*

\*

J	NU	NR	NL	NC1	NC2	NCASE	NPRINT	NPNT	NRP
42	0	0	0	0	0	1	1	0	0

---

---

XL	W	S	ZR	ZL	BW	DIAM	R1	R2
114.0	8.0	0.10	0.0	0.0	0.0	0.0	0.1	0.0

---

FMIN	G	POR	SI	SMAX	ROC	RECS	DINTR
0.5	5.0	0.453	0.9	1.0	0.0	0.6	0.01

---

LAW	CF	CG	CH	CO-CS	D50	RHOS	PAVE	SIGMAS
2	32.49	0.001	7.99	0.0	0.0012	2.5	0.0	0.0018

---

\*

# KINEROS Parameter Input File

```
#
*****
***** SYSTEM *****
*****
* NELE NRES NPART CLEN TFIN DELT THETA TEMP
  8  1  0  200.0 100.0 1  0.8 -1.
#
*****
***** OPTIONS *****
*****
  NTIME NUNITS NEROS
    2    1    2
#
*****
**** COMPUTATION ORDER ****
*****
  There must be NELE elements in the list. NLOG
  must be sequential. ELEMENT NUM. need not be.
#
  COMP. ORDER  ELEMENT
    (NLOG)    NUM. (J)
  -----
    1          1
    2          2
    3          3
    4          4
    5          5
    6          6
    7          7
    8          8
#
*****
***** ELEMENT-WISE INFO ***
*****
  There must be NELE sets of the ELEMENT-WISE prompts and data
  records; duplicate records from * to * for each element. The
  elements may be entered in any order.
*
  J  NU  NR  NL  NC1  NC2  NCASE  NPRINT  NPNT  NRP
  1  0  0  0  0  0  0  1  0  0
-----
    XL  W  S  ZR  ZL  BW  DIAM  R1  R2
    113.75 188.5 0.05 0.0 0.0 0.0 0.0 0.10 0.0
-----
    FMIN  G  POR  SI  SMAX  ROC  RECS  DINTR
    0.55  5.0 0.49 0.75 1.0 0.0 0.6 0.1
-----
    LAW  CF  CG  CH  CO-CS  D50  RHOS  PAVE  SIGMAS
    1  32.49 0.001 7.99 0.0001 0.0012 2.5 0.0 0.0018
*
*
```

J	NU	NR	NL	NC1	NC2	NCASE	NPRINT	NPNT	NRP
2	1	0	0	0	1	1	0	0	

XL	W	S	ZR	ZL	BW	DIAM	R1	R2
227.5	97.5	0.12	0.0	0.0	0.0	0.0	0.10	0.0

FMIN	G	POR	SI	SMAX	ROC	RECS	DINTR
0.55	5.0	0.453	0.75	1.0	0.0	0.6	0.1

LAW	CF	CG	CH	CO-CS	D50	RHOS	PAVE	SIGMAS
1	32.49	0.001	7.99	0.0001	0.0012	2.5	0.0	0.0018

\*

\*

J	NU	NR	NL	NC1	NC2	NCASE	NPRINT	NPNT	NRP
3	0	0	0	0	1	1	0	0	

XL	W	S	ZR	ZL	BW	DIAM	R1	R2
269.75	97.5	0.02	0.0	0.0	0.0	0.0	0.10	0.0

FMIN	G	POR	SI	SMAX	ROC	RECS	DINTR
0.55	5.0	0.453	0.75	1.0	0.0	0.6	0.1

LAW	CF	CG	CH	CO-CS	D50	RHOS	PAVE	SIGMAS
1	32.49	0.001	7.99	0.0001	0.0012	2.5	0.0	0.0018

\*

\*

J	NU	NR	NL	NC1	NC2	NCASE	NPRINT	NPNT	NRP
4	0	0	0	0	1	1	0	0	

XL	W	S	ZR	ZL	BW	DIAM	R1	R2
243.75	130.0	0.03	0.0	0.0	0.0	0.0	0.10	0.0

FMIN	G	POR	SI	SMAX	ROC	RECS	DINTR
0.55	5.0	0.453	0.75	1.0	0.0	0.6	0.1

LAW	CF	CG	CH	CO-CS	D50	RHOS	PAVE	SIGMAS
1	32.49	0.001	7.99	0.0001	0.0012	2.5	0.0	0.0018

\*

\*

J	NU	NR	NL	NC1	NC2	NCASE	NPRINT	NPNT	NRP
5	2	4	3	0	0	1	1	0	0

XL	W	S	ZR	ZL	BW	DIAM	R1	R2
276.25	0.0	0.06	1.5	1.5	3.0	0.3	0.01	0.0

FMIN	G	POR	SI	SMAX	ROC	RECS	DINTR
0.55	5.0	0.453	0.75	1.0	0.0	0.6	0.1

LAW	CF	CG	CH	CO-CS	D50	RHOS	PAVE	SIGMAS
1	32.49	0.001	7.99	0.0001	0.0012	2.5	0.0	0.0018

\*

\*

J	NU	NR	NL	NC1	NC2	NCASE	NPRINT	NPNT	NRP
---	----	----	----	-----	-----	-------	--------	------	-----

6 0 0 0 0 0 1 1 0 0

---

XL	W	S	ZR	ZL	BW	DIAM	R1	R2
243.75	65.0	0.03	0.0	0.0	0.0	0.0	0.10	0.0

---

FMIN	G	POR	SI	SMAX	ROC	RECS	DINTR
29.0	5.0	0.453	0.75	1.0	0.0	0.6	0.1

---

LAW	CF	CG	CH	CO-CS	D50	RHOS	PAVE	SIGMAS
1	32.49	0.001	7.99	0.0001	0.0012	2.5	0.0	0.0018

\*

\*

J	NU	NR	NL	NC1	NC2	NCASE	NPRINT	NPNT	NRP
7	0	0	0	0	1	1	0	0	

---

XL	W	S	ZR	ZL	BW	DIAM	R1	R2
260.0	48.75	0.02	0.0	0.0	0.0	0.0	0.10	0.0

---

FMIN	G	POR	SI	SMAX	ROC	RECS	DINTR
29.0	5.0	0.453	0.75	1.0	0.0	0.6	0.1

---

LAW	CF	CG	CH	CO-CS	D50	RHOS	PAVE	SIGMAS
1	32.49	0.001	7.99	0.0001	0.0012	2.5	0.0	0.0018

\*

\*

J	NU	NR	NL	NC1	NC2	NCASE	NPRINT	NPNT	NRP
8	0	7	6	5	0	1	1	0	0

---

XL	W	S	ZR	ZL	BW	DIAM	R1	R2
308.75	0.0	0.05	1.5	1.5	3.5	0.3	0.01	0.0

---

FMIN	G	POR	SI	SMAX	ROC	RECS	DINTR
0.55	5.0	0.453	0.75	1.0	0.0	0.6	0.1

---

LAW	CF	CG	CH	CO-CS	D50	RHOS	PAVE	SIGMAS
1	32.49	0.001	7.99	0.0001	0.0012	2.5	0.0	0.0018

\*



## Appendix C. Sediment Transport Capacity Relations

The following transport capacity relations were evaluated in this test of KINEROS.

Most of the symbols have been previously defined. Some definitions are listed below.

$$u_* = \sqrt{(gh_d S)} \quad [L/T]$$

$$h_d = \text{hydraulic depth, flow area divided by top width } [L]$$

$$\rho_s = \text{particle density } [m/L^3]$$

Ackers and White (1973) (only for  $d \geq 0.04$  mm):

$$C_{mx} = dC_p/h [u/u_*]^n [F_g/A_p - 1]^m (10^6)$$

in which

$$F_g = u_*^n / \sqrt{d_g (S_s - 1)} \{u / \sqrt{32 \log_{10} (10h/d)}\}^{1-n}$$

and in which, defining dimensionless grain diameter as:

$$d_g = d [g(S_s - 1)/v^2]^{1/3}$$

the following parameter definitions apply:

$$n = 1 - 0.56 d_g \quad \text{for } 1 < d_g \leq 60$$

or

$$n = 0 \quad \text{for } d_g > 60$$

$$A_p = 0.23/\sqrt{d_g} + 0.14 \quad \text{for } 1 < d_g \leq 60$$

or

$$A_p = 0.170 \quad \text{for } d_g > 60$$

$$m = 9.66/d_g + 1.34 \quad \text{for } 1 < d_g \leq 60$$

or

$$m = 1.50 \quad \text{for } d_g > 60$$

and

$$\log C_p = 2.86 \log d_g - [\log(d_g)]^2 - 3.53 \quad \text{for } 1 < d_g \leq 60$$

or

$$C_p = 0.025 \quad \text{for } d_g > 60$$

Yalin (1963):

$$C_{mx} = 0.635 du_* S_s A_n / u h [1 - 1/B_p A_n \ln(1 + A_n B_p)]$$

in which

$$A_n = Y/Y_c - 1 \quad \text{for } Y > Y_c$$

$$A_n = 0 \quad \text{otherwise}$$

$$B_p = [2.45/(S_s)^{0.4}] \sqrt{Y_c}$$

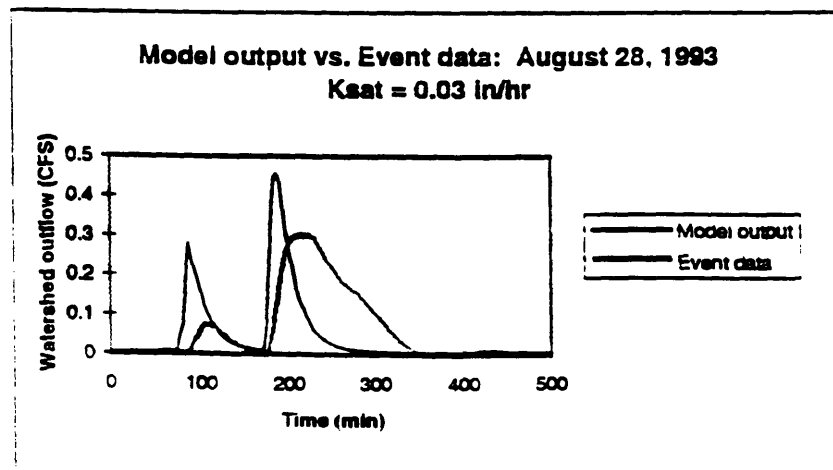
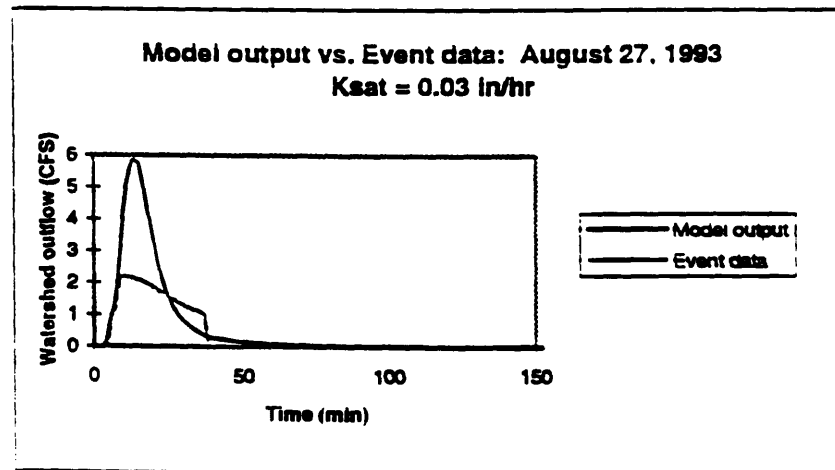
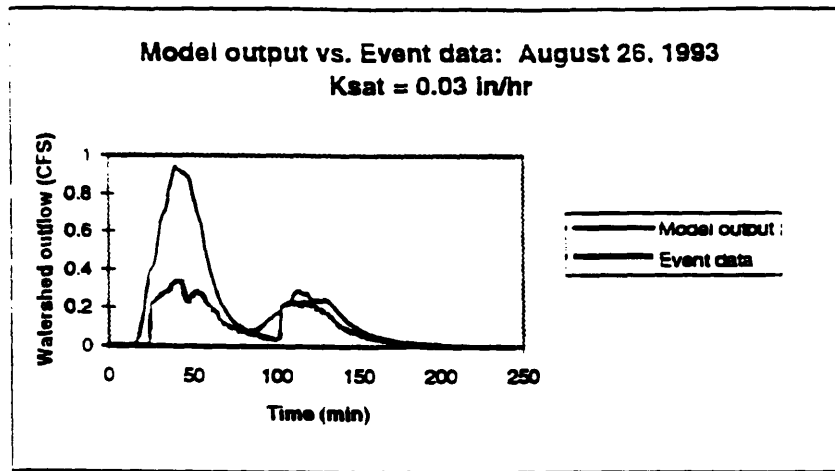
$$Y = u_*^2 / (S_s - 1) g d$$

$Y_c$  = critical tractive force, based on particle Reynolds number

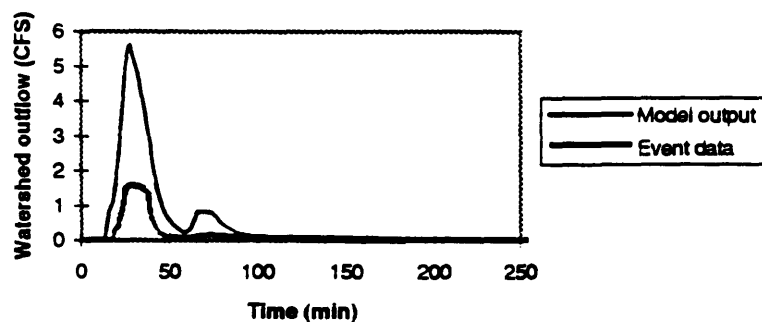
Engelund and Hansen (1967):

$$C_{mx} = (0.05 u_*^3) / (g^2 d h (S_s - 1)^2)$$

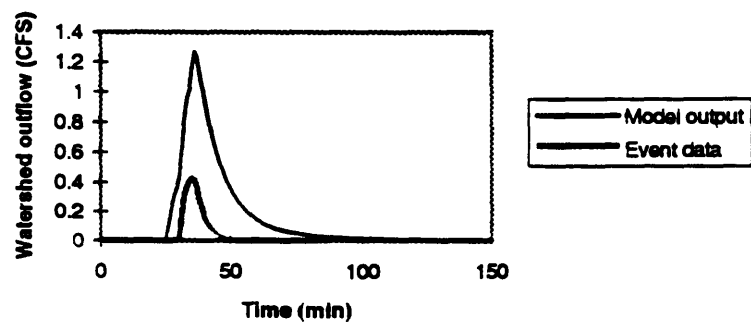
Appendix D. Model vs. Storm Hydrographs for  $K_{sat} = 0.03, 0.2$  and  $0.55$  in/hr



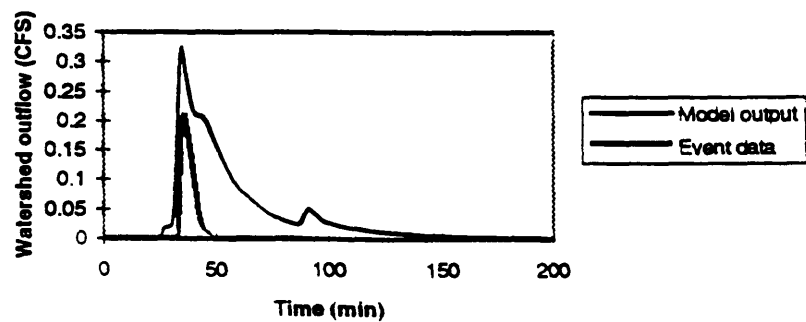
**Model output vs. Event data: July 28, 1993**  
**Ksat = 0.03 in/hr**

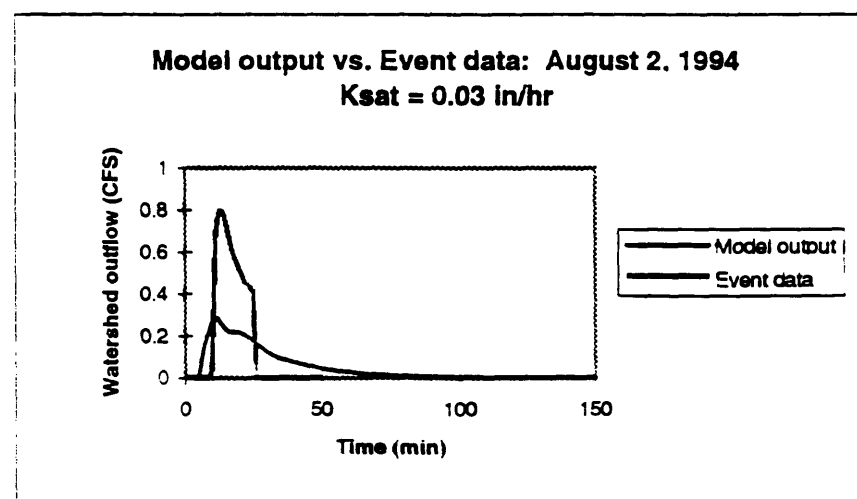
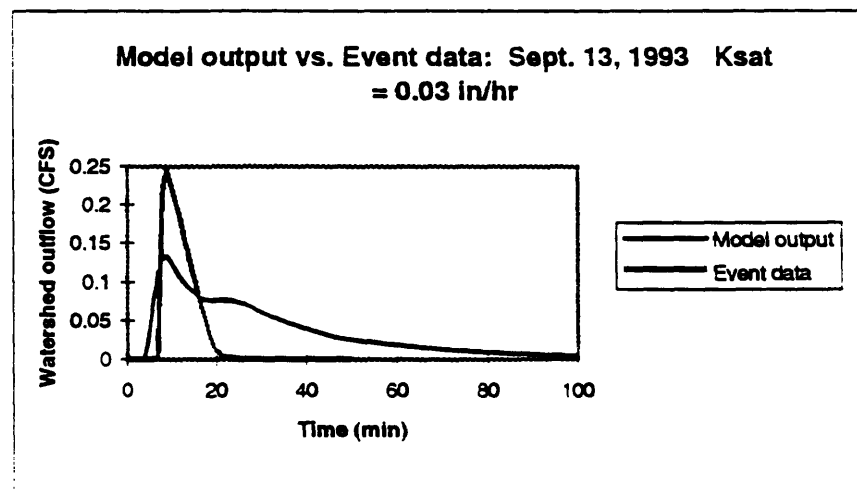
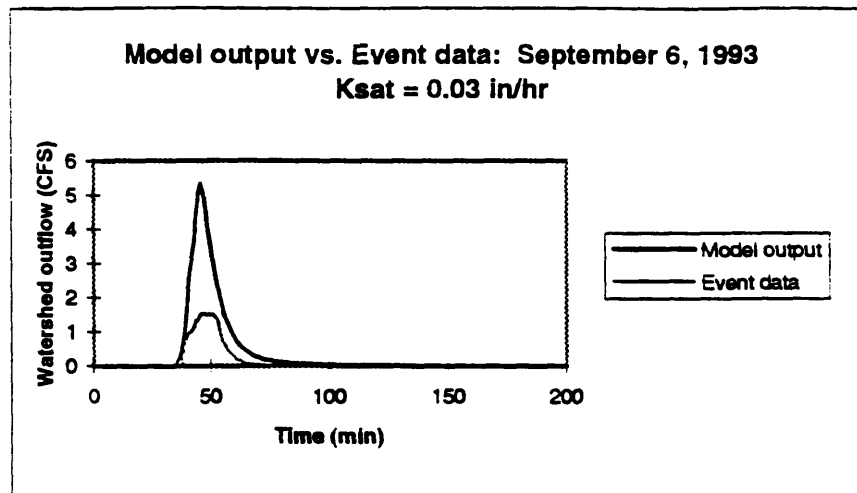


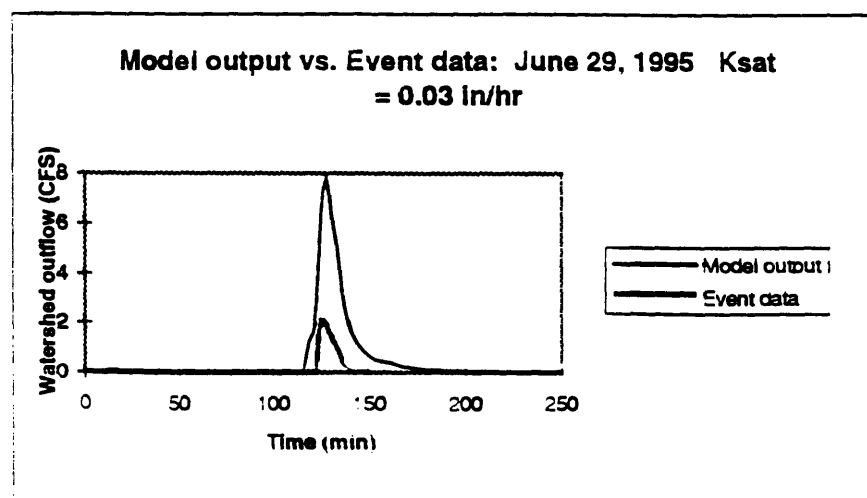
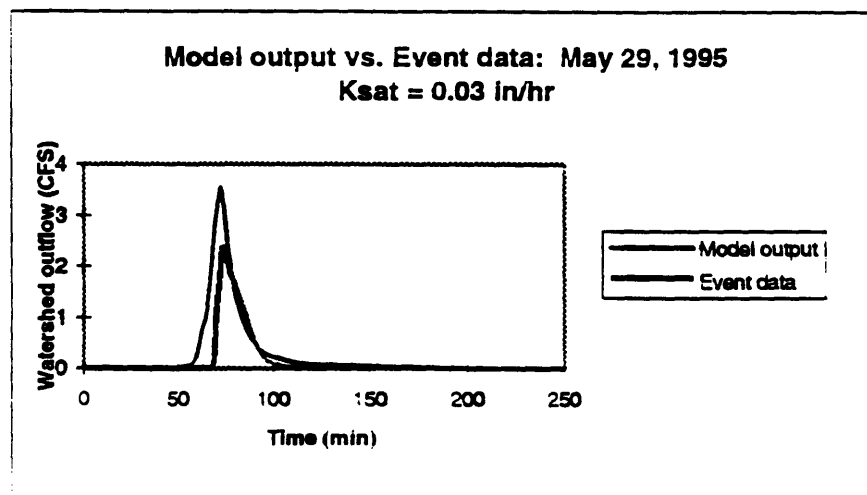
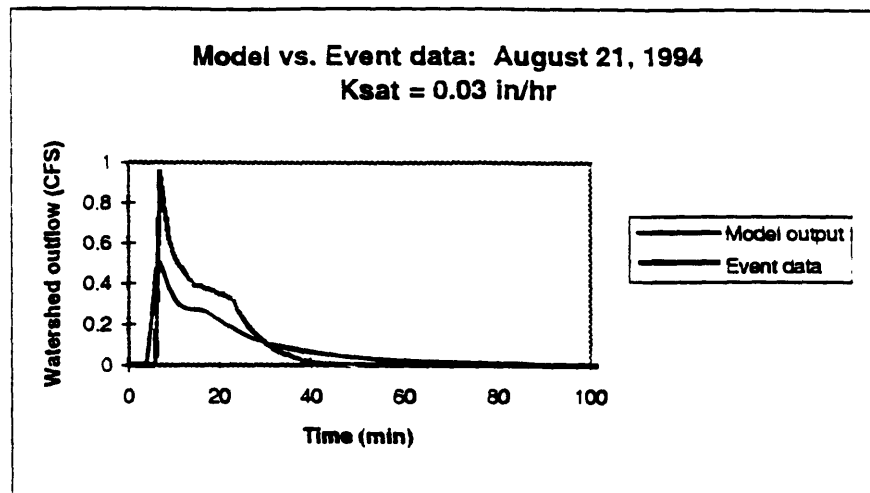
**Model output vs. Event data: August 6, 1993**  
**Ksat = 0.03 in/hr**



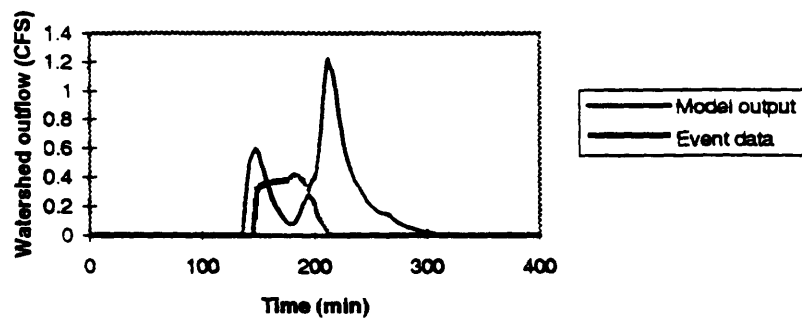
**Model output vs. Event data: August 13, 1995**  
**Ksat = 0.03 in/hr**



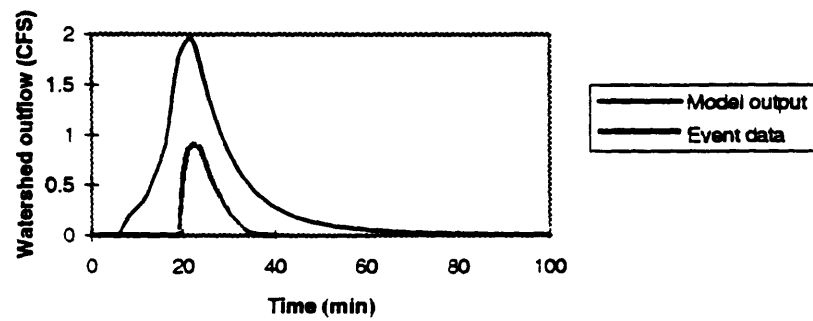


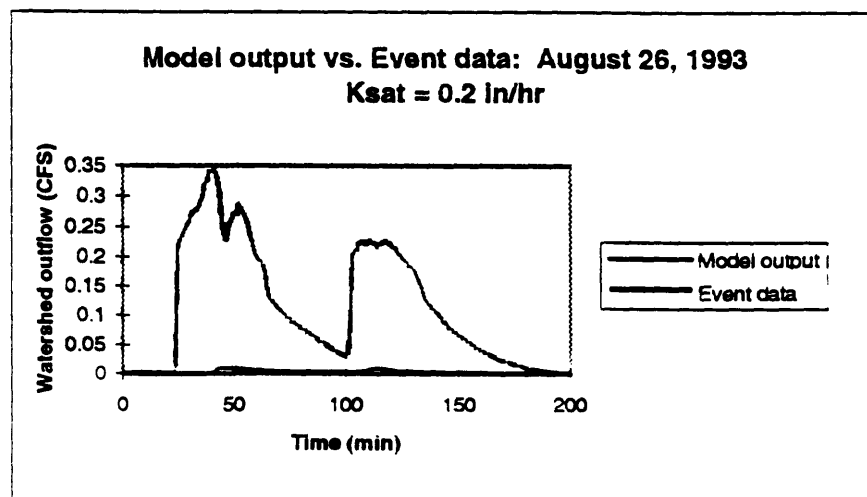
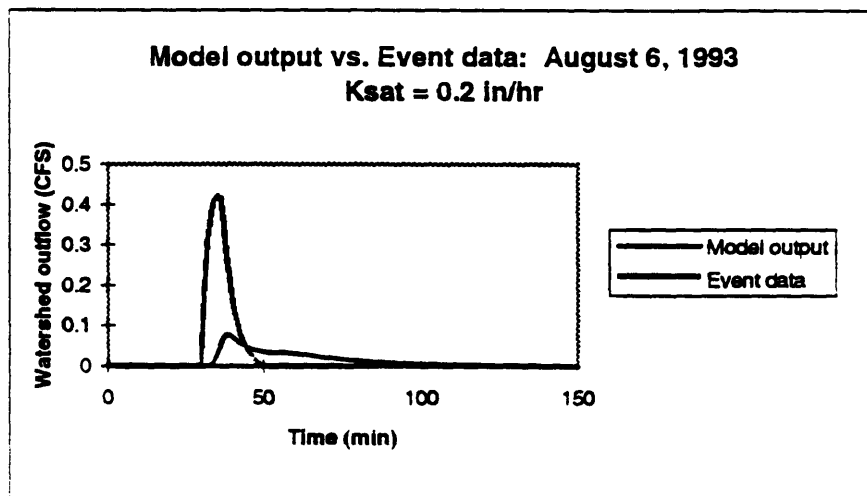
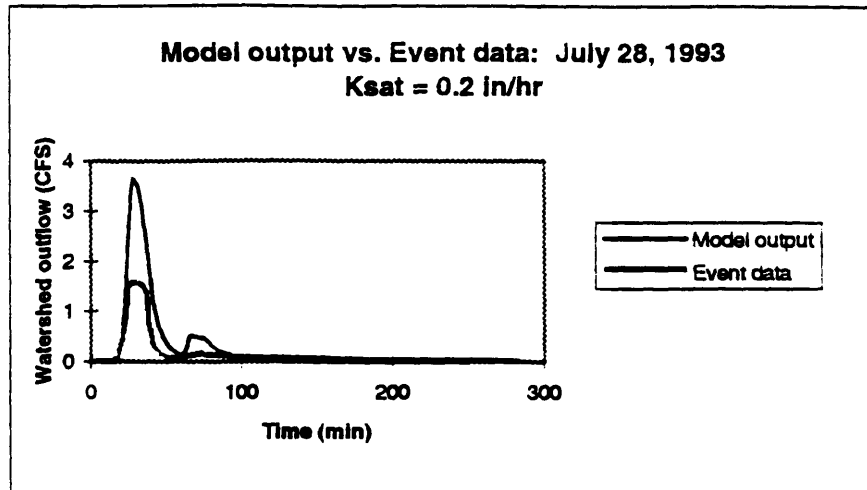


**Model output vs. Event data: July 18, 1995 Ksat = 0.03 in/hr**

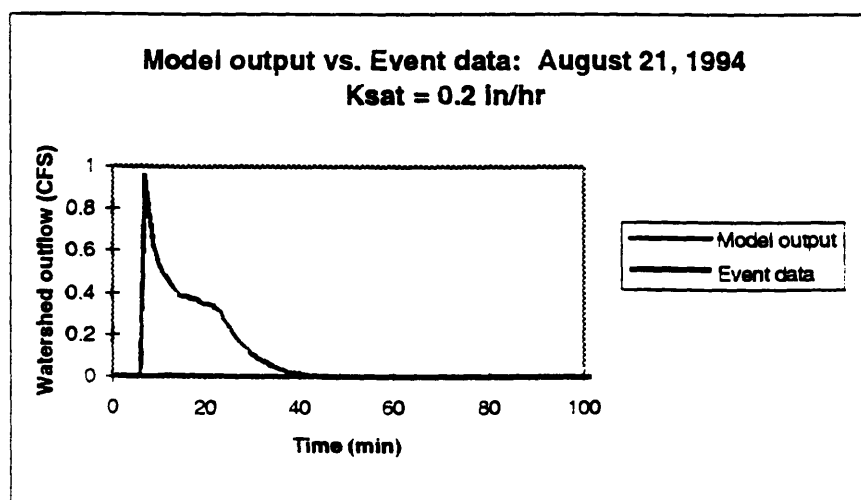
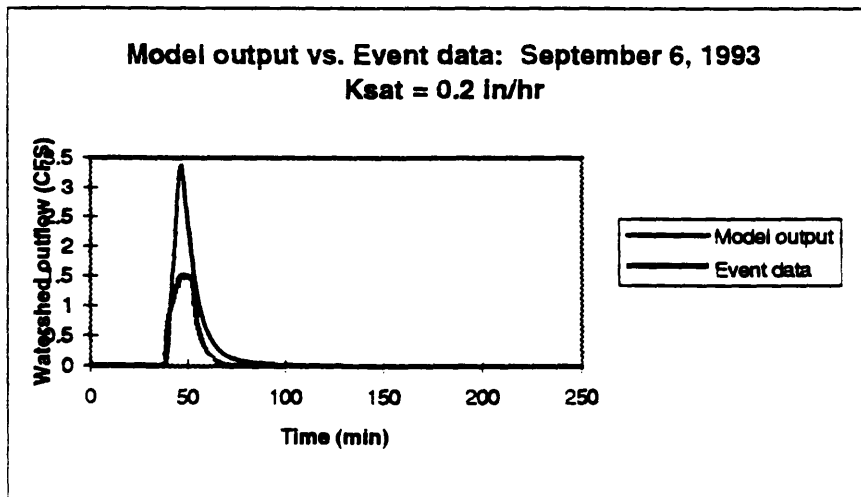
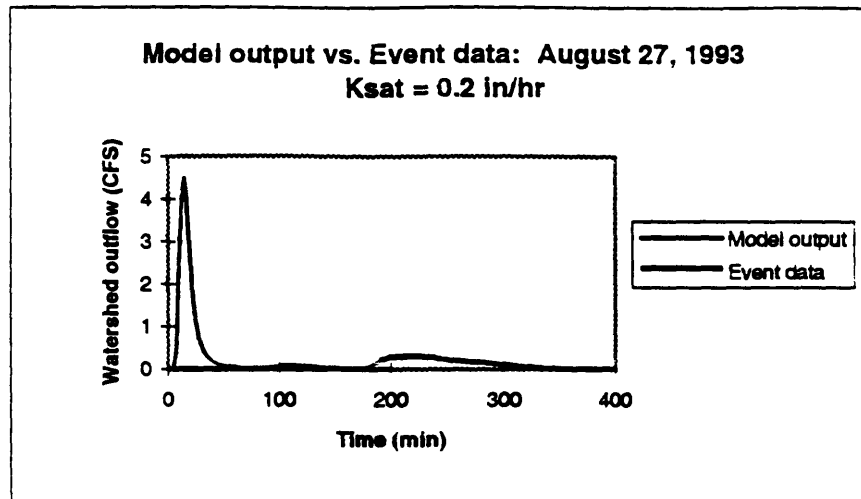


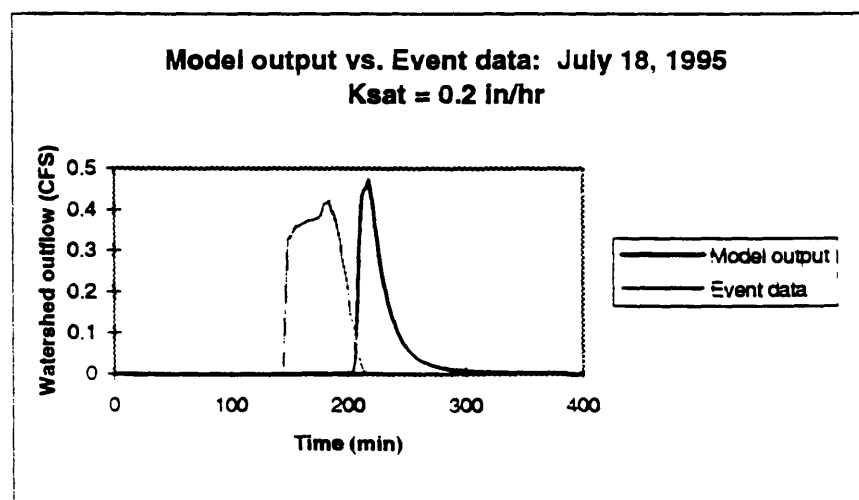
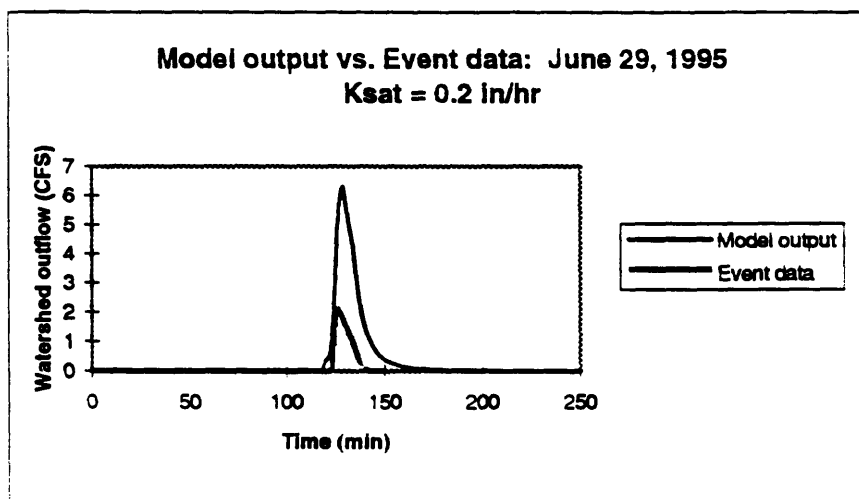
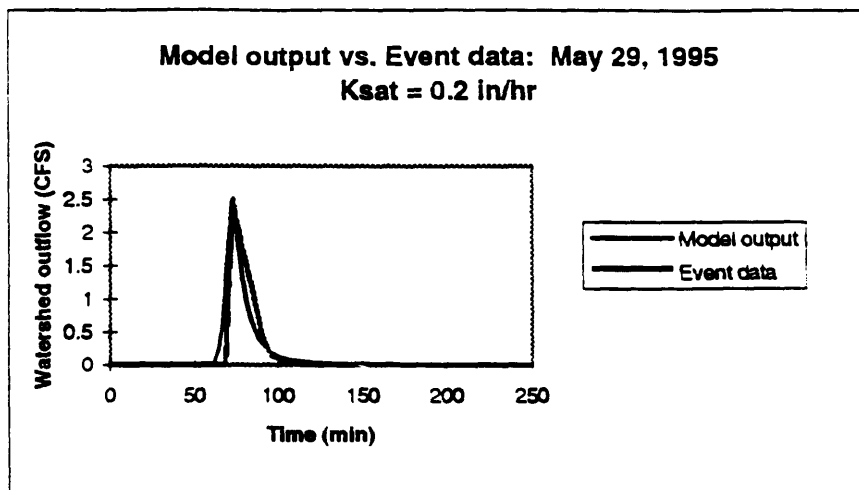
**Model output vs. Event data: August 13, 1995 Ksat = 0.03 in/hr**



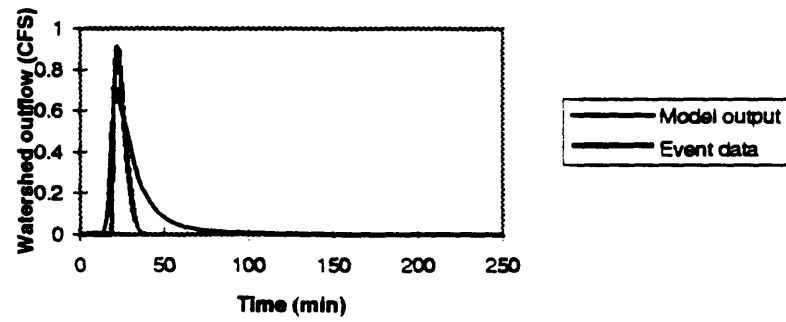




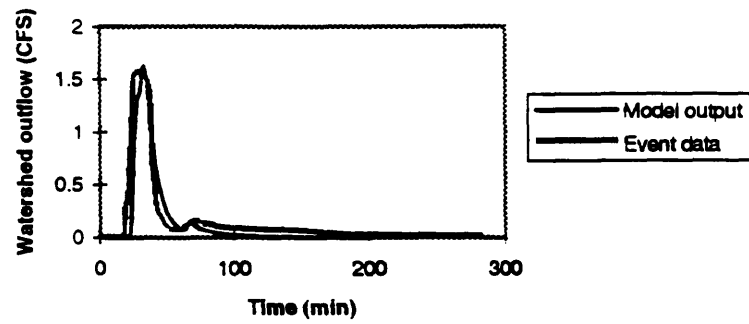




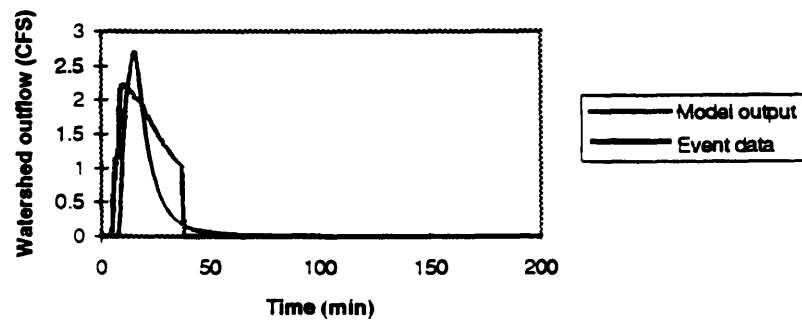
**Model output vs. Event data: August 13, 1995**  
**Ksat = 0.2 in/hr**



**Model output vs. Event data: July 28, 1993**  
**Ksat = 0.55 in/hr**



**Model output vs. Event data: August 27, 1993**  
**Ksat = 0.55 in/hr**



**Model output vs. Event data: September 6, 1993**  
**Ksat = 0.55 in/hr**

